Soukendai lecture note

English Lectures on Fusion Basics Oct.2010~Mar.2011

NIFS Room 701 (7th floor) from 13:30 to 15:10

MHD Equilibrium and stability

K.Y. Watanabe

Index of lecture

1. Introduction of MHD	Jan. 5
2. MHD equilibrium	Jan. 5
3. Pressure driven MHD instabilities	Jan. 12
4. Current driven MHD instabilities	Jan. 19
5. Hot topics of MHD equilibrium and instability	Jan. 27/28

What is MHD?

short for **<u>M</u>**agneto**<u>H</u>**ydro**<u>D</u>**ynamics

The study in which the behavior of a lot of charged particles (plasmas) is treated as motion (dynamics) of a group (fluid) taking interaction between the group and magnetic/electric field into account.

Hydrodynamics;
The fluid consists of a lot of particles. Each particle is in the different position in the real space and the velocity space.
When we study the properties, we do not care each particle's property and we characterize it by using "density", "temperature", "pressure", "velocity", "electric charge density" and "current" as the averaged value with some kind of "weigh". And we analyze the averaged values when we study the fluid properties.

"MHD equilibrium and stability" means the force balance and the stability from view point of "MagnetoHydroDynamics"

What is the study of MHD equilibrium and stability?

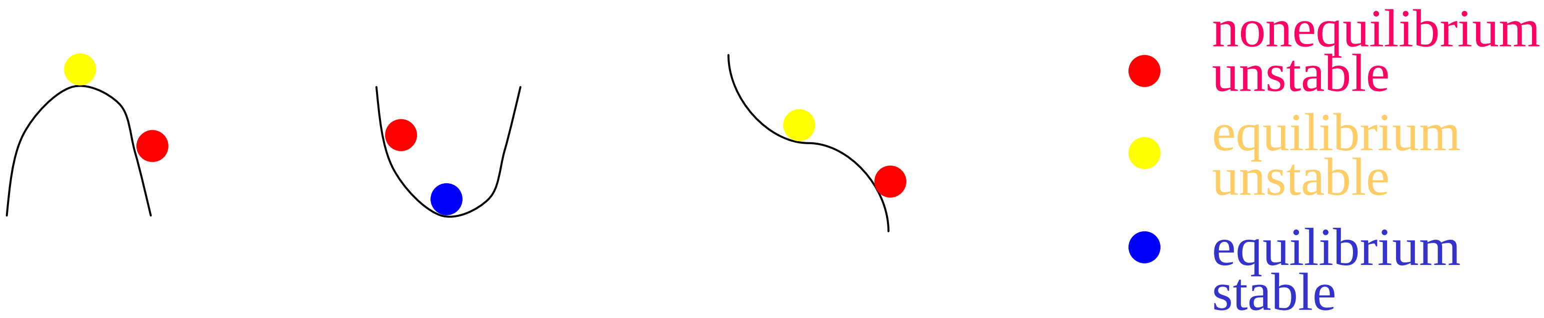

MHD equilibrium study;

Does plasma move or not **when plasma is softly put in** the bottle made of the magnetic field? Is the bottle crushed?

What is the condition for plasma not to move?

MHD stability study;

Does plasma in the bottle made of the magnetic field move or not when plasma is slightly pushed? Does the whole of it or the part of it moves? What is the condition for plasma to stay?

Moving plasma leads to the source of the magnetic field

=> Situation is very complicated.

Index of lecture

1. Introduction of MHD	Jan. 5
2. MHD equilibrium	Jan. 5
3. Pressure driven MHD instabilities	Jan. 12
4. Current driven MHD instabilities	Jan. 19
5. Hot topics of MHD equilibrium and instability	Jan. 27/28

MHD equil. study = Study of Bottle of mag. field (mag. configuration)

Trace of mag. field line =>
Closed line in 2 dimension

Coil of LHD (purple)
& plasma (yellow)

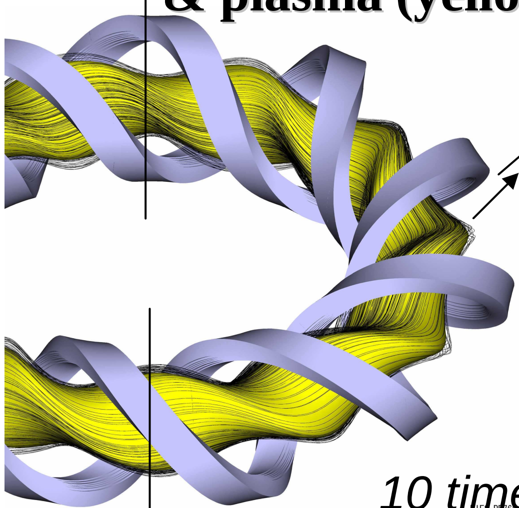

Tangential View of LHD

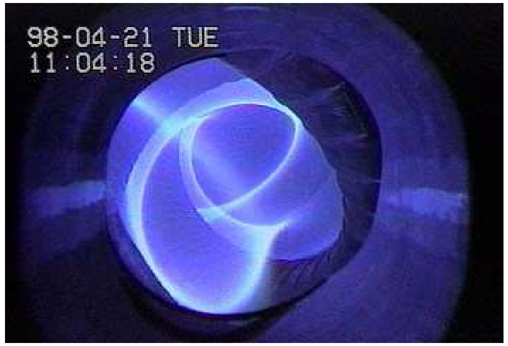

10 times poloidally rotating during 1 toroidal rotating

1 field line makes a "basket"
Field lines make nested "baskets"
=> magnetic surfaces

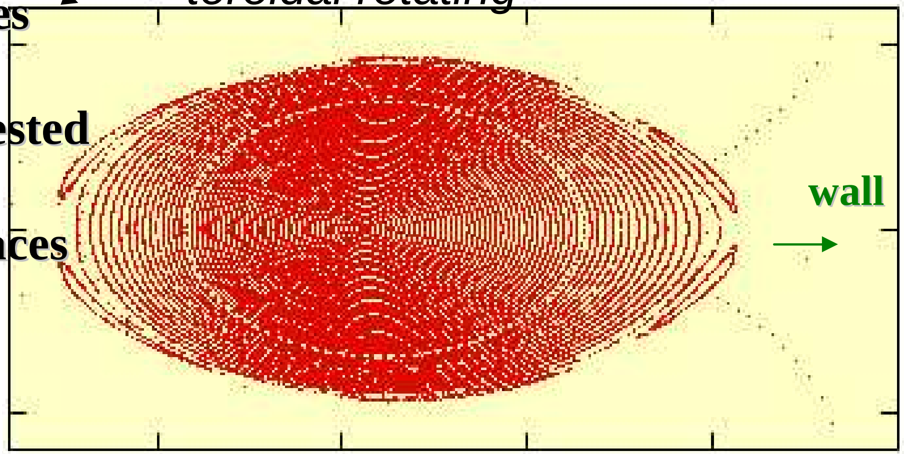

Nested baskets made of mag. field lines keep away plasma from wall
=>
Good magnetic surfaces improve insulation between plasmas and wall

Change of mag. bottle by finite plasma pressure gradient; Fluid picture

Density and temperature grad in mag. bottle induce current

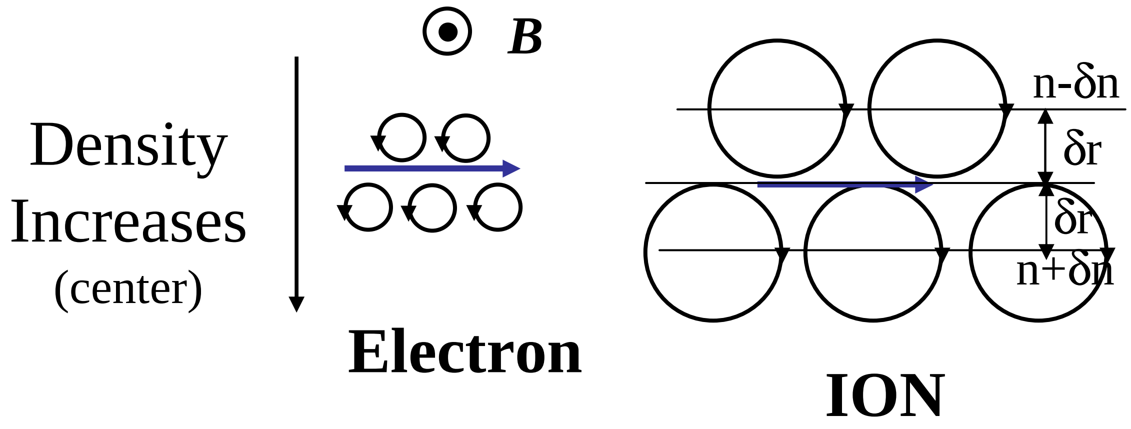

$j_i = q_i e v_i x 2\delta n$ (i ; ion)

$\delta n = (dn/dr)\delta r$

$M_i v_i^2/\delta r = q_i e v_i B$ (centrifugal vs electromag. force)

$\Downarrow$

$j_i = (1/B)(2M_i v_i^2)(dn/dr)$

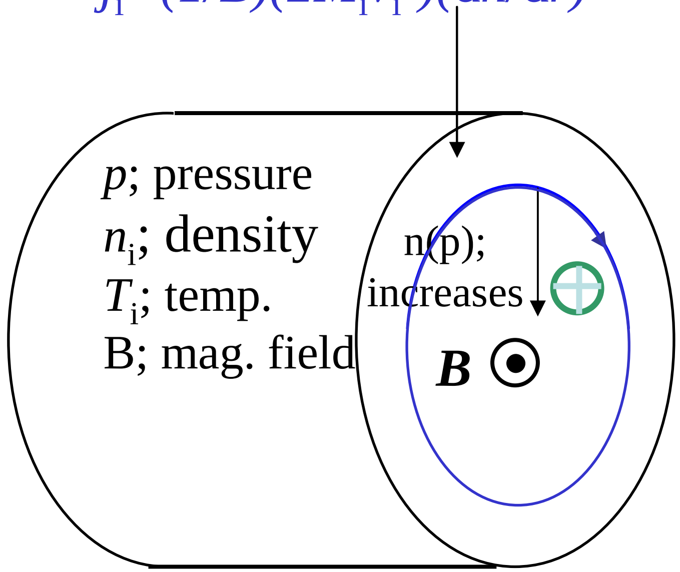

In increases of temp., δv_i exists instead of δn_i.
=> Current flows (cf; $T_i = M_i v_i^2/2$).
For electron, similar current flows (cf; $p = (n_e T_e + n_i T_i)$).
=> Total current;

$$\boxed{j \propto \left| \frac{1}{B} \frac{\partial p}{\partial r} \right|}$$

Current direction; reduces the original mag. field
=> Diamagnetic current

Diamag. current; orthogonal to both B and grad p => $\mathbf{j}\mathrm{x}\mathbf{B}$=grad $\boldsymbol{P}$

=> Diamag. current; source of changing mag. field from vacuum

cf. Relationship between density, temp., press. and velocity of plasma (I)

In thermal equilibrium state (collisional and steady state);
Distribution func. is isotropic, and gauss func. in the velocity (Maxwell distribution func.)
The dispersion is defined by *T*/*m*, the average velocity is by **u**,

$$f \propto \exp\left(\frac{m(\mathbf{v}-\mathbf{u})^2/2}{T}\right);\ \text{Boltzman constant Omitted}$$

$$N \equiv \int f d\mathbf{v};\ \text{Total number of paticles is defined by } N$$

$$\Rightarrow f = N\left(\frac{m}{2\pi T}\right)^{1.5}\exp\left(\frac{m(\mathbf{v}-\mathbf{u})^2/2}{T}\right)$$

$$\int \frac{m(\mathbf{v}-\mathbf{u})^2}{2} f d\mathbf{v} \Rightarrow \frac{3}{2}NT$$

Energy of particles in the moving coordinate system with **u** (thermal energy)

cf. Relationship between density, temp., press. and velocity of plasma (II)

For simplicity, we consider the pressure under the assumption $\mathbf{u}=0$

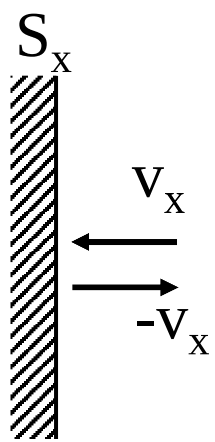

The momentum which 1 particle gives a wall

$2mv_x$

The number of particles per unit of time which reach the wall with area size S_x,

$v_x S_x n$ (n denote density)

Then, the momentum per unit of time (force) by which the wall with area size S_x is pushed,

$2mv_x^2 S_x n$

The pressure, p, corresponds to the above force divided by area size, (here isotropic pressure is assumed)

$p=2mn\langle v^2\rangle/3=nT$

=> Pressure is density times temp.

Diamag. current in the presence of non-unform mag. field

$$j_R = \frac{|\nabla p|}{B}$$

Condition is achieved in simple torus mag. field (external current flows along z axis)

Here non-uniform mag. field is assumed as $B=R_0B_0/R$.

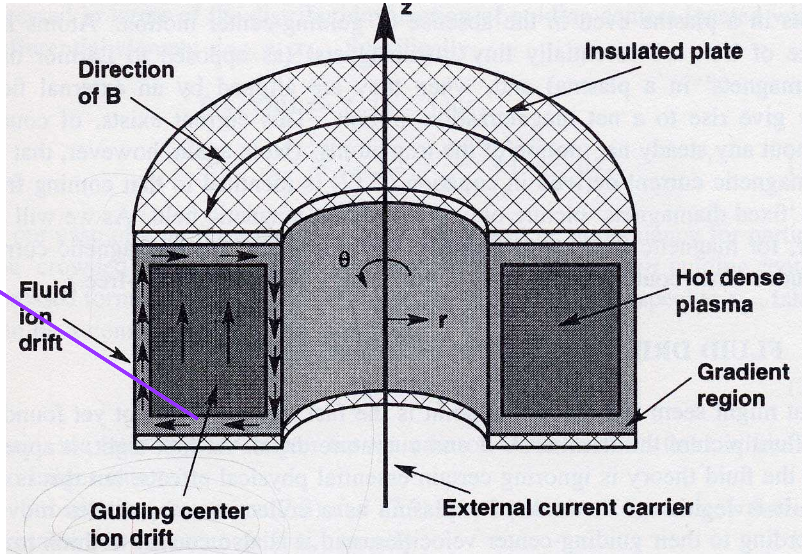

$$j_R = R\frac{|\nabla p|}{R_0 B_0}$$

Current density increases as more torus outwardly

Divergence of j is as the below

$$div \quad j = \frac{1}{R}\frac{\partial}{\partial R}\left(R \times R\frac{|\nabla p|}{R_0 B_0}\right) \approx \frac{2\nabla p}{RB} \neq 0$$

$$\frac{d\sigma}{dt} + div \quad \mathbf{j} = 0 \quad \Rightarrow \frac{d\sigma}{dt} \neq 0$$

The charge appears at torus top and bottom ($d\sigma/dt=/0$)

Time evolution of charge (due to the connection of top and bottom) is necessary to satisfy the charge conservation

The current along mag. field line should be induced

=>

Pfirsh-Schluter (PS) current

Evaluation of PS current (From $\nabla \cdot \mathbf{j} = 0$)

$$\mathbf{j}_{//} \equiv \frac{(\mathbf{j}\cdot\mathbf{B})\mathbf{B}}{B^2}, \nabla\cdot\mathbf{j}_{//} = \nabla\cdot\left(\frac{j_{//}}{B}\mathbf{B}\right) = \mathbf{B}\cdot\nabla\left(\frac{j_{//}}{B}\right) = B\frac{\partial}{\partial s}\left(\frac{j_{//}}{B}\right) \sim \frac{\partial j_{//}}{\partial s},$$

$$\mathbf{j}_{\perp} \equiv \frac{B^2\mathbf{j} - (\mathbf{j}\cdot\mathbf{B})\mathbf{B}}{B^2} = \frac{\mathbf{B}\times\nabla p}{B^2},$$

$$\nabla\cdot\mathbf{j}_{\perp} = \nabla\cdot\left(\frac{\mathbf{B}}{B^2}\times\nabla p\right) = \nabla p\cdot\nabla\times\left(\frac{1}{B^2}\mathbf{B}\right)$$

$$= \nabla p\cdot\left(-\frac{2}{B^3}\nabla B\times\mathbf{B}\right) = -2\nabla p\cdot\left(\frac{\nabla B\times\mathbf{b}}{B^2}\right)$$

$$\nabla p \sim \hat{\mathbf{r}}\frac{\partial p}{\partial r}, \hat{\boldsymbol{\theta}}\cdot\nabla B \sim B_0\frac{\partial}{r\partial\theta}(1-\varepsilon\cos\theta), \frac{\partial}{\partial s} = \frac{\partial\theta}{\partial s}\frac{\partial}{\partial\theta} = \frac{\iota}{2\pi R_0}\frac{\partial}{\partial\theta}$$

$$\nabla\cdot\mathbf{j}_{//} = -\nabla\cdot\mathbf{j}_{\perp} \Longrightarrow \frac{\partial j_{//}}{\partial s} = 2\nabla p\cdot\left(\frac{\nabla B\times\mathbf{b}}{B^2}\right)$$

$$\Longrightarrow \frac{\iota}{2\pi R_0}\frac{\partial j_{//}}{\partial\theta} \sim \frac{\partial p}{\partial r}\frac{1}{R_0 B_0}\sin\theta \Longrightarrow j_{//} \sim -\frac{2\pi}{\iota B_0}\frac{\partial p}{\partial r}\cos\theta$$

Current along mag. field line (PS current) increases with press. grad. and decreases with rotational transform, ι, and magnetic field strength, B_0.

Plasma consists of a lot of charged particles (MHD equil. picture based on each particle's motion)

Basis of behavior of charged particles; Drift

Charged particle follows gyro-orbit along the magnetic field line in uniform mag. field w/o elec. field. In non-uniform mag. field and/or with elec. field, it makes the additional motion in perpendicular to mag. field (drift). This is the basis to understand the charged particle behavior.

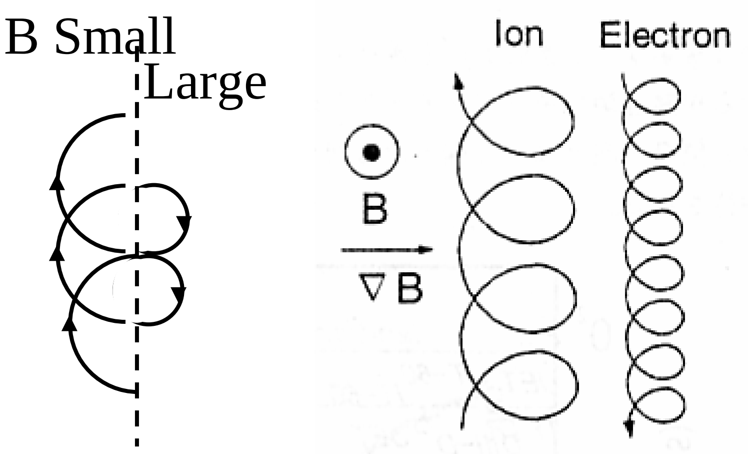

$$\frac{mv^2}{r} = qvB \Rightarrow r = \frac{mv}{qB}$$

Bx∇B drift

Ion moves in the direction to **Bx∇B** due to change of gyro-radius during gyro-motion.

Direction of elec. drift is opposite.

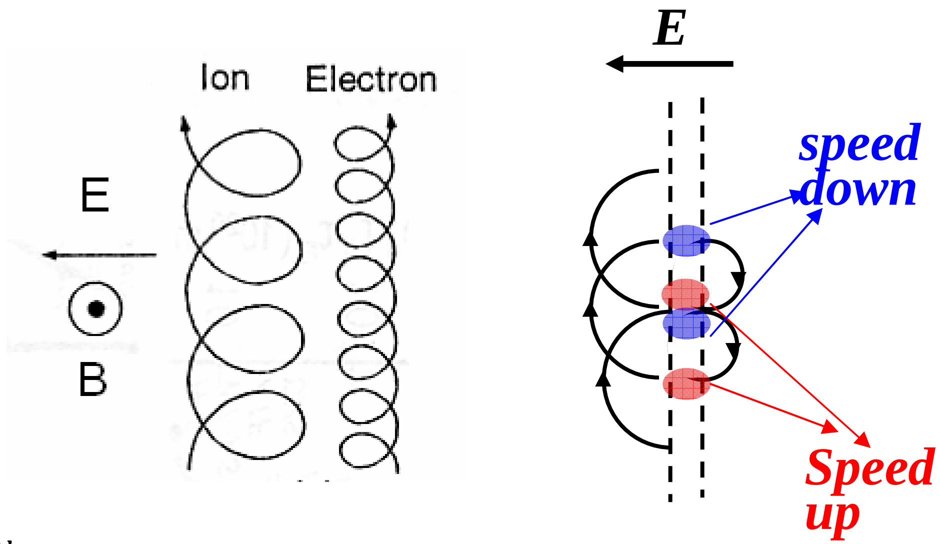

ExB drift

Ion moves in the direction to **ExB** due to change of velocity during gyro-motion.

Direction of elec. drift is same.

Change of mag. bottle due to plasma I -- based on particle motion --

Plasma cannot be confined by only toroidal mag. field (it moves even when plasma is softly put).

Only toroidal field exists
($B_t \neq 0$, $B_p = 0$)

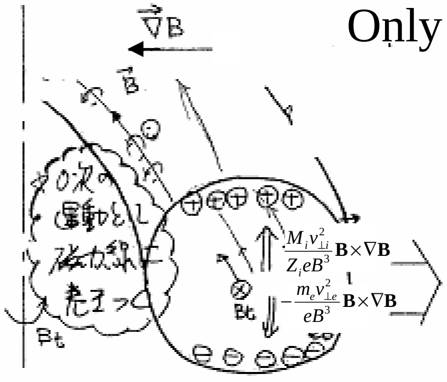

Bx∇B ドリフト

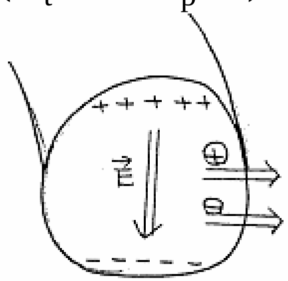

ExBドリフト

Reason

(1) Charge separation occurs due to Bx∇B drift.
(2) The charges induce Elec. field => Both ion and elec. move to torus outwardly due to ExB drift.

A countermeasure

Add the poloidal mag. field ($B_p \neq 0$) to connect the separated charges in torus-top and bottom due to the mag. filed line.

⇓

Elec. field is reduced, which suppresses ExB drift.

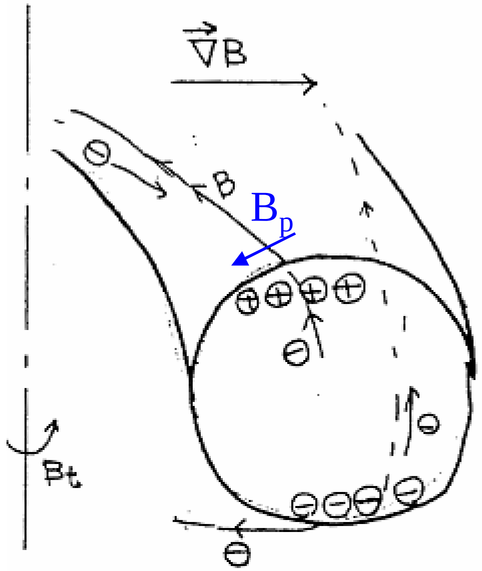

Elec. easily moves because it is light to cancel separated charges.

How to produce B_p

Tokamaks; toroidal current is induced.
Heliotron/Helical; external coils are helically wound.

Change of mag. bottle due to plasma II -- mag. axis moves --

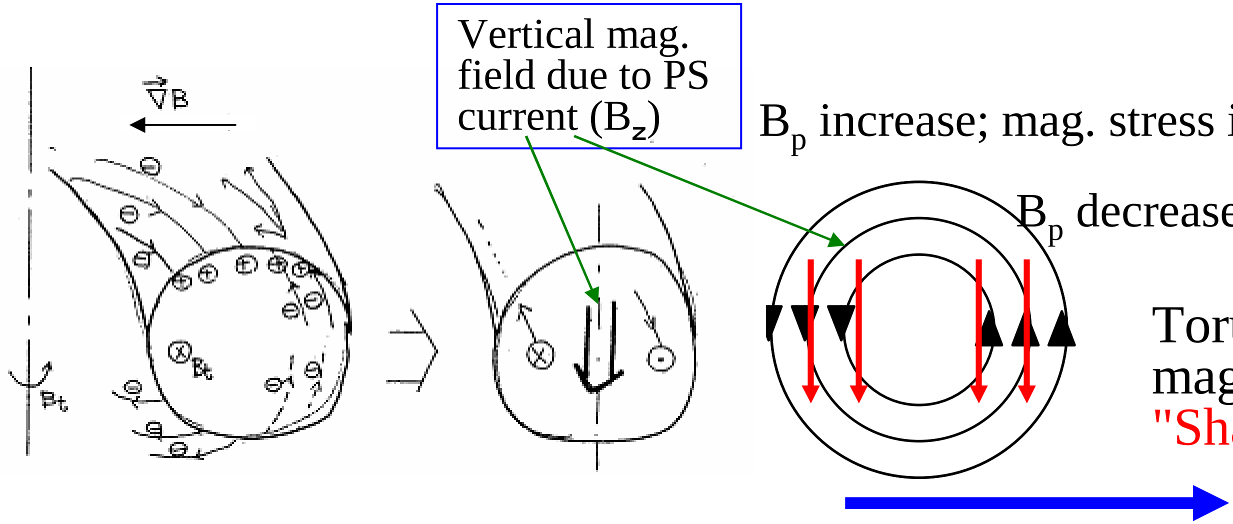

Torus outwardly
mag. axis shift
"Shafranov shift"

<u>Suppression of ExB drift due to production of B_p</u>
<u>(Suppression of charge separation)</u>

$\Downarrow$

Pfirsh-Schuter current(Equilibrium current) is induced

$\Downarrow$

Mag. axis torus outwardly shifts due to vertical field by PS current **=> Change of mag. bottle**

Large B_p=> Large pitch of mag. field line (rotational transform ι) => Small toroidal component of PS current
=> Small Shafranov shift
Large plasma pressure (Large dp/dρ)
=> Large PS current => Large Shafranov shift

Top View of torus

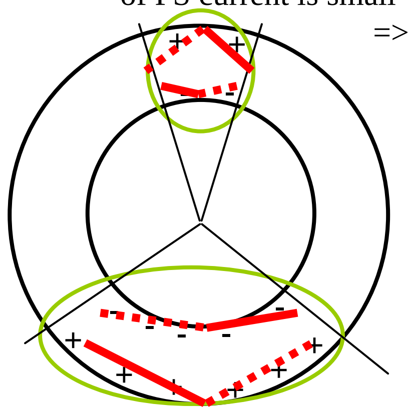

Summary of PS current (from viewpoints of different aspects)

From the viewpoint of fluid and particle, driving mechanism of PS current is reviewed. From both viewpoints, it is indispensable to confine finite pressure plasma.

1. In toroidal mag. configuration (grad ***B*** */=0), only diamag. current does not satisfy* div ***j*** =0 *condition and charges increase both in the torus top and the bottom. The finite poloidal mag. field in addition to toroidal field is necessary to satisfy* div ***j*** =0 *and PS current appears.*

2. In toroidal mag. configuration (grad ***B*** */=0), charge separation occurs due to* ***B****x* ∇*B drift. In order to suppress* ***E****x****B*** *drift due to the charge separation, the poloidal mag. field* ($B_p \neq 0$) *is necessary to connect the torus-top and bottom of the mag. filed line. When the charges are cancelled, a current flows in the opposite direction inside and outside of torus, which is PS current's another aspect.*

How is poloidal field produced
ー Helical and Tokamak ー

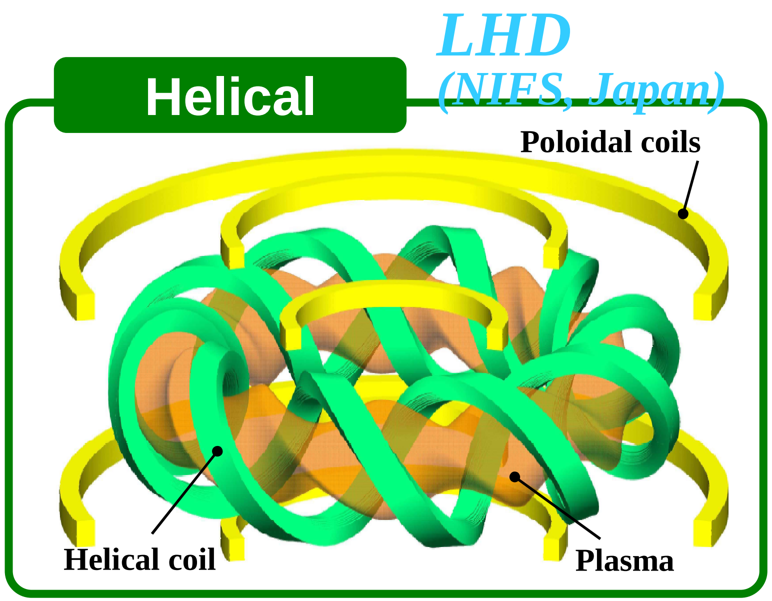

External coils (helical coils) produces poloidal mag. field.

More suitable for steady state operation than tokamak

Construction is difficult because of complicated structure and needs of high accurate alignment.

Japanese scientist poroposed this concept.

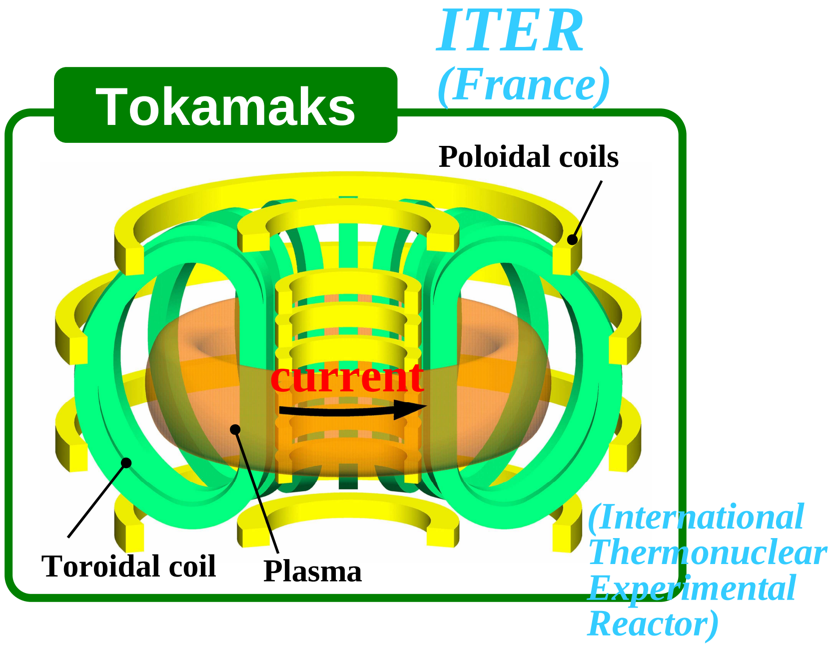

Toroidal current produces poloidal mag. field.

For steady state operation, innovative concept on stationary toroidal current drive is necessary.

Construction is rather easy because of simpler structure than helical.

Why can helical coils produce B_p (finite poloidal field) ?

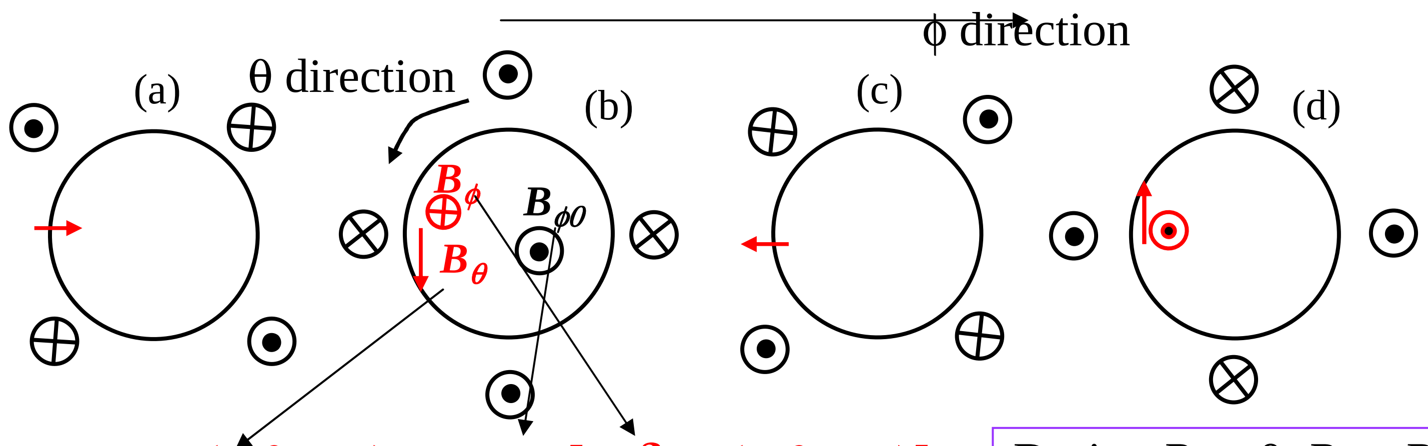

$B_\theta \sim \cos(L\theta - M\phi)$, $B_\phi \sim B_{\phi 0}[1-\delta\cos(L\theta - M\phi)]$

L; poloidal pole number, M; toroidal period
In the above figure, L=2.

During $B_\theta > 0$, $B_\phi < B_{\phi 0}$.
During $B_\theta < 0$, $B_\phi > B_{\phi 0}$.
=>
During $B_\theta > 0$, mag. field line proceeds slowly in troidal direction. During $B_\theta < 0$, mag. field line proceeds fast.

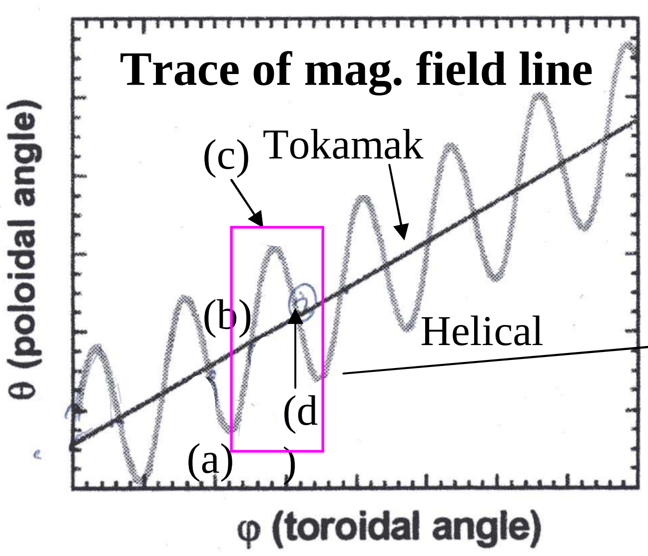

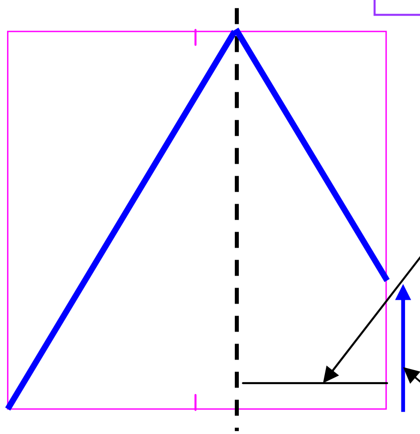

This phase is shorter than the previous phase.
=>
Mag. field line does not reach the starting point of the previous phase.
=>
Mag. field line proceeds in the poloidal direction.

MHD equilibrium equation I

Starting from MHD equations

$\rho\left(\frac{\partial}{\partial t}+\mathbf{v}\cdot\nabla\right)\mathbf{v}=\mathbf{j}\times\mathbf{B}-\nabla p,$	Motion eq.
$\frac{\partial\rho}{\partial t}+\nabla\cdot(\rho\mathbf{v})=0,$	Continuity eq.
$\left(\frac{\partial}{\partial t}+\mathbf{v}\cdot\nabla\right)\left(\frac{p}{\rho^{\gamma}}\right)=0,$	State eq.
$\mathbf{E}+\mathbf{v}\times\mathbf{B}=\eta\mathbf{j},$	Ohms low
$\nabla\times\mathbf{B}=\mu_0\mathbf{j},\quad \nabla\times\mathbf{E}=-\frac{\partial\mathbf{B}}{\partial t},\quad \nabla\cdot\mathbf{B}=0.$	Maxwell eq.

ρ; mass density
$\mathbf{v}$; fluid velocity
p; pressure
$\mathbf{j}$; current density
$\mathbf{B}$; magnetic field
$\mathbf{E}$; electric field
η; resistivity
γ; rate of specific heat
μ_0; space permeability

Here we consider the MHD equilibrium ($\partial / \partial t = 0$) under the assumption $v << v_{th}$ ($v=0$).
(This assumption is valid in typical fusion plasma)

$$
\begin{aligned}
&0=\mathbf{j}\times\mathbf{B}-\nabla p,\\
&0+0=0,\\
&0+0=0,\\
&\mathbf{E}+0=\eta\mathbf{j},\\
&\nabla\times\mathbf{B}=\mu_0\mathbf{j},\quad \nabla\times\mathbf{E}=-\frac{\partial\mathbf{B}}{\partial t},\quad \nabla\cdot\mathbf{B}=0.
\end{aligned}
$$

$\rightarrow$

MHD equilibrium equation

$$
\boxed{
\begin{aligned}
&\mathbf{j}\times\mathbf{B}=\nabla p,\\
&\nabla\times\mathbf{B}=\mu_0\mathbf{j},\\
&\nabla\cdot\mathbf{B}=0.
\end{aligned}
}
$$

MHD equilibrium equation II

Starting from MHD equil. eq.

$$\mathbf{j}\times\mathbf{B}=\nabla p,\quad \nabla\times\mathbf{B}=\mu_0\mathbf{j},\quad \nabla\cdot\mathbf{B}=0.$$

$$\mathbf{j}-j_{//}\frac{\mathbf{B}}{B}\equiv\mathbf{j}_\perp=\frac{\mathbf{B}\times\nabla p}{B^2},$$
$$\nabla\cdot\mathbf{j}=\nabla\cdot(\nabla\times\mathbf{B})=0.$$

$$\mathbf{B}\cdot\nabla p=0,\quad \mathbf{j}\cdot\nabla p=0.$$

1. Mag. field line and current lie on contour of pressure.
2. Contours of pressure coincide with mag. surfaces.

$$\nabla\cdot\mathbf{B}=0$$
$$\Rightarrow \mathbf{B}=\nabla\psi\times\nabla\alpha$$

(Clebsh expression)

$$\mathbf{B}\cdot\nabla\psi=0,\quad \mathbf{B}\cdot\nabla\alpha=0$$

1. Both ∇Ψ and ∇α are orthogonal to mag. field line.
2. When contour of Ψ is defined by mag. surface, a=constat on mag. surf. denotes magnetic field line.

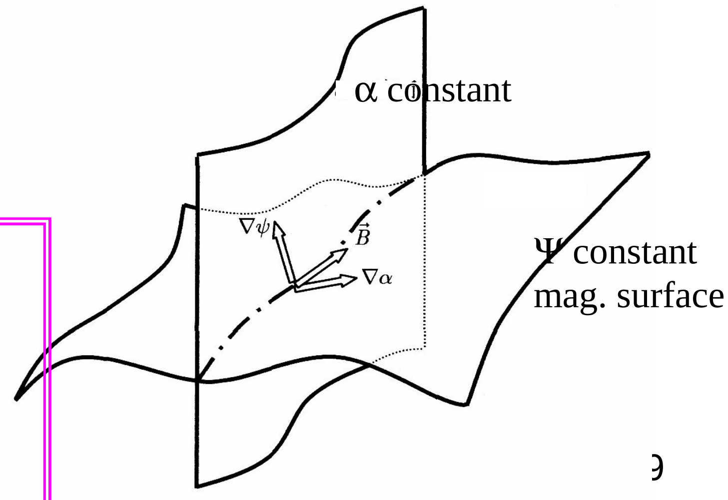

Ex. of change of mag. bottle (mag. structure) due to plasma press.

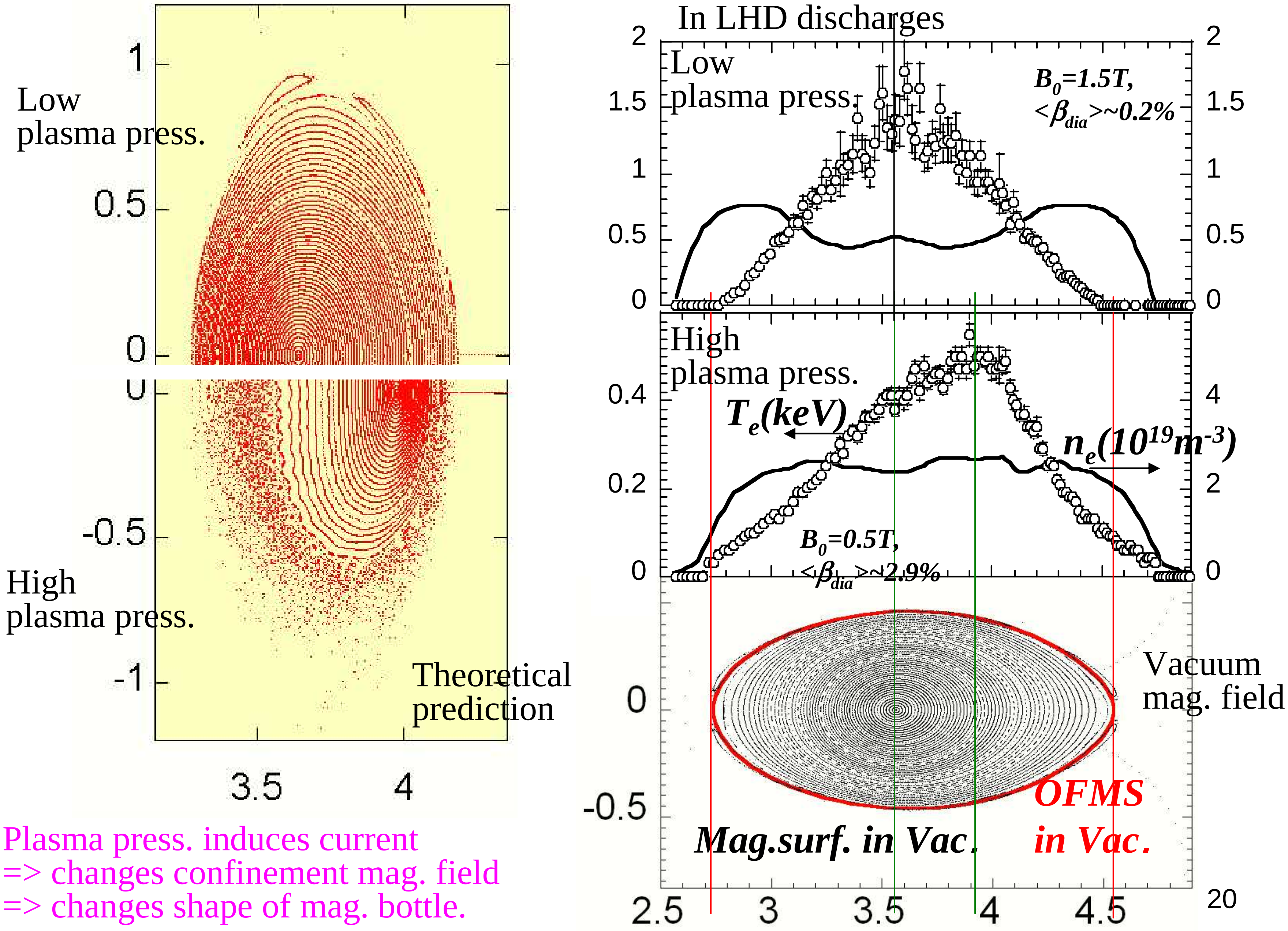

Plasma press. induces current
=> changes confinement mag. field
=> changes shape of mag. bottle.

プラズマ中にはいろんな電流が流れる

1. 反磁性電流
2. Pfirsh-Schluter(フィルシュ.シュルター)電流
 (MHD平衡が成り立つために必要な電流として
説明済み)
3. オーミック電流
4. ビーム駆動(大河)電流
5. ブートストラップ電流
6. その他(電磁波駆動電流など)

これらの電流が、プラズマ閉込め容器(磁場配位)の形状を変化させる => その影響を定量的に調べることがMHD平衡研究
閉込め容器の形状が変わればプラズマの閉込め特性も影響を受けるので、MHD平衡研究は基盤的な研究。

3. オーミック電流

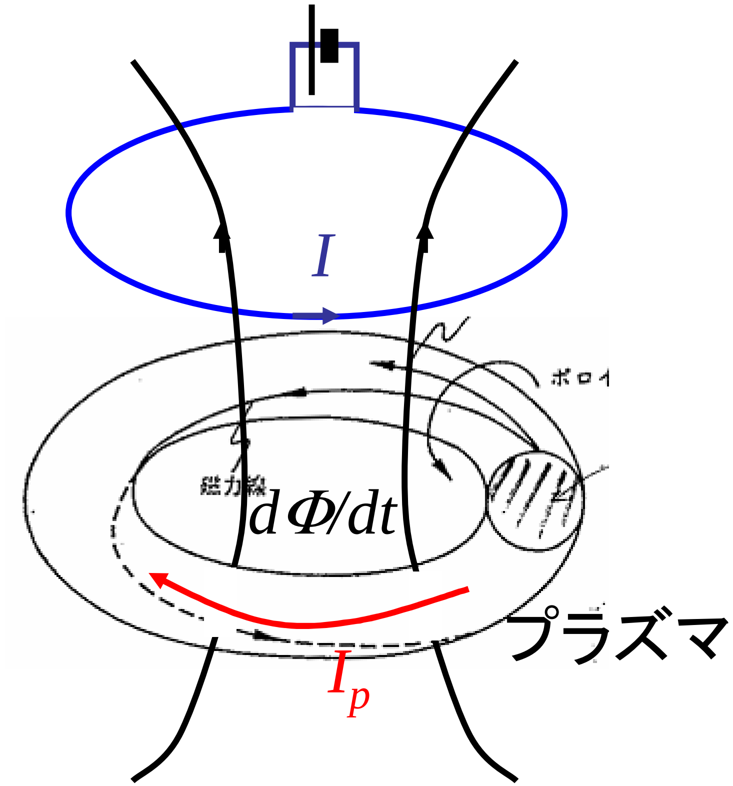

$d\Phi/dt=RI_p$

4. ビーム駆動(大河)電流

米国、GA社の大河博士が予言

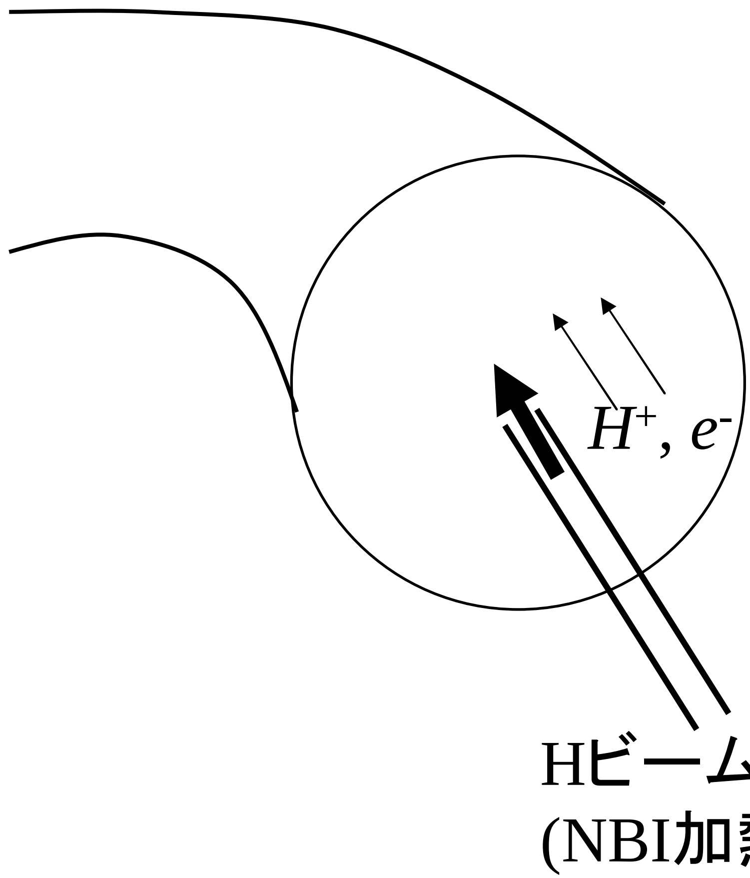

水素イオンと電子の衝突の差により電流が流れる

5.ブートストラップ電流の駆動機構 (I)

磁場強度に強弱がある時の荷電粒子の運動

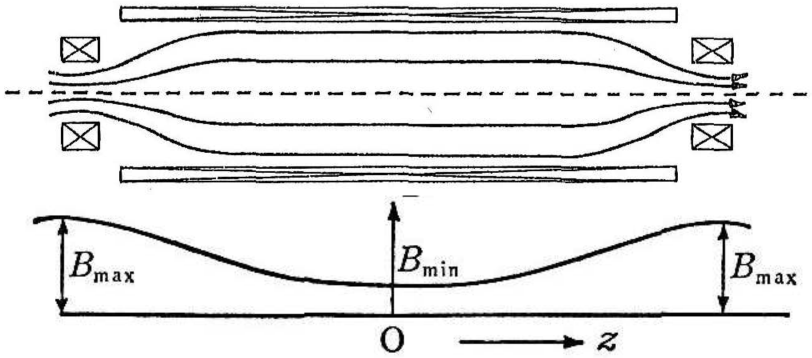

電場がゼロで磁場がゆっくり変化している場の荷電粒子は、運動エネルギーの他に磁気モーメントが保存する。

$$\frac{mv_{//}^2}{2} = E - \mu_m B$$ より

$E < \mu_m B_{\max}$ の粒子は$B = B_{\max}$の領域に到達できない。

$$=> \frac{mv_{//0}^2}{2} + \frac{mv_{\perp 0}^2}{2} < \frac{mv_{\perp 0}^2}{2}\frac{B_{\max}}{B_{\min}}$$

$=> \mathrm{z} = 0$で、$\left|\frac{v_{//0}}{v_{\perp 0}}\right| < \sqrt{\frac{B_{\max}}{B_{\min}} - 1}$ の荷電粒子は

$B = B_{\max}$の領域に到達する前に磁場の弱い方へ反射される。

=> 捕捉粒子と呼ばれる粒子が存在する。

μ_mの保存($\left|\frac{1}{\Omega}\frac{1}{B}\frac{\partial B}{\partial t}\right| << 1$ の時)

$$\frac{\mathrm{d}}{\mathrm{d}t}(m\mathbf{v}) = q(\mathbf{E} + \mathbf{v}_\perp \times \mathbf{B})$$

$$\frac{\mathrm{d}}{\mathrm{d}t}\left(\frac{m\mathbf{v}_\perp^2}{2}\right) = q\mathbf{v}_\perp \cdot \mathbf{E}$$

$$\Delta W_\perp = \int q\mathbf{E}\cdot\mathbf{v}_\perp \mathrm{d}t = \int q\mathbf{E}\cdot\mathrm{d}\mathbf{s} = \int q(\nabla\times\mathbf{E})\cdot\mathbf{n}\mathrm{d}S = q\int\frac{\partial\mathbf{B}}{\partial t}\cdot\mathbf{n}\mathrm{d}S$$

$$\sim q\frac{\partial}{\partial t}\int\mathbf{B}\cdot\mathbf{n}\mathrm{d}S \sim q\frac{\partial B}{\partial t}\pi\rho_B^2 = \frac{2\pi}{\Omega}\frac{\partial B}{\partial t}\frac{q\Omega\rho_B^2}{2} \sim \Delta B\frac{W_\perp}{B}$$

$$\frac{\Delta W_\perp}{\Delta B} = \frac{W_\perp}{B} => \mu_m \equiv \frac{W_\perp}{B} = \mathrm{const.}$$

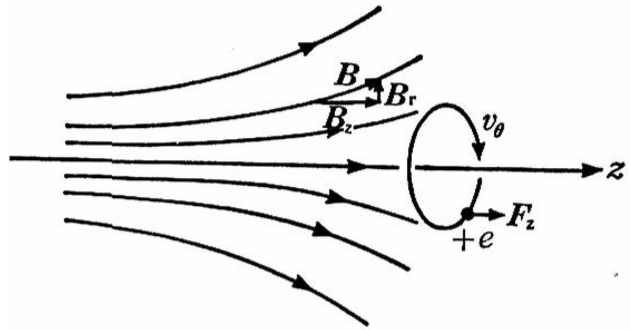

磁場に強弱があると、磁場弱い方向に凸に磁力線が曲がる。
図中でBr成分が発生。この磁場と荷電粒子の運動方向から、磁場の弱い方向に力を受ける

5.ブートストラップ電流の駆動機構 (II)

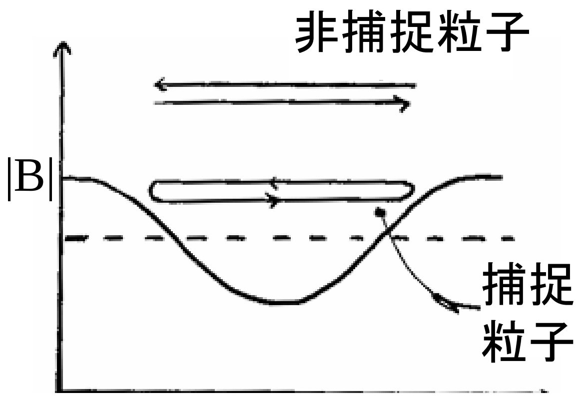

磁力線の距離

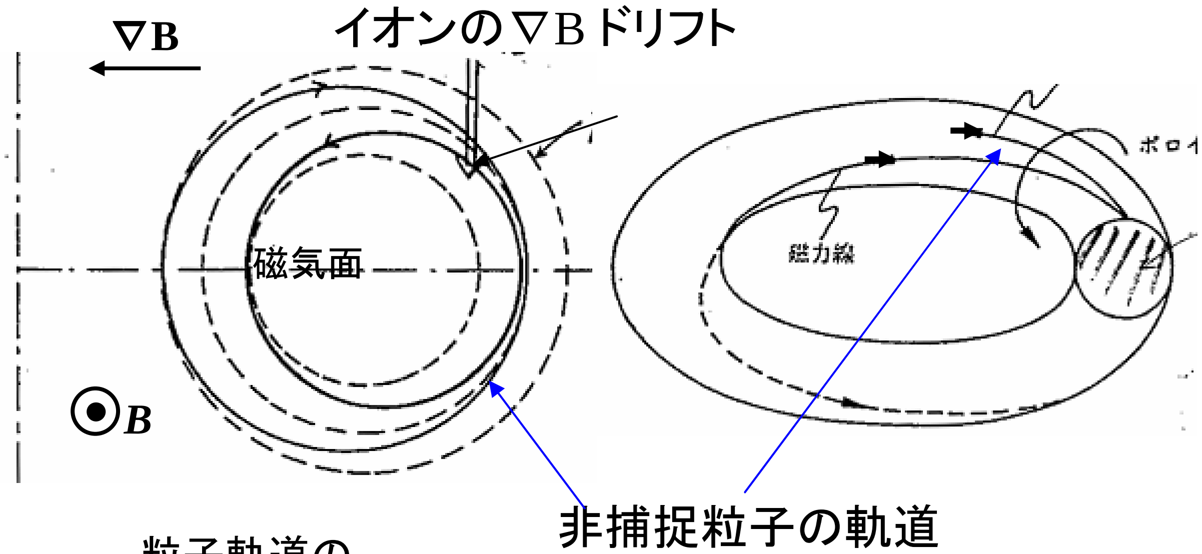

粒子軌道の
ポロイダル断面

磁場の弱いところに捕捉される捕捉粒子の存在と密度、温度勾配によりトロイダル方向に余剰のモーメンタム源が現れる

➔

圧力勾配が駆動する電流"ブートストラップ電流"が流れる。

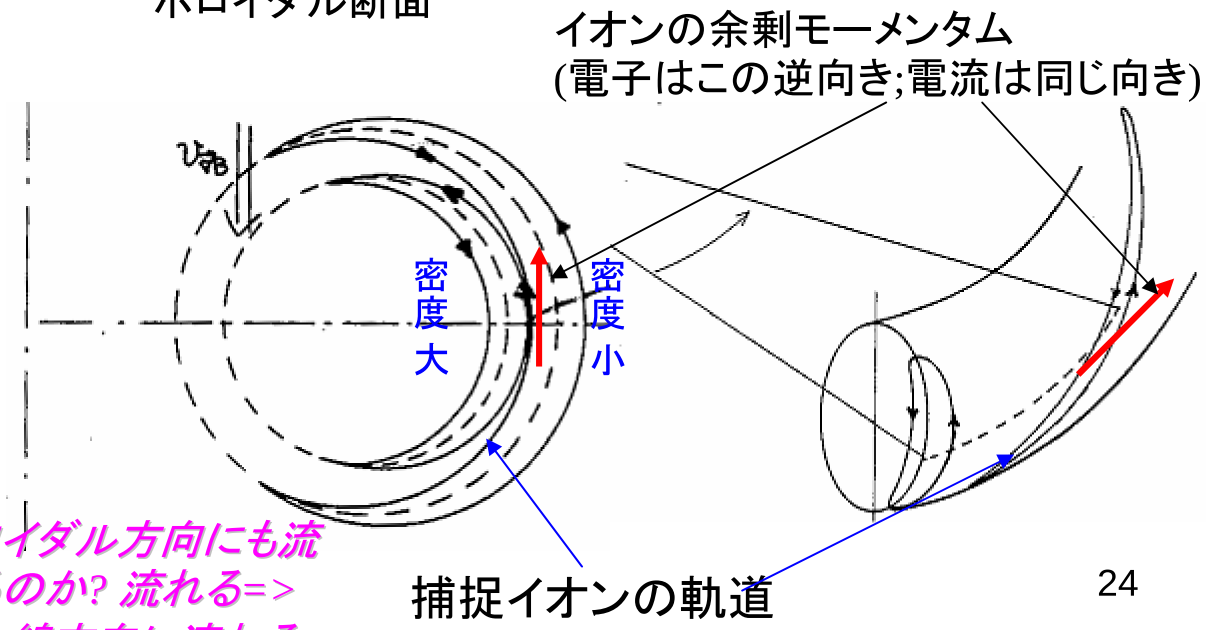

ポロイダル方向にも流れるのか? 流れる=>
磁力線方向に流れる

ヘリカルコイルで回転変換(磁場の捩じれ)が生じる理由

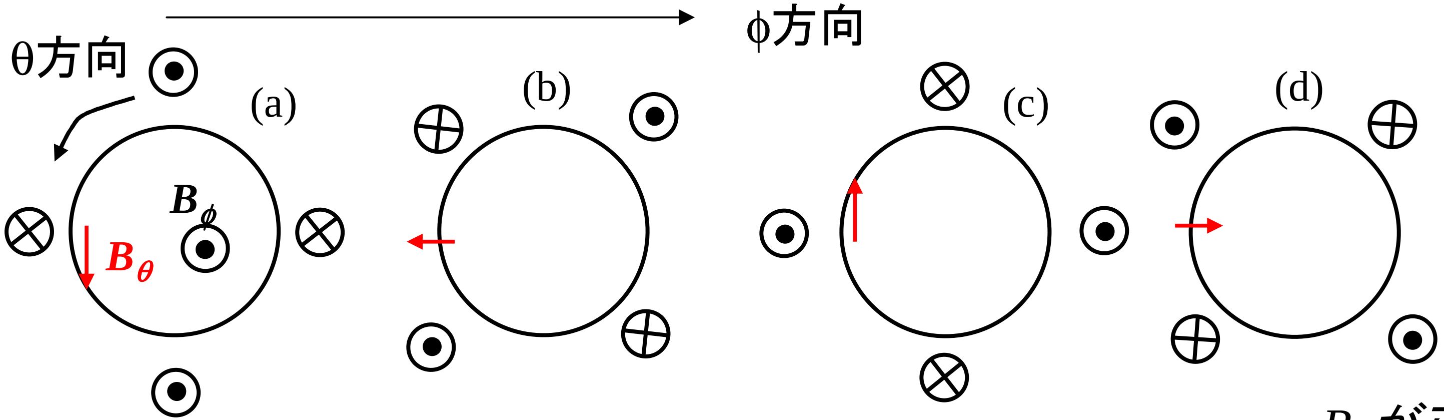

B_θ~cos(Lθ-Mϕ), B_ϕ~[1-δcos(Lθ-Mϕ)]
L,Mはそれぞれポロイダル局数，トロイダル周期数
図の例では，L=2.

B_θが正の間はB_ϕが1より小さく，B_θが負の間はB_ϕが1より大きい．つまり，B_θが正の間は磁力線は方向にあまり進まず，B_θが負の間に磁力線は早く前に進む.

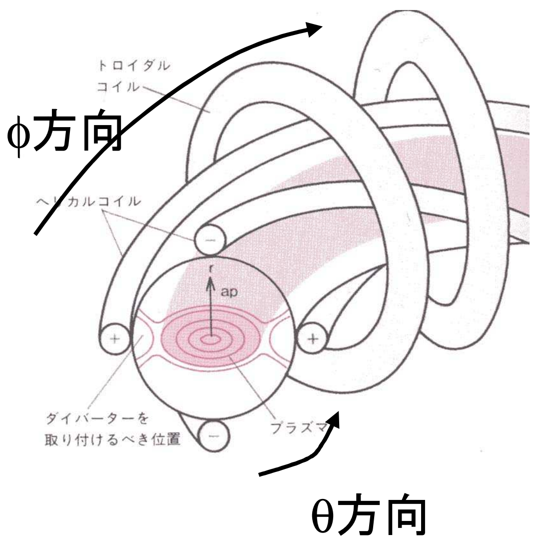

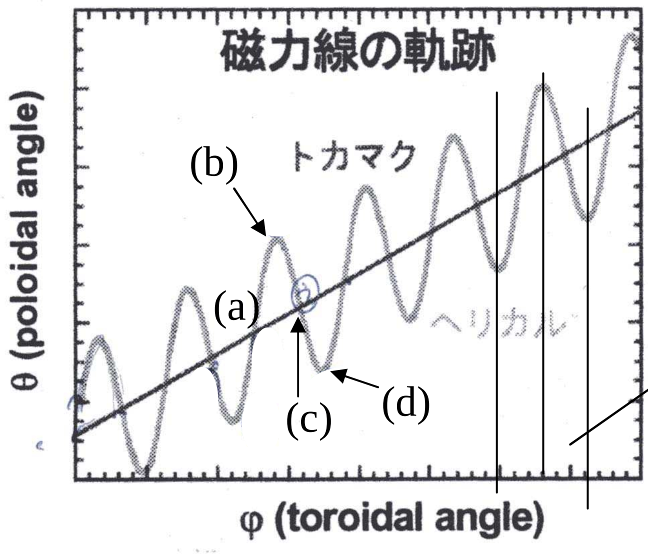

こちらのほうが短い，その前の半周期でθ方向に進んだ分，戻ってこない
＝＞
磁力線はθ方向に進む

Index of lecture

What drives MHD instabilities in magnetized plasmas?

Two driving mechanism are considered.
(1) Pressure gradient (pressure driven mode)
(2) Plasma current (current driven mode)

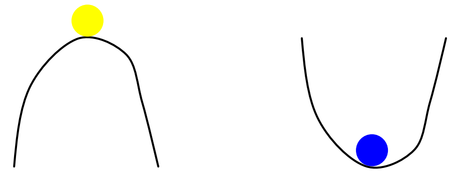

equilibrium unstable

equilibrium stable

(1) =>
appears in both helical and tokamak plasmas.
Interchange/Ballooning mode

(2) =>
appears in only tokamak plasmas.
Kink/Tearing mode

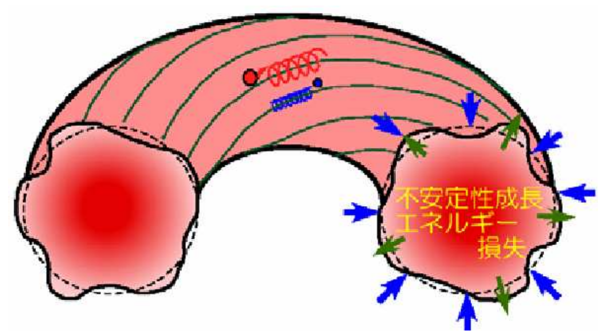

MHD Stable on not?

Does plasma in mag. bottle move or not when plasma is slightly pushed?

Does the whole of it or the part of it moves?

Physical picture of pressure driven instabilities

Unstable conditions;
Pressure increases as magnetic field strength increses.

Physical picture of instability
(1) Density perturbation appears
(2) Direct. of density gradients coincide with mag. field strength gradient (Bad curvature).
=> Charges separates due to **B**x∇B drift.
(3) Charge separation due to **E**x**B** drift enhances density perturbation.

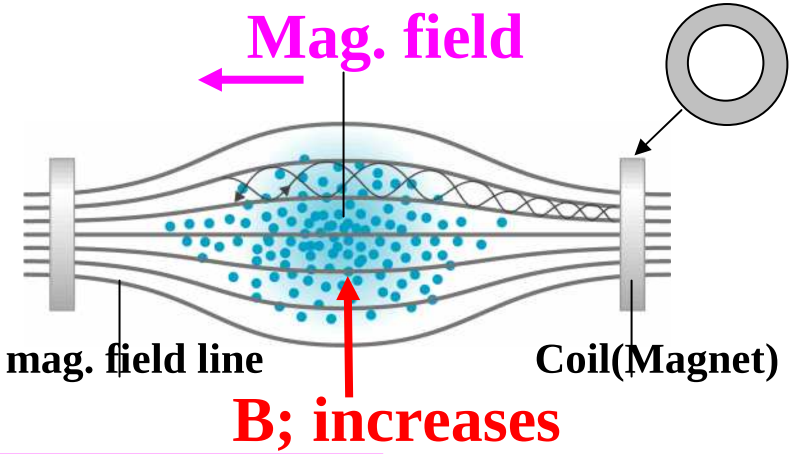

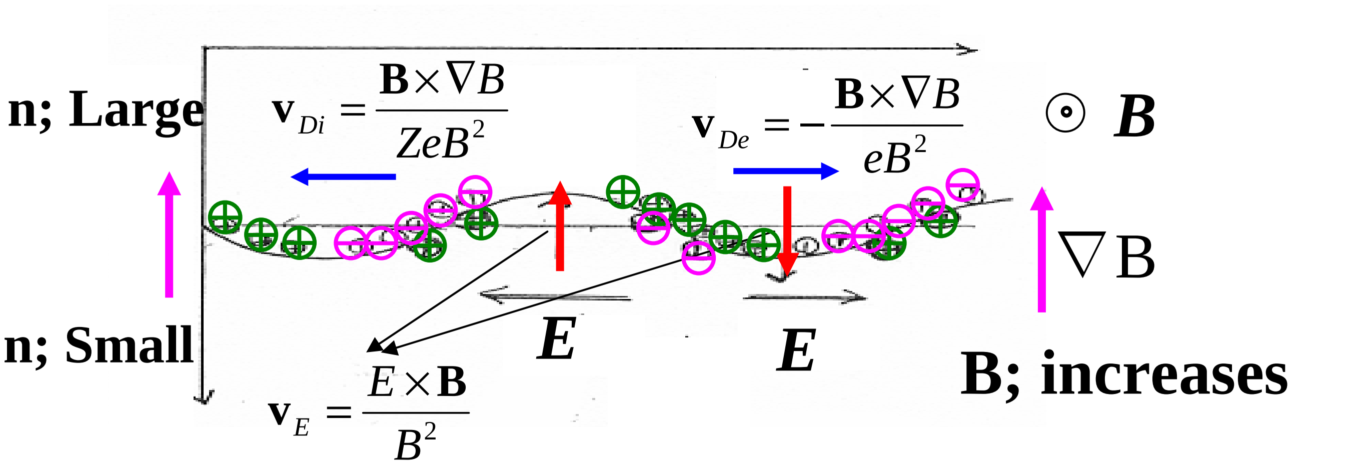

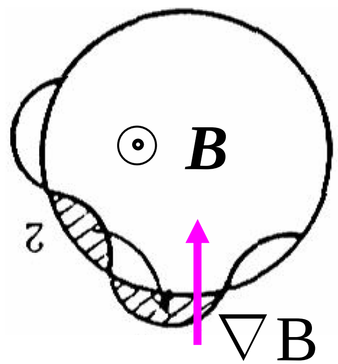

Plasma consists of a lot of charged particles (MHD equil. picture based on each particle's motion)

Basis of behavior of charged particles; Drift

Charged particle follows gyro-orbit along the magnetic field line in uniform mag. field w/o elec. field. In non-uniform mag. field and/or with elec. field, it makes the additional motion in perpendicular to mag. field (drift). This is the basis to understand the charged particle behavior.

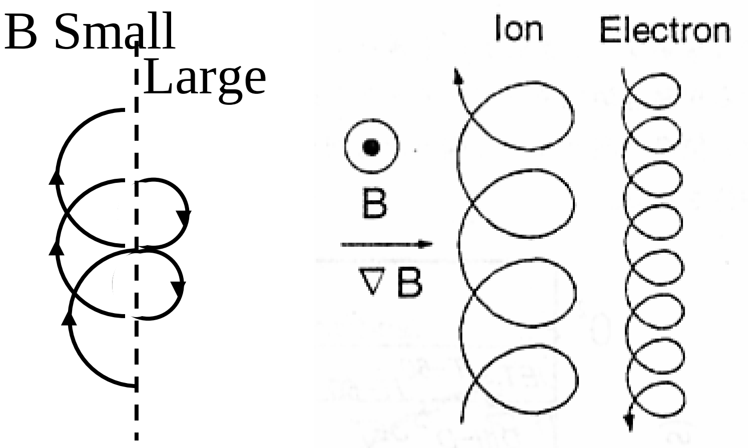

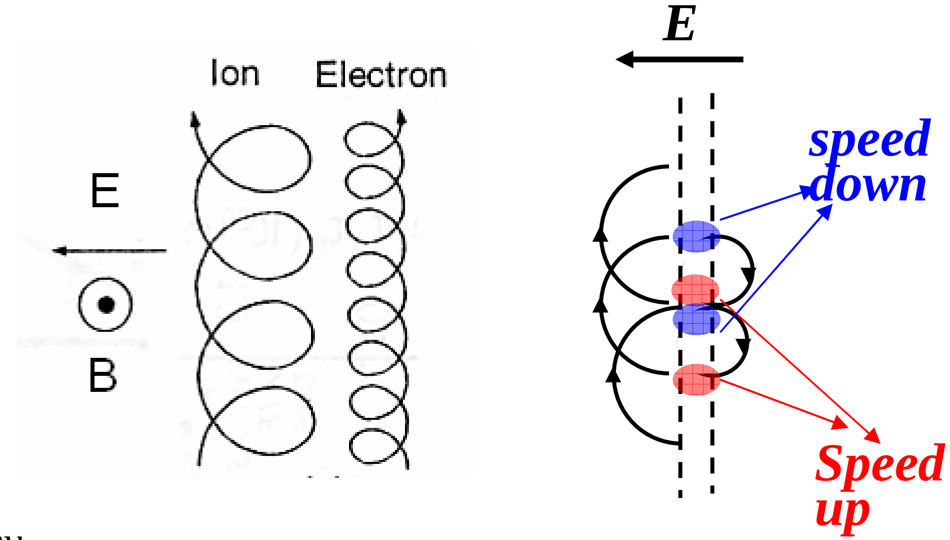

$$\frac{mv^2}{r} = qvB => r = \frac{mv}{qB}$$

Bx∇B drift

Ion moves in the direction to **Bx∇B** due to change of gyro-radius during gyro-motion.

Direction of elec. drift is opposite.

ExB drift

Ion moves in the direction to **ExB** due to change of velocity during gyro-motion.

Direction of elec. drift is same.

Physical picture of pressure driven instabilities II

Here we consider a unstable system as analogs of the pressure driven instability.

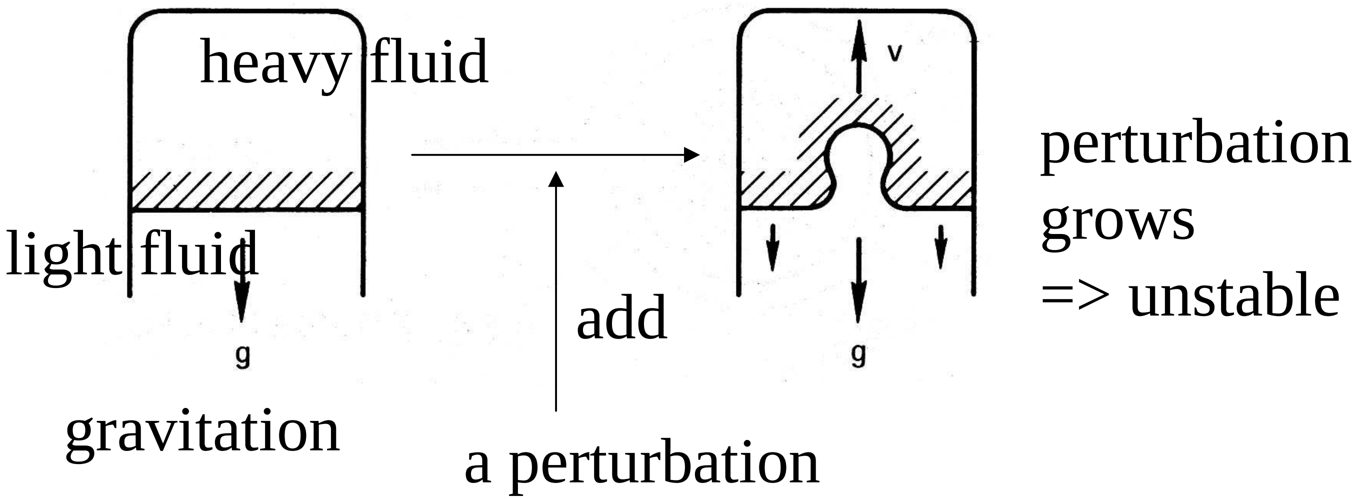

gravitational instability	*pressure driven instabilities in plasma*

destabilizing term;
gravitation and deference of weight between 2 fluids

grad B drift force (magnetic well/hill)
deference of pressure (pressure gradient)

stabilizing term;
Nothing

field line bending (magnetic shear)

Physical picture of pressure driven instabilities III

Charge separation due to **E**x**B** drift enhances density perturbation

In the rational surface resonated with the wave number of dens. fluc., separated charges cannot be canceled.
=> Den. fluc. with resonated wave numbers grows.
(Unstable)

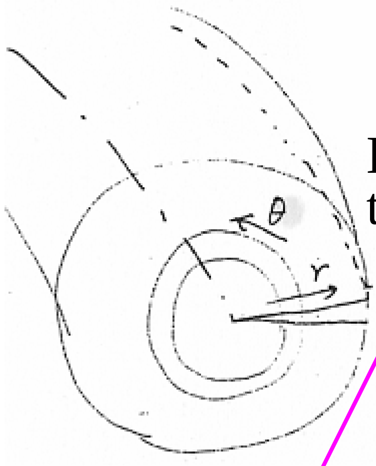

Expands to slab.

Rational surface resonated with dens. fluc.

Rotational transform (pitch of mag. field line winding) = m/n
=>
When mag. field line turns toroidally n times, it turns poloidally m times.

Wave number of m and n (toroidal and ploidal mode num.)
=>
When fluc. goes around toroidally n times, it turns poloidally m times, min. and max. of the amp. of fluc. coincides each other before and after.

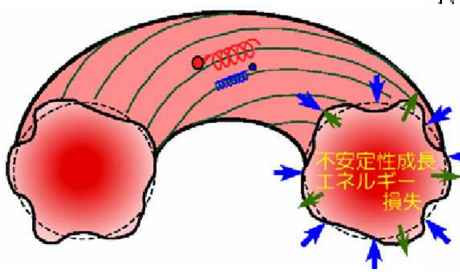

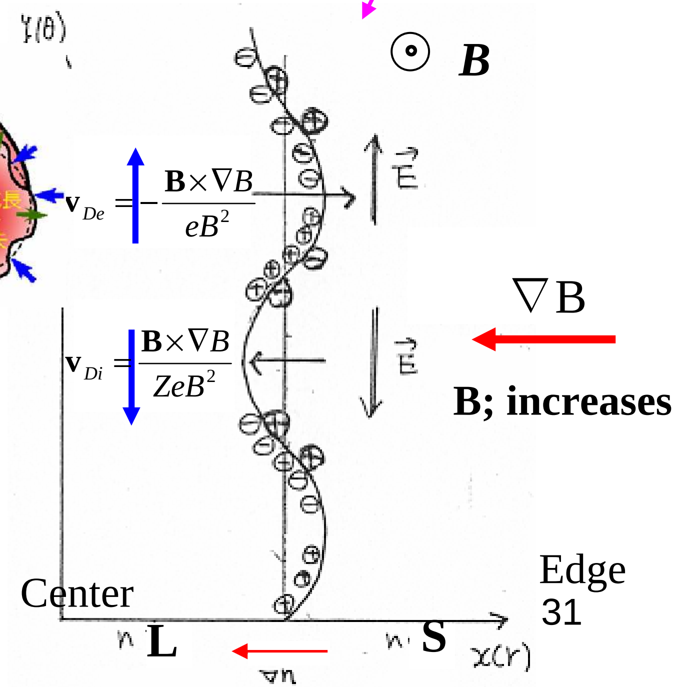

Physical picture of pressure driven instabilities IV

The effect of the magnetic field shear in the radila direction on the ideal interchange mode

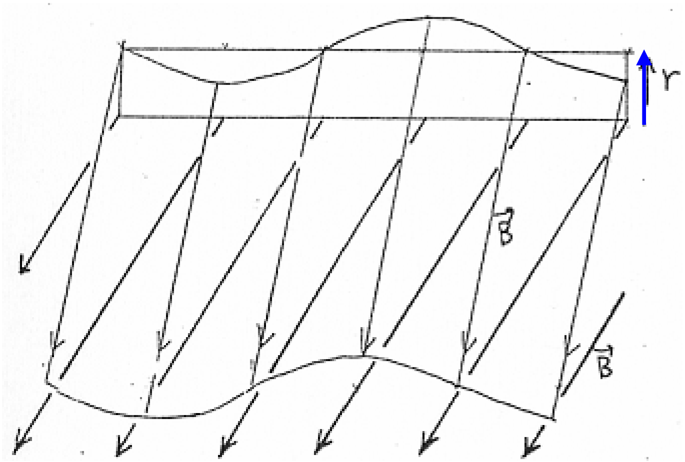

Minor radial outward direction

In order that the perturbation grows over the resonant surface, it is necessary to bend the magnetic field line so that it makes the direction of the field line same with that of the resonant surface.

Unless it bends the field line, the electron motion on the next surfaces cancels the separated charges for the ExB drift.

rational surface; ι=*n*/*m*.
ι; rotational transform =1/*q*.
n, *m; integer*.

➔
Mag. shear has the stabilizing effet.

The electron moving on a rational surface returns to the exact same position after *n* toroidal turns.
There the charge cancellation due to the electron does not occurs for the resonant modes

Physical picture of pressure driven instabilities V

What is the effect of resistive in pressure driven instability?

Hint!

Charge separation due to **E**x**B** drift enhances density perturbation

In the rational surface resonated with the wave number of dens. fluc., separated charges cannot be canceled.
=> Den. fluc. with resonated wave numbers grows. (Unstable)

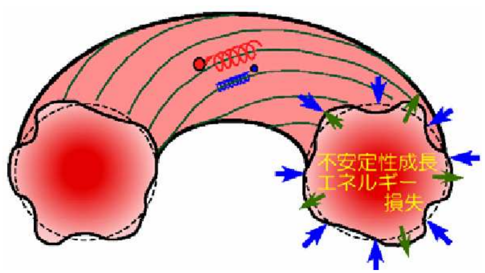

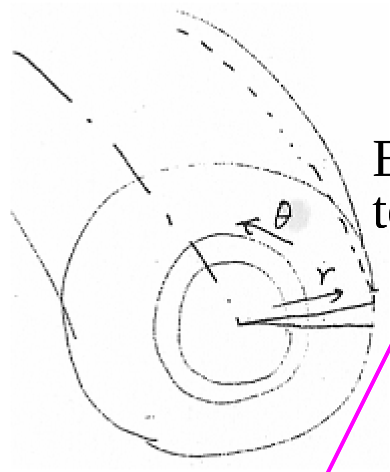

Expands to slab.

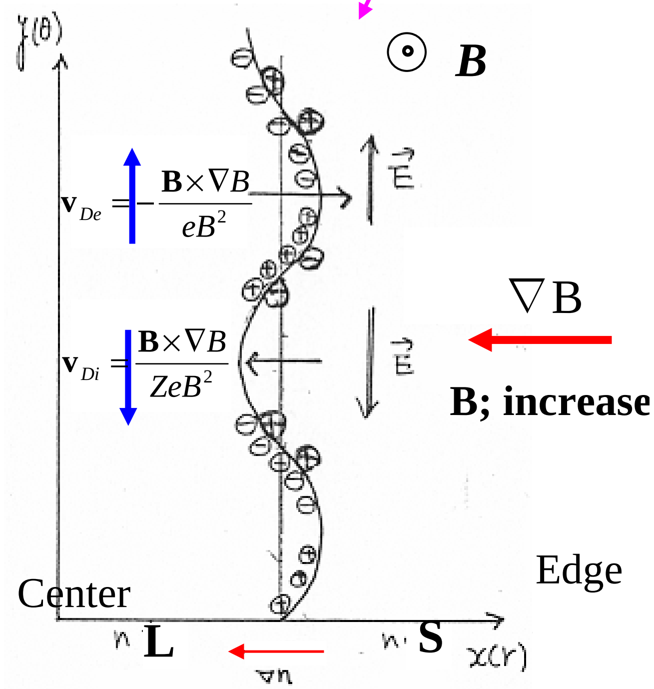

---MHD stability analysis?---

Here we consider several possible mechanical system as analogs of the MHD stability.

In Fig.(a), if the ball is moved a small distance from equilibrium position, it simply oscillates around this point. Even though the ball neverreturns to rest at its equilibrium position, this status is “stable”. In Fig.(b), a small perturbation off the top of the hill sets the ball rolling further away from its equilibrium position, this status is “unstable”.

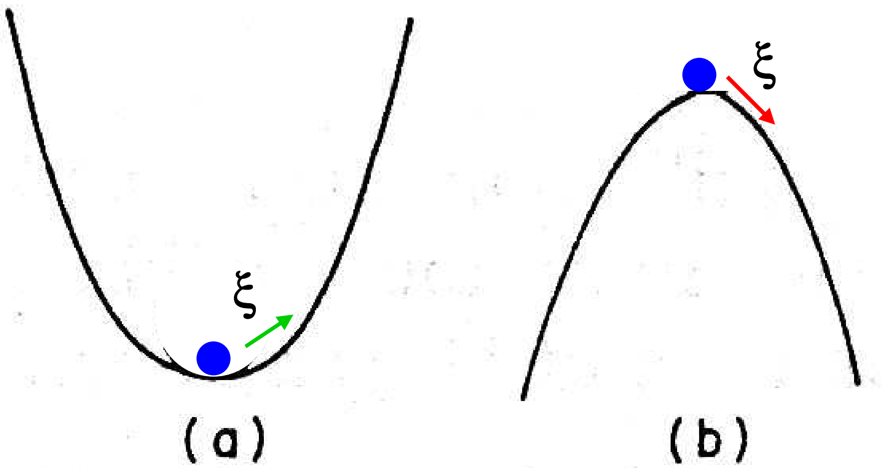

There are two methods to analyze the MHD stability.
(1) Analyzing the time evolution of the displacement, ξ, in MHD equations, especially momentum equation.
(2) Analyzing the change of the potential energy when a displacement occurs. Since the total energy is conserved in the frictionless system, when the kinetic energy increases, the potential energy decreases. When the potential energy decreases, the system is unstable.

Here only linear stabilities are considered.

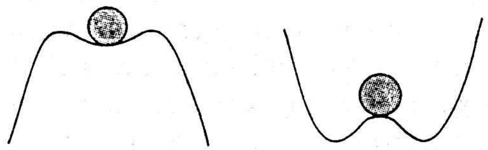

linearly stable / non-linearly unstable   linearly unstable / non-linearly stable

Linearized MHD Eq. I

Starting from ideal MHD equations

$$\rho\left(\frac{\partial}{\partial t}+\mathbf{v}\cdot\nabla\right)\mathbf{v}=\mathbf{j}\times\mathbf{B}-\nabla p,$$

$$\frac{\partial\rho}{\partial t}+\nabla\cdot(\rho\mathbf{v})=0,$$

$$\left(\frac{\partial}{\partial t}+\mathbf{v}\cdot\nabla\right)\left(\frac{p}{\rho^{\gamma}}\right)=0,$$

$$\mathbf{E}+\mathbf{v}\times\mathbf{B}-0,$$

$$\nabla\times\mathbf{B}=\mu_0\mathbf{j},\quad \nabla\times\mathbf{E}=-\frac{\partial\mathbf{B}}{\partial t},\quad \nabla\cdot\mathbf{B}=0.$$

Here some quantities are linearlized (separate the equilibrium part (suffix 0) and the perturbed part (suffix 1).).

$$\mathbf{v}(\mathbf{r},t)=\mathbf{v}_0(\mathbf{r})+\mathbf{v}_1(\mathbf{r},t),\ \mathbf{v}_0(\mathbf{r})=0,\qquad \mathbf{j}(\mathbf{r},t)=\mathbf{j}_0(\mathbf{r})+\mathbf{j}_1(\mathbf{r},t),\ |\mathbf{j}_1|<<|\mathbf{j}_0|,$$

$$\mathbf{B}(\mathbf{r},t)=\mathbf{B}_0(\mathbf{r})+\mathbf{B}_1(\mathbf{r},t),\ |\mathbf{B}_1|<<|\mathbf{B}_0|,\quad \mathbf{E}(\mathbf{r},t)=\mathbf{E}_0(\mathbf{r})+\mathbf{E}_1(\mathbf{r},t),\ \mathbf{E}_0(\mathbf{r})=0,$$

$$\rho(\mathbf{r},t)=\rho_0(\mathbf{r})+\rho_1(\mathbf{r},t),\ \rho_1<<\rho_0,\qquad p(\mathbf{r},t)=p_0(\mathbf{r})+p_1(\mathbf{r},t),\ p_1<<p_0.$$

The 1st order momentum equations are as follows:

$$\rho_0\frac{\partial\mathbf{v}_1}{\partial t}=-\nabla p_1+\mathbf{j}_1\times\mathbf{B}_0+\mathbf{j}_0\times\mathbf{B}_1,\ \frac{\partial\rho_1}{\partial t}+\nabla\cdot(\rho_0\mathbf{v}_1)=0,$$

$$\frac{\partial p_1}{\partial t}=-\mathbf{v}_1\cdot\nabla p_0-\gamma p_0\nabla\cdot\mathbf{v}_1,\ \mathbf{E}_1+\mathbf{v}_1\times\mathbf{B}_0=0,$$

$$\nabla\times\mathbf{B}_1=\mu_0\mathbf{j}_1,\quad \nabla\times\mathbf{E}_1=-\frac{\partial\mathbf{B}_1}{\partial t},\quad \nabla\cdot\mathbf{B}_1=0.$$

Linearized MHD Eq. II

Summarizing the above equations,

$$\rho_0 \frac{\partial^2 \mathbf{v}_1}{\partial t^2} = -\nabla\{\mathbf{v}_1 \cdot \nabla p_0 + \gamma p_0 \nabla \cdot \mathbf{v}_1\}_1 + \mathbf{j}_0 \times \{\nabla \times (\mathbf{v}_1 \times \mathbf{B}_0)\} + \frac{1}{\mu_0}[\nabla \times \{\nabla \times (\mathbf{v}_1 \times \mathbf{B}_0)\}] \times \mathbf{B}_0.$$

When $\mathbf{v}_1$ replaces a Lagrangian valiable, $\partial \xi / \partial t$,

$$\rho_0 \frac{\partial^2 \boldsymbol{\xi}}{\partial t^2} = \mathbf{F}(\boldsymbol{\xi}),$$

$$\mathbf{F}(\boldsymbol{\xi}) \equiv -\nabla\{\boldsymbol{\xi} \cdot \nabla p_0 + \gamma p_0 \nabla \cdot \boldsymbol{\xi}\} + \frac{1}{\mu_0}(\nabla \times \mathbf{B}_0) \times \mathbf{Q} + \frac{1}{\mu_0}(\nabla \times \mathbf{Q}) \times \mathbf{B}_0.$$

where $\mathbf{Q} \equiv \nabla \times (\boldsymbol{\xi} \times \mathbf{B}_0).$

In the linear stability analysis, the followin expression of the time evolution of the perturbation is useful,

$$\boldsymbol{\xi}(\mathbf{r}, t) = \boldsymbol{\xi}_\omega(\mathbf{r}) \exp(-\mathrm{i}\omega t).$$ If ω is imaginary, the mode grows (unstable).

Then $$-\rho_0 \omega^2 \boldsymbol{\xi} = \mathbf{F}(\boldsymbol{\xi}).$$

Here it should be noticed that $\mathbf{F}$ is a self-adjoint operator, $\int dV \mathbf{x} \cdot \mathbf{F}(\mathbf{y}) = \int dV \mathbf{y} \cdot \mathbf{F}(\mathbf{x}).$

$$\frac{1}{2}\rho_0 \omega^2 \int \mathrm{d}V \boldsymbol{\xi}^* \boldsymbol{\xi} = -\frac{1}{2}\int \mathrm{d}V \boldsymbol{\xi}^* \mathbf{F}(\boldsymbol{\xi}),\ \frac{1}{2}\rho_0 \omega^{*2} \int \mathrm{d}V \boldsymbol{\xi}\boldsymbol{\xi}^* = -\frac{1}{2}\int \mathrm{d}V \boldsymbol{\xi}\mathbf{F}(\boldsymbol{\xi}^*).$$

$$\Rightarrow \frac{1}{2}\rho_0 \omega^2 \int \mathrm{d}V \boldsymbol{\xi}^* \boldsymbol{\xi} = \frac{1}{2}\rho_0 \omega^{*2} \int \mathrm{d}V \boldsymbol{\xi}\boldsymbol{\xi}^* \Rightarrow \omega^2 = \omega^{*2}.$$ => ω^2 should be real.

Here * denotes a complex conjugate.

Linearized MHD Eq. III

$$\frac{1}{2}\rho_0\omega^2\int dV\xi^*\xi = -\frac{1}{2}\int dV\xi^*\mathbf{F}(\xi) \Rightarrow \mathrm{K} \equiv \frac{1}{2}\rho_0\int dV\xi^*\xi,\ \delta\mathrm{W} \equiv -\frac{1}{2}\int dV\xi^*\mathbf{F}(\xi).$$

$$\Rightarrow \omega^2\mathrm{K} = \delta\mathrm{W}.$$

$$\Rightarrow \omega^2 = \frac{\delta\mathrm{W}}{\mathrm{K}}.$$

Because K is positive, the sign of δW determines the stability of the system.
$\delta W>0$ => stable. $\delta W<0$ => unstable.
Here K and δW correspond to the kinetic energy and the potential energy.
After some calculations, δW is rewritten as

$$\delta W = \frac{1}{2}\int_{plasma} dV\left[\gamma p_0(\nabla\cdot\xi)^2 + (\xi\cdot\nabla p_0)(\nabla\cdot\xi) + \frac{|\mathbf{Q}|^2}{\mu_0} + \mathbf{j}_0(\mathbf{Q}\times\xi)\right].$$

$$-\xi\cdot(\mathbf{j}_0\times\mathbf{B}_1)$$

Change of the internal energy of plasma without magnetic energy

Change of the magnetic energy

Work against the unbalanced magnetic force

Linearized MHD Eq. IV

$$\delta W = \frac{1}{2}\int_{plasma} \mathrm{d}V \left[\frac{|\mathbf{Q}_\perp|^2}{\mu_0} + \frac{B_0{}^2}{\mu_0}|\nabla\cdot\xi_\perp + 2\xi_\perp\cdot\boldsymbol{\kappa}|^2 + \gamma p_0(\nabla\cdot\xi)^2 - 2(\xi_\perp\cdot\nabla p_0)(\xi_\perp\cdot\boldsymbol{\kappa}) - \mathbf{j}_{//}\cdot(\mathbf{Q}_\perp\times\xi_\perp) \right]$$

shear alfven wave
(line bending term)

$(k_\perp a)^2(k_{//}a)^2$

sound wave of plasma

compressional alfven wave

stabilizing term

current driven
destabilizing term

$(k_\perp a)(k_{//}a)$

pressure driven
destabilizing term

$(k_\perp a)^2$

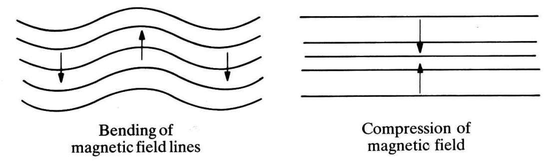

When the mode is localized $k_\perp a >> 1$,
pressure driven modeis dominant.

Current driven mode;
The global mode is more easily
unstable than the localized mode.
$k_\perp a \sim 1$

Ideal Interchange mode I ---Reduced MHD equation---

When the high aspect approximation ($\varepsilon = a/R_0 << 1$) and the high beta ordering ($\beta \sim \varepsilon$) are applied to the full MHD equations, in a quasi toroidal coordinates, (r, θ, φ), the following reduced MHD equation is obtained. [ξ =***grad*** U x **z** ($\xi = mU/r\omega$)]

$$\frac{\partial \psi}{\partial t} = \mathbf{B}\cdot\nabla U, \quad \left(\frac{\partial}{\partial t} + \mathbf{B}\cdot\nabla\right) p = 0, \quad \rho\left(\frac{\partial}{\partial t} + \mathbf{v}\cdot\nabla\right)\nabla_\perp{}^2 U = -\mathbf{B}\cdot\nabla j_\varphi - \hat{\varphi}\times\boldsymbol{\kappa}_r\cdot\nabla p.$$

Here $R = R_0 + r\cos\theta$, R_0; major radius, $r = a$; minor radius. and are the poloidal flux and a stream function, respectively. And

$$\mathbf{B} = B_0\hat{\varphi} + \nabla\psi\times\hat{\varphi}, \quad \mathbf{v} = \nabla U\times\hat{\varphi}, \quad j_\varphi = -\nabla_\perp{}^2 A_\varphi, \quad \psi = A_\varphi + \psi_V(r,\theta), \quad \boldsymbol{\kappa}_r = -\nabla\Omega, \quad \Omega = \frac{r}{R_0} + \Omega_V(r,\theta).$$

ψ_V, and Ω_V are the averaged vacuum poloidal flux and the vacuum magnetic curvature potential, respectively, which are zero for tokamaks, and non-zero for heliotron.

The potential energy based on reduced MHD equation is as the following;

$$\delta W(\xi,\xi) = \frac{1}{2}\int_{V_p} \mathrm{d}r \left[\left|\mathbf{Q}_\perp\right|^2 - 2(\xi_\perp\cdot\nabla p)(\boldsymbol{\kappa}_r\cdot\xi_\perp) - j_\varphi(\xi_\perp\times\hat{\varphi})\cdot\mathbf{Q}_\perp\right]$$

The terms with the compressional alfven wave and the magnetic sound wave disappear. Here $\xi_\perp = \nabla_\perp U\times\hat{\varphi}, \quad \mathbf{Q}_\perp = \nabla_\perp(\mathbf{B}\cdot\nabla U)\times\hat{\varphi}.$

Ideal Interchange mode II ---Sydum Criterion---

In order to linearlize Eqs.(1), we assume $U = \tilde{U}(r,\theta,\varphi),\quad p = p_0 + \tilde{p}(r,\theta,\varphi),\quad A_\varphi = A_0 + \tilde{A}(r,\theta,\varphi)$
and
$$\{\tilde{U}, \tilde{p}, \tilde{A}\} = \{\hat{U}, \hat{p}, \hat{A}\}\exp[\mathrm{i}(m\theta - n\varphi) - \mathrm{i}\omega t].$$

The following eigenmode equation for U is derived in the cylinder geometry,

$$\omega^2\left(\frac{1}{r}\frac{\mathrm{d}}{\mathrm{d}r}r\frac{\mathrm{d}}{\mathrm{d}r} - k_\theta{}^2\right)\hat{U} = \omega k_{//}\left(\frac{1}{r}\frac{\mathrm{d}}{\mathrm{d}r}r\frac{\mathrm{d}}{\mathrm{d}r} - k_\theta{}^2\right)\left(\frac{k_{//}\hat{U}}{\omega}\right) + k_\theta{}^2 p_0'\Omega'\hat{U}$$

where $k_{//}=m\iota-n$, $k_\theta=m/r$ and primes denote the derivative with respect to r.
In order to analyze the radially localized mode in the neighborhood of a resonant surface, the following relations are used; $x=r-r_0$, $k_{//}=k_{//}'x$, $k_{//}'=m\iota'|_{r=r0}$.

$$\frac{\mathrm{d}^2}{\mathrm{d}r^2}\hat{U} - \left\{\frac{k_{\theta 0}{}^2 p_0'\Omega'}{k'_{//}{}^2} + k_{\theta 0}{}^2\right\}\hat{U} = 0$$

The solution of U is assumed as $U \sim x^\nu$. U crosses 0 around x=0 infinite times when $-k_{\theta 0}{}^2 p_0'\Omega' / k'_{//}{}^2 > 1/4$.
According to Sydum, when U crosses 0 without boundaries, the system is always unstable. Then $-\dfrac{p_0'\Omega'}{r^2} > \dfrac{1}{4}\iota'^2$ is a sufficient condition of the localized instabilities.

Mercier criterion corresponds to the extended Sydum criterion to the toroidal system.

Ideal Interchange mode III ---Relationship between the Sydum criterion and global mode stability---

Generally speaking, the global mode is stable even that the sydum's criterion is unstable. Why the global mode is stable there nevertheless sydum's criterion is a sufficient condition of the instability?

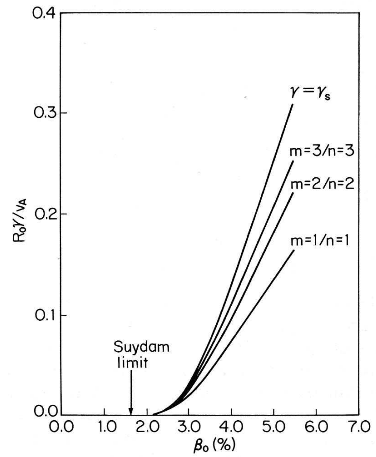

The mode width of the interchange mode becomes narrower as the growth rate decreases.
Usually the stability analysis is calculated with finite mesh size. Then the only unstable modes with finite size and finite growth rate can be analyzed. The sydum's criterion corresponds to the instability condition for the limit of the radially localized mode.

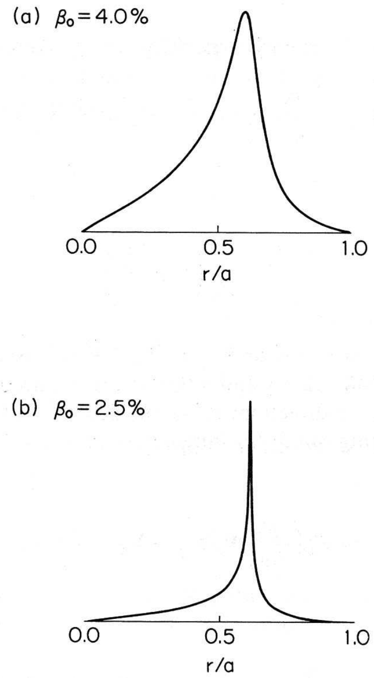

Caution!!
The stability limit of the global unstable mode depends on the calculation mesh size especially in the interchange mode.

M.Wakatani; Chap.5.6 in "Stellarator and Heliotron devices", Oxford (1998).

Ideal Interchange mode IV ---Example of the mode structure and growth rate of the interchange mode---

$\xi = mU/r\omega,$

$\boldsymbol{\xi} = \mathbf{grad}\ U \times \mathbf{z}$

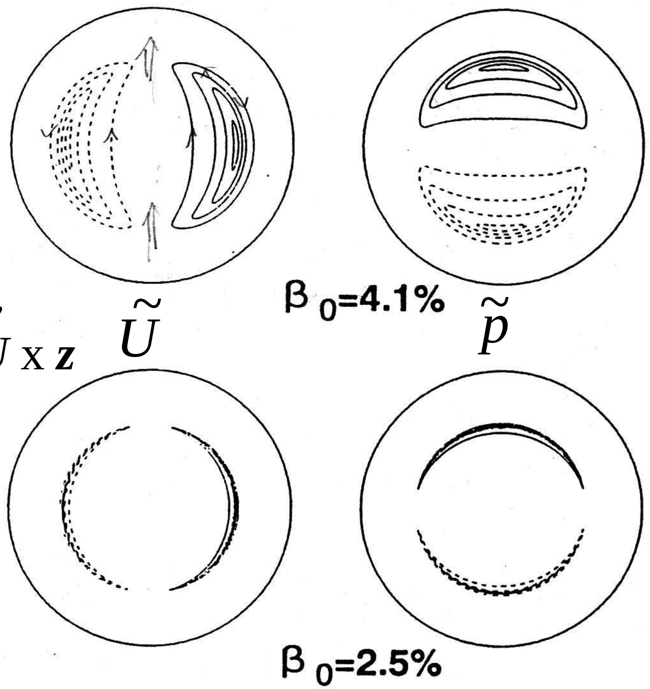

$$\tilde{p} = k_\theta p_0' \tilde{U} \big/ \omega$$

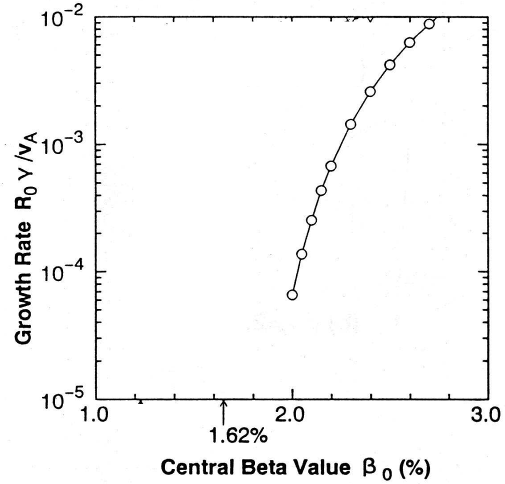

K.Watanabe; Nuclear Fusion 32, 1647 (1992).

Because w is a imaginary, the difference of the phase between U and p is $\pi/2$.

Index of lecture

1. Introduction of MHD Jan. 5

2. MHD equilibrium Jan. 5

3. Pressure driven MHD instabilities
   Interchange mode Jan. 12
   Ballooning mode Jan. 19

4. Current driven MHD instabilities Jan. 19

5. Hot topics of MHD equilibrium and instability
   Jan. 27

磁力線の曲率と磁場強度の強弱

$\nabla \cdot B=0$(磁力線は閉じるという性質)より、磁力線の曲率が凸に曲がっている方向に，磁場強度は弱まる。

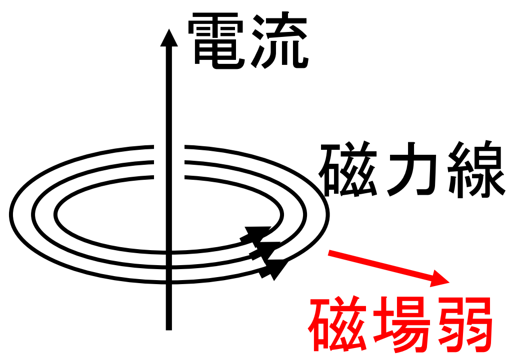

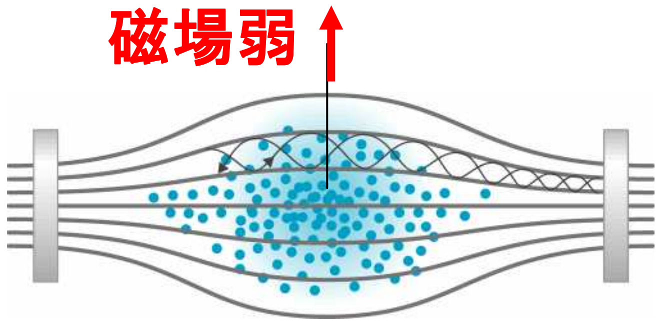

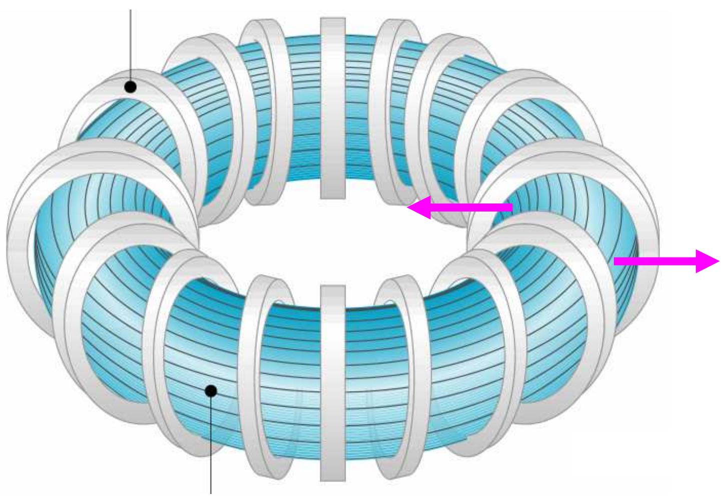

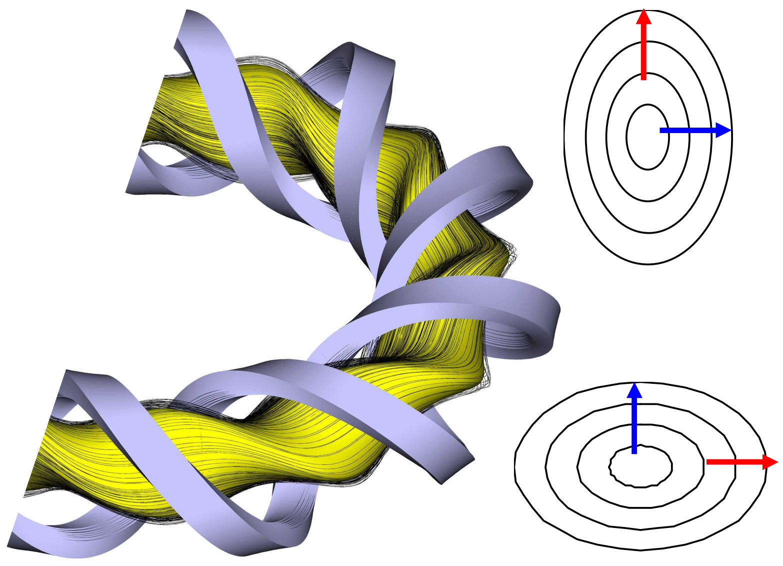

環状磁場プラズマでの交換型MHD不安定特性 II

環状磁場プラズマ閉じ込め装置では、ドーナッツの内、外で磁場の曲率が異なる

=>

悪い曲率での不安定性の発現

=>

磁気面上で不均一な不安定性 (バルーニングモード)

バルーニングの前に、あるところでよい曲率で、あるところで悪い曲率である場合、まず何が起こるか????の導入要

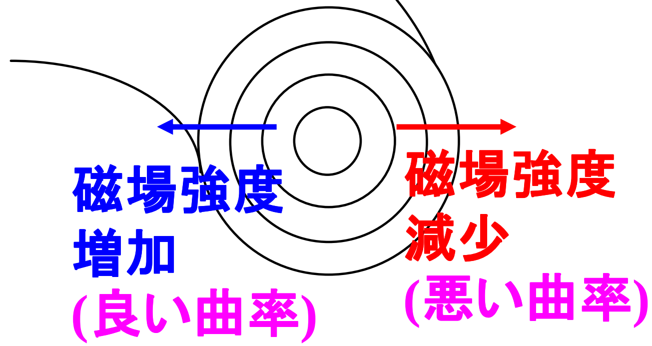

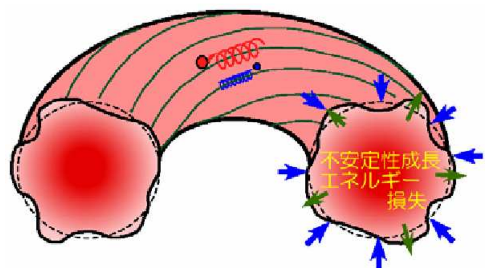

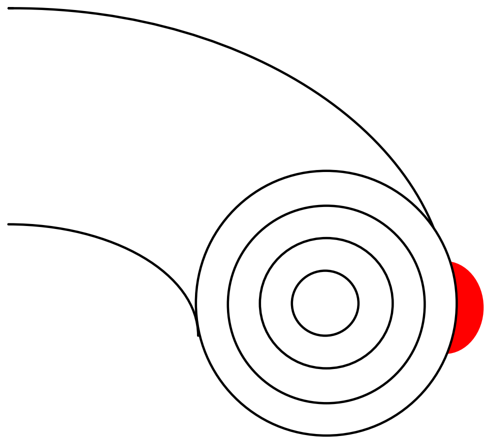

Pressure driven instabilities in torus plasmas

magnetic hill and well

minor radial direction

When mag. flux averaged ∇B is negative (positive), it is magnetic hill (well) config.

∇B is locally negative (positive).=> bad (good) curvature.

1. Tokamaks

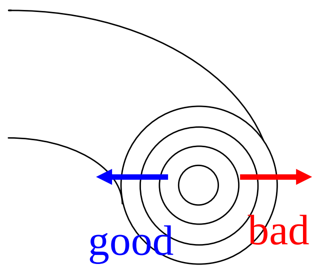

Mag. axis torus-outwardly shifted case

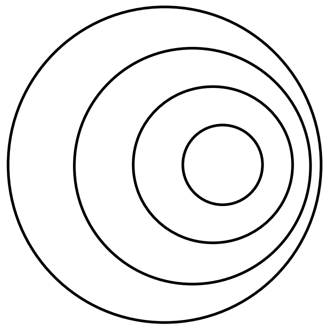

2. "Straight" heliotron

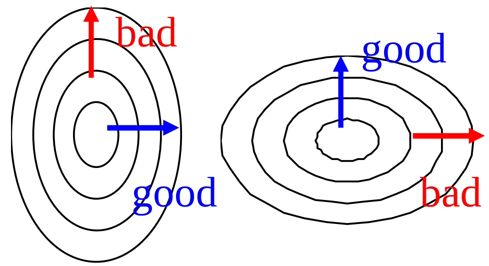

Well/Hill depends on the relative location between 2 neighboring surfaces.

The averaging location of the mag. surf. is more torus inward as the minor radius increases.
=> The averaged B of mag. surf. increases as the larger minor radius .

Averaged B of mag.surf. decreases as the larger minor radius.

=> ***Mag. Well.***

Characteristics MHD equil. related to stability in LHD

Straight stellarator's mag. field is expressed as the followings.

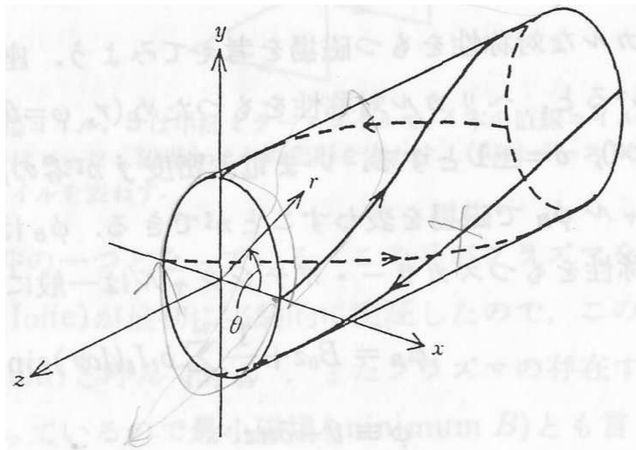

$$\mathbf{B} = \mathbf{B}_h + B_0\mathbf{z} = \nabla\Phi + B_0\mathbf{z}$$

(helical field by l pair of helical coils + constant toridal field)

Mag. field by helical coils is expressed by a scalar potential Φ

$$\boxed{\Phi = \sum_{l=1}^{l=\infty} \Phi_l(r) I_l(lMr/R_0)\sin(l\theta - Mz/R_0)}$$

In torus, M; toridal pitch number, R_0; plasma majior radius, $\phi = z/R_0$ (toroidal angle)

Here mag. flux due to helical coil, ψ_h, is introduced.

$$\boxed{\psi_h = -\frac{1}{2B_0}\sum_{l,m}\Phi_l(r)\Phi_m(r)\frac{m}{r}I_l^{'}(lMr/R_0)I_m(lMr/R_0)\cos((l-m)\theta)}$$

By using , averaged mag. field strength and rotational transform are expressed

$$\Omega \equiv \frac{B^2}{B_0^{\,2}} = \frac{\left|\nabla\Phi\right|^2}{B_0^{\,2}} = -\frac{M}{lR_0B_0}\frac{1}{r}\frac{\mathrm{d}}{\mathrm{d}r}\left(r^2\psi_h\right), \quad \text{and} \quad \iota_h = -\frac{R_0}{rB_0}\frac{\mathrm{d}\psi_h}{\mathrm{d}r}.$$

$$\boxed{\Rightarrow \quad \frac{\mathrm{d}\Omega}{\mathrm{d}r} = -\frac{M}{lR_0^{\,2}}\frac{1}{r^2}\frac{\mathrm{d}}{\mathrm{d}r}\left(r^4\iota_h\right).}$$

When $d\iota_h/dr > 0$,
=> Magnetic hill structure.

M.Wakatani et al, Phys. Fluids 29, 905 (1986).

Characteristics MHD equil. related to stability in LHD II

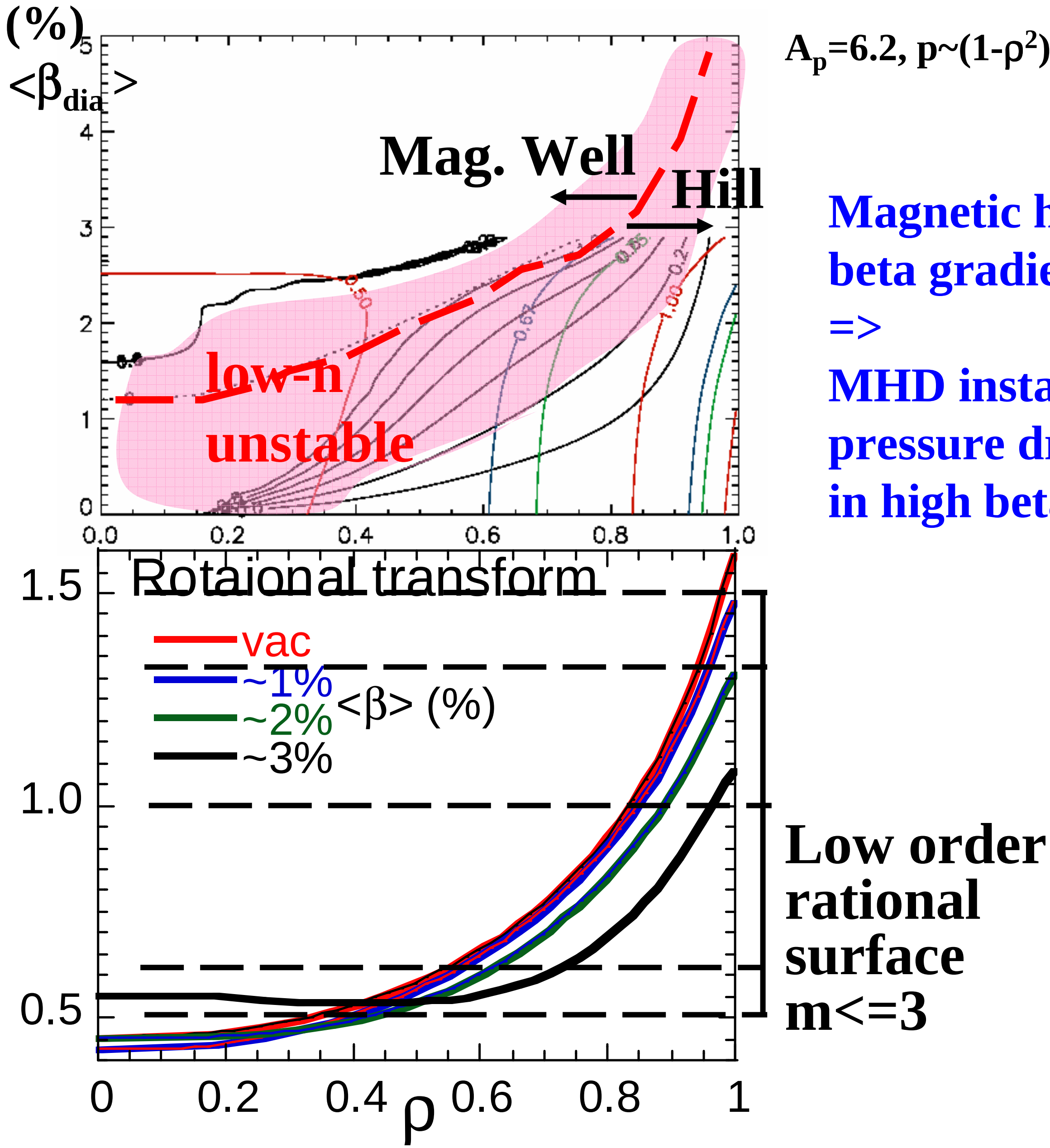

A_p=6.2, p~$(1-\rho^2)(1-\rho^8)$

Magnetic hill exists in the finite beta gradients region

=>

MHD instabilities (interchange/ pressure driven) would appear in high beta regime.

Observation of the mode structure of the interchange mode in LHD

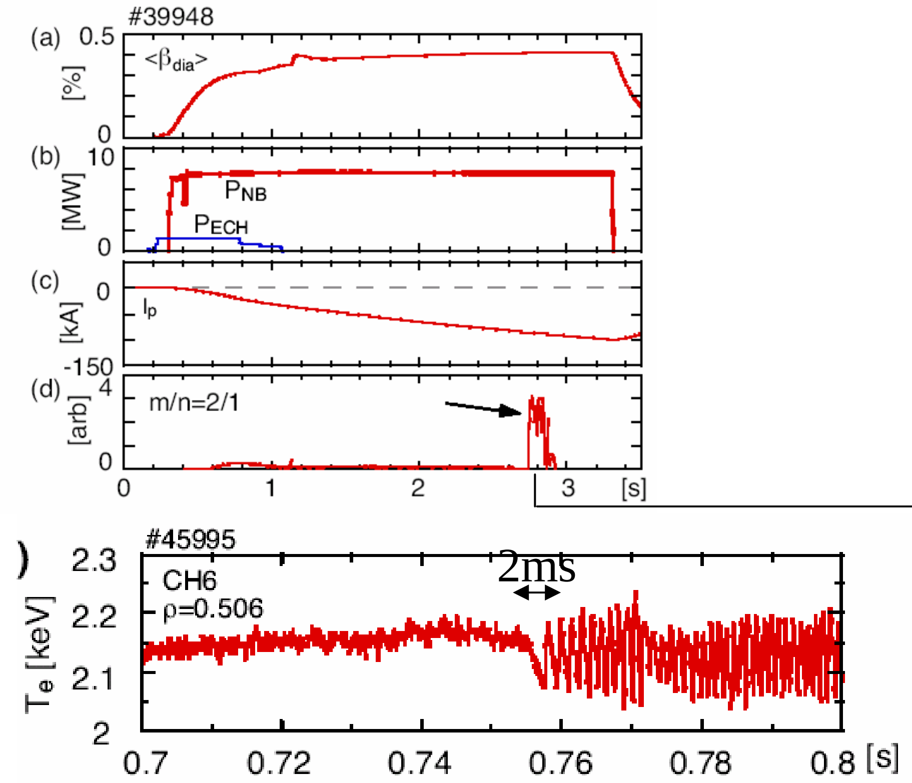

Evolution of the ECE perturbation

Toroidal Alfven freq. ~5.3x10^{6}Hz @2.75T, n_e=10^{19}m^{-3}, R_0=3,6m

According to theoretical prediction, the growth rate is around ~1.6x10^{4}Hz (63μs).

There is discrepancy between the prediction and observation in the growth rate.

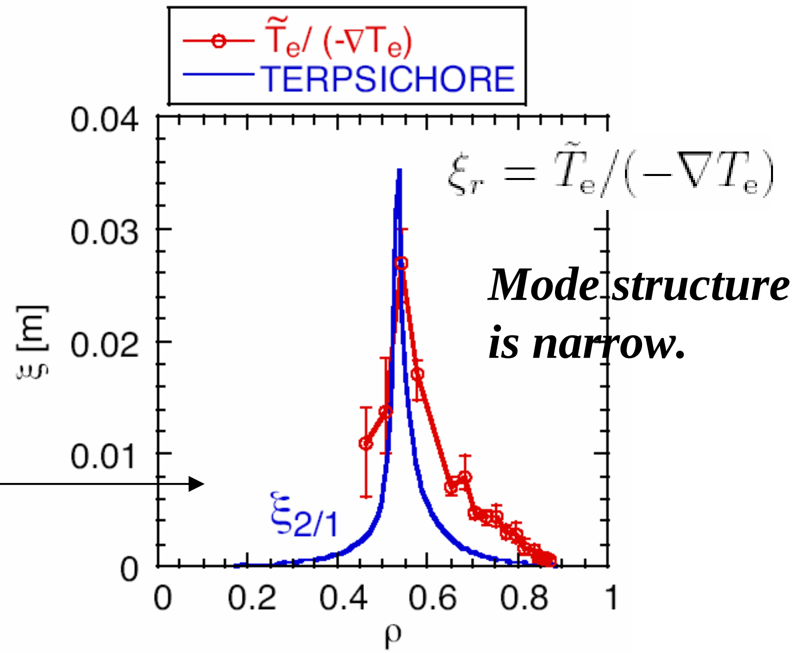

Profile of the radial displacement by ECE measurement and theoretical prediction

The prediction of the ideal interchange mode is quite consistent with the observation on the mode structure.

A.Isayama et al; Plasma Phys. Contr. Fus. to be published (2005).

Reduced MHD Equation

$$\rho\left(\frac{\partial}{\partial t}+\mathbf{v}\cdot\nabla\right)\mathbf{v}=\mathbf{j}\times\mathbf{B}-\nabla p,$$

Motion eq.

$$\frac{\partial\rho}{\partial t}+\nabla\cdot(\rho\mathbf{v})=0,\qquad\left(\frac{\partial}{\partial t}+\mathbf{v}\cdot\nabla\right)p=0,$$

Eq. of continuity and state for γ=0

$$\frac{\partial\mathbf{B}}{\partial t}=-\nabla\times\mathbf{E},\quad\nabla\times\mathbf{B}=\mu_0\mathbf{j},\quad\nabla\cdot\mathbf{B}=0,\quad\mathbf{E}+\mathbf{v}\times\mathbf{B}=0\quad(\eta\mathbf{j}),$$

Ohm's low Maxwell eq.

Here some quantities are linearlized (separate the equilibrium part (suffix 0) and the perturbed part (suffix 1).).

$$\mathbf{v}(\mathbf{r},t)=0+\mathbf{v}_1(\mathbf{r},t),\qquad\mathbf{j}(\mathbf{r},t)=\mathbf{j}_0(\mathbf{r})+\mathbf{j}_1(\mathbf{r},t),\left|\mathbf{j}_1\right|<<\left|\mathbf{j}_0\right|,$$
$$\mathbf{B}(\mathbf{r},t)=\mathbf{B}_0(\mathbf{r})+\mathbf{B}_1(\mathbf{r},t),\left|\mathbf{B}_1\right|<<\left|\mathbf{B}_0\right|,\quad\mathbf{E}(\mathbf{r},t)=0+\mathbf{E}_1(\mathbf{r},t),$$
$$\rho(\mathbf{r},t)=\rho_0(\mathbf{r})+\rho_1(\mathbf{r},t),\,\rho_1<<\rho_0,\qquad p(\mathbf{r},t)=p_0(\mathbf{r})+p_1(\mathbf{r},t),\,p_1<<p_0.$$

The 1st order momentum equations are as follows:

$$\rho_0\frac{\partial\mathbf{v}_1}{\partial t}=-\nabla p_1+\mathbf{j}_1\times\mathbf{B}_0+\mathbf{j}_0\times\mathbf{B}_1,$$
$$\frac{\partial\rho_1}{\partial t}+\nabla\cdot(\rho_0\mathbf{v}_1)=0,\quad\frac{\partial p_1}{\partial t}=-\mathbf{v}_1\cdot\nabla p_0-\gamma p_0\nabla\cdot\mathbf{v}_1,$$
$$\mathbf{E}_1+\mathbf{v}_1\times\mathbf{B}_0=\mu\mathbf{j}_1,$$
$$\frac{\partial\mathbf{B}_1}{\partial t}=-\nabla\times\mathbf{E}_1,\quad\nabla\times\mathbf{B}_1=\mu_0\mathbf{j}_1,\quad\nabla\cdot\mathbf{B}_1=0.$$

$$\boxed{\begin{aligned}&\rho_0\frac{\partial\mathbf{v}_1}{\partial t}=-\nabla p_1+\mathbf{j}_1\times\mathbf{B}_0+\mathbf{j}_0\times\mathbf{B}_1,\\&\frac{\partial\rho_1}{\partial t}+\nabla\cdot(\rho_0\mathbf{v}_1)=0,\quad\frac{\partial p_1}{\partial t}=-\mathbf{v}_1\cdot\nabla p_0,\\&\frac{\partial\mathbf{B}_1}{\partial t}=\nabla\times(\mathbf{v}_1\times\mathbf{B}_0-\eta\nabla\times\mathbf{B}_1),\quad\nabla\cdot\mathbf{B}_1=0.\end{aligned}}$$

Reduced MHD Equation II

The 1st order momentum equations are as follows:

$$\rho_0 \frac{\partial \mathbf{v}_1}{\partial t} = -\nabla p_1 + \mathbf{j}_1 \times \mathbf{B}_0 + \mathbf{j}_0 \times \mathbf{B}_1,$$
$$\frac{\partial \rho_1}{\partial t} + \nabla \cdot (\rho_0 \mathbf{v}_1) = 0, \quad \frac{\partial p_1}{\partial t} + \mathbf{v}_1 \cdot \nabla p_0 = 0,$$
$$\frac{\partial \mathbf{B}_1}{\partial t} = \nabla \times (\mathbf{v}_1 \times \mathbf{B}_0 - \eta \nabla \times \mathbf{B}_1), \quad \nabla \cdot \mathbf{B}_1 = 0.$$

Here $\nabla \cdot \mathbf{v}_1 = 0$ is assumed. $\dfrac{\partial \rho_1}{\partial t} + \mathbf{v}_1 \cdot \nabla \rho_0 = 0.$

Here $\nabla \cdot (\mathbf{B} \times)$ for 1st eq., and by using $\nabla \cdot \mathbf{v}_1 = 0$ and $\nabla \cdot \mathbf{B}_1 = 0$.

$$\mathbf{B} \cdot \frac{\rho_0}{B_0^2} \nabla \times \frac{\partial \mathbf{v}_1}{\partial t} = (\mathbf{B} \cdot \nabla) \frac{\mathbf{j}_1 \cdot \mathbf{B}_0}{B_0^2} + \mathbf{B} \cdot \frac{\nabla B_0^2 \times \nabla p_1}{B_0^4},$$
$$\frac{\partial p_1}{\partial t} + \mathbf{v}_1 \cdot \nabla p_0 = 0.$$
$$\frac{\partial \mathbf{B}_1}{\partial t} = (\mathbf{B}_0 \cdot \nabla)\mathbf{v}_1 - (\mathbf{v}_1 \cdot \nabla)\mathbf{B}_0 + \eta \nabla^2 \mathbf{B}_1.$$

$\eta = 0$, $\mathbf{v}_1 = \nabla U \times \vec{\varphi}$, and $\mathbf{B}_1 = \nabla \psi_1 \times \vec{\varphi}$ are assumed. $\mathbf{B}_0 = B_0 \vec{\varphi} + \nabla \psi_0 \times \vec{\varphi}$, $j_\varphi = -\nabla_\perp^2 (\psi - \psi_V(r,\theta))$, $\psi = \psi_0 + \psi_1$.

$$\frac{\partial \psi}{\partial t} = \mathbf{B} \cdot \nabla U, \quad \left(\frac{\partial}{\partial t} + \mathbf{B} \cdot \nabla\right) p = 0, \quad \rho\left(\frac{\partial}{\partial t} + \mathbf{v} \cdot \nabla\right) \nabla_\perp^2 U = -\mathbf{B} \cdot \nabla j_\varphi - \hat{\varphi} \times \boldsymbol{\kappa}_r \cdot \nabla p.$$

Ideal Interchange mode I ---Reduced MHD equation---

When the high aspect approximation ($\varepsilon = a/R_0 << 1$) and the high beta ordering ($\beta \sim \varepsilon$) are applied to the full MHD equations, in a quasi toroidal coordinates, (r, θ, φ), the following reduced MHD equation is obtained. [ξ =***grad*** U x **z** ($\xi = mU/r\omega$)]

$$\frac{\partial \psi}{\partial t} = \mathbf{B}\cdot\nabla U,\quad \left(\frac{\partial}{\partial t} + \mathbf{B}\cdot\nabla\right)p = 0,\quad \rho\left(\frac{\partial}{\partial t} + \mathbf{v}\cdot\nabla\right)\nabla_\perp{}^2 U = -\mathbf{B}\cdot\nabla j_\varphi - \hat{\varphi}\times\boldsymbol{\kappa}_r\cdot\nabla p.$$

Here $R = R_0 + r\cos\theta$, R_0; major radius, $r = a$; minor radius. and are the poloidal flux and a stream function, respectively. And

$$\mathbf{B} = B_0\hat{\varphi} + \nabla\psi\times\hat{\varphi},\quad \mathbf{v} = \nabla U\times\hat{\varphi},\quad j_\varphi = -\nabla_\perp{}^2 A_\varphi,\quad \psi = A_\varphi + \psi_V(r,\theta),\quad \boldsymbol{\kappa}_r = -\nabla\Omega,\quad \Omega = \frac{r}{R_0} + \Omega_V(r,\theta).$$

ψ_V, and Ω_V are the averaged vacuum poloidal flux and the vacuum magnetic curvature potential, respectively, which are zero for tokamaks, and non-zero for heliotron.

The potential energy based on reduced MHD equation is as the following;

$$\delta W(\xi,\xi) = \frac{1}{2}\int_{V_p} \mathrm{d}r\left[\left|\mathbf{Q}_\perp\right|^2 - 2(\xi_\perp\cdot\nabla p)(\boldsymbol{\kappa}_r\cdot\xi_\perp) - j_\varphi(\xi_\perp\times\hat{\varphi})\cdot\mathbf{Q}_\perp\right]$$

The terms with the compressional alfven wave and the magnetic sound wave disappear. Here $\xi_\perp = \nabla_\perp U\times\hat{\varphi},\ \mathbf{Q}_\perp = \nabla_\perp(\mathbf{B}\cdot\nabla U)\times\hat{\varphi}.$

Ideal Interchange mode II ---Sydum Criterion---

In order to linearlize Eqs.(1), we assume $U = \tilde{U}(r,\theta,\varphi), \quad p = p_0 + \tilde{p}(r,\theta,\varphi), \quad A_\varphi = A_0 + \tilde{A}(r,\theta,\varphi)$
and

$$\{\tilde{U}, \tilde{p}, \tilde{A}\} = \{\hat{U}, \hat{p}, \hat{A}\}\exp[\mathrm{i}(m\theta - n\varphi) - \mathrm{i}\omega t].$$

The following eigenmode equation for U is derived in the cylinder geometry,

$$\omega^2\left(\frac{1}{r}\frac{\mathrm{d}}{\mathrm{d}r}r\frac{\mathrm{d}}{\mathrm{d}r} - k_\theta{}^2\right)\hat{U} = \omega k_{//}\left(\frac{1}{r}\frac{\mathrm{d}}{\mathrm{d}r}r\frac{\mathrm{d}}{\mathrm{d}r} - k_\theta{}^2\right)\left(\frac{k_{//}\hat{U}}{\omega}\right) + k_\theta{}^2 p_0'\Omega'\hat{U}$$

where $k_{//}=m\iota-n$, $k_\theta=m/r$ and primes denote the derivative with respect to r.
In order to analyze the radially localized mode in the neighborhood of a resonant surface, the following relations are used; $x=r-r_0$, $k_{//}=k_{//}'x$, $k_{//}'=m\iota'|_{r=r0}$.

$$\frac{\mathrm{d}^2}{\mathrm{d}r^2}\hat{U} - \left\{\frac{k_{\theta 0}{}^2 p_0'\Omega'}{k'_{//}{}^2} + k_{\theta 0}{}^2\right\}\hat{U} = 0$$

The solution of U is assumed as $U \sim x^\nu$. U crosses 0 around $x=0$ infinite times when $\quad -k_{\theta 0}{}^2 p_0'\Omega' / k'_{//}{}^2 > 1/4.$
According to Sydum, when U crosses 0 without boundaries, the system is always unstable. Then $\quad -\frac{p_0'\Omega'}{r^2} > \frac{1}{4}\iota'^2 \quad$ is a sufficient condition of the localized instabilities.

Mercier criterion corresponds to the extended Sydum criterion to the toroidal system.

Ballooning instability

When locally bad curvature exists in a magnetic flux surface, poloidally (and/or toroidally) localized pressure driven unstable mode appear there.
=> ballooning mode

Ex. Tokamak

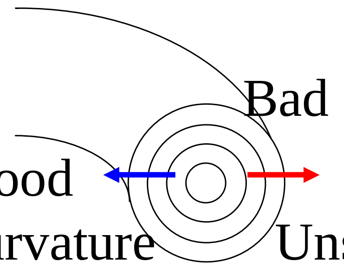

Stability condition of ballooning instability

It is principlely same with that in interchange mode.
However local value of the curvature and magnetic shear are important in the bad curvature region.

$$-\frac{p_0'\Omega'}{r^2} > \frac{1}{4}\iota'^2 \quad \Rightarrow \quad -q^2 p_0'\tilde{\Omega}' > \frac{1}{4}\tilde{s}^2 \quad \left(\tilde{s} \equiv \frac{r}{q}\tilde{q}' = -\frac{r}{\iota}\tilde{\iota}'\right)$$

$\sim$ means the value at bad curvature.

Even in tokamaks, $\tilde{\Omega}'$ is positive.

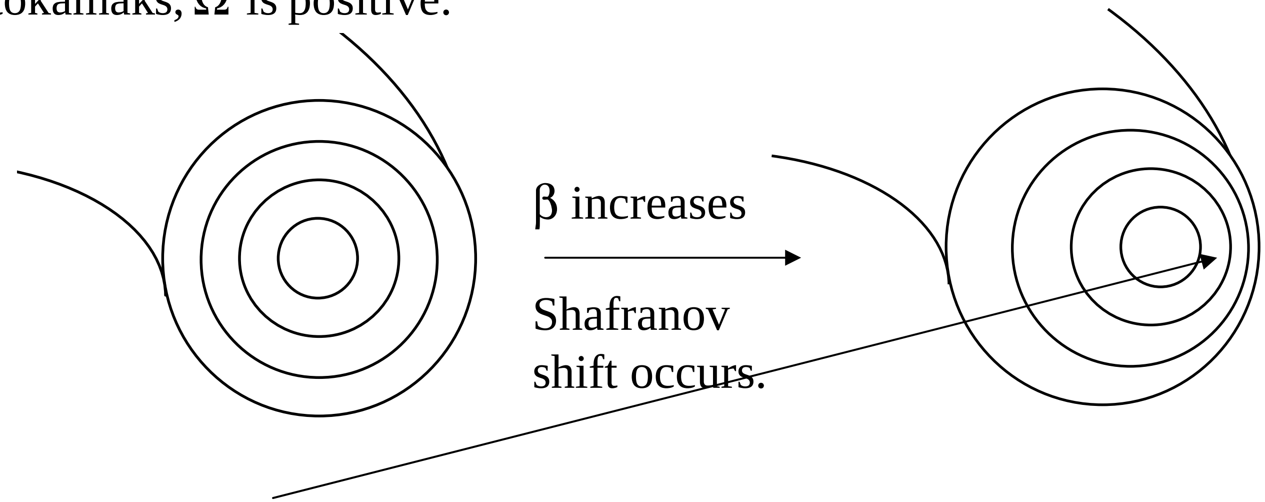

B_p increases where the magnetic fields becomes dense.
Increment of B_p is larger where the the magnetic fields becomes more dense (the relative shift of the magnetic surface to the next magnetic surface is larger. In edge region, the relative shift is larger). => $d\Delta B_p/dr > 0$.

Stability condition of ballooning instability

Here $\tilde{s} \equiv \frac{r}{q} q' - \alpha$, $-\alpha \propto (\Delta q)'$ is the modification due to shafranov shift.

$$(\Delta q)' = \frac{d}{dr}\left(\frac{r}{\Delta B_p}\frac{B_p}{R}\right) \sim \frac{rB_p}{R}\frac{d}{dr}\left(\frac{1}{\Delta B_p}\right) < 0 \Rightarrow \alpha > 0.$$

$$(s-\alpha)^2 < k\alpha \Rightarrow s^2 - 2\alpha s + \alpha^2 - k\alpha < 0$$

$$\Rightarrow \alpha - \sqrt{k\alpha} < s < \alpha + \sqrt{k\alpha}$$

According to more detail calculation, $0 < k < 1$.

In tokamak, $s > 0$.

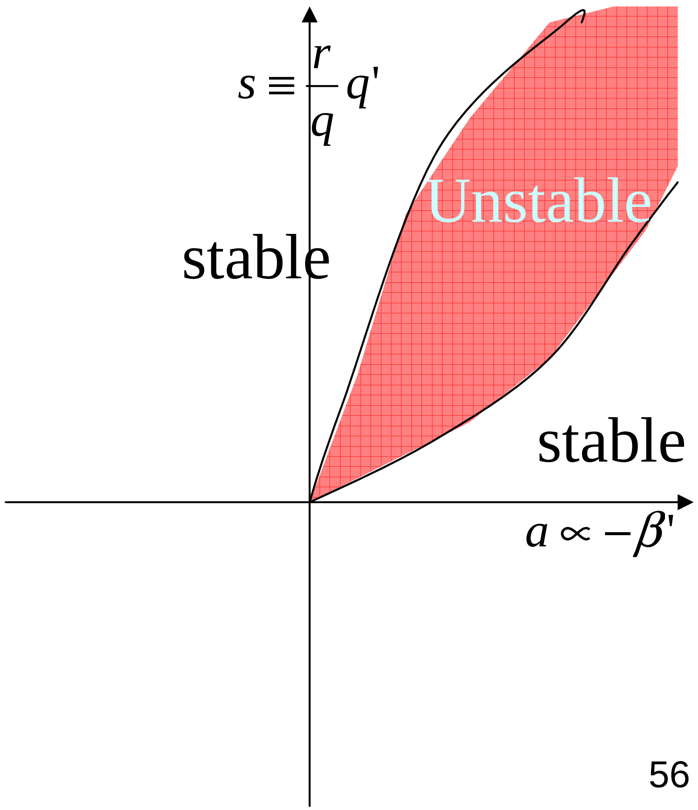

More exact treatment of stability analysis of ballooning mode

In order to exactly analyze the ballooning mode stability, we introduce the Eikonal approximation.

resonant surface

$$A = F(r)\exp(\mathrm{i}S),\ S(r,\theta,\phi) = -n[\phi - q(r)(\theta-\theta_0)] \Rightarrow -[n\phi - m(r)(\theta-\theta_0)],\ n \gg 1.$$

$$A = F(r)\exp\left(\mathrm{i}\mathbf{k}\cdot\mathbf{r} + nq_r'(r\text{-}r_r)(\theta-\theta_0)\right) \Rightarrow F(r)\exp\left(nq_r'(r\text{-}r_r)(\theta-\theta_0)\right)\exp(\mathrm{i}\mathbf{k}\cdot\mathbf{r});\ \text{near } q = q_r.$$

cf. $S = -[n\phi - m(\theta-\theta_0)]$; in fourier analysis.

Change of this part at resonance is relatively large near resonant surface

When the Eikonal approximation is introduced, the potential energy is rewritten as follows. $RB_p\xi_r \Rightarrow A$

$$\delta W = \int\left[\left(1+\Lambda^2\right)\left(\frac{\mathrm{d}F}{\mathrm{d}\theta}\right)^2 - \alpha(\Lambda\sin\theta + \cos\theta)F^2\right]\mathrm{d}\theta,\ \text{where } \Lambda = s\theta - \alpha\sin\theta,\ s = \frac{r}{q}\frac{\mathrm{d}q}{\mathrm{d}r},\ \alpha = -\frac{2\mu_0 Rq^2}{B^2}\frac{\mathrm{d}p}{\mathrm{d}r}.$$

Minimization of the above potential energy leads to the following Euler equation,

$$\frac{\mathrm{d}}{\mathrm{d}\theta}\left[\left(1+\Lambda^2\right)\left(\frac{\mathrm{d}F}{\mathrm{d}\theta}\right)^2 - \alpha(\Lambda\sin\theta + \cos\theta)F\right] = 0.$$

[ref] J.Wesson; Chap.6.13-14 in “Tokamaks --2nd edit.--” Clarendon press (1997).

More exact treatment of stability analysis of ballooning mode

There is no simple analytic solution of the Ballooning eq.
Here just show a numerical calculation result. (If you want to know more detail analyzing procedure, please see refs.[1], [2],[3]).

According to refs.[2], the stability boundary is expressed as the following on s-α diagram. Here δ is the amplitude of the magnetic well (averaged good curvature).
It shows that in the averaged good curvature, the no ballooning mode unstable operation is possible.

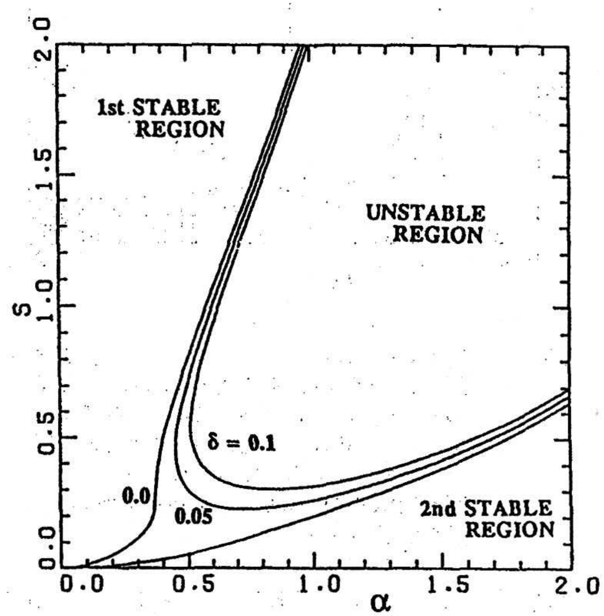

[1] J.P.Freidberg; Chap.10.5 in “Ideal Magneto hydrodynamics” Plenum press (1987).
[2] M.Azumi and M.Wakatani; J.Plasma Fus. Res., 66 (1991) 494.
[3] J.Wesson; Chap.6.14 in “Tokamaks --2nd edit.--” Clarendon press (1997).

ELM (Edge Localized Mode) I

Phenomena that heat and particles in the plasma edge region are oscillatingly exhausted in H-mode plasmas (Typically observed signal is the spick of Hα (Dα) emission).

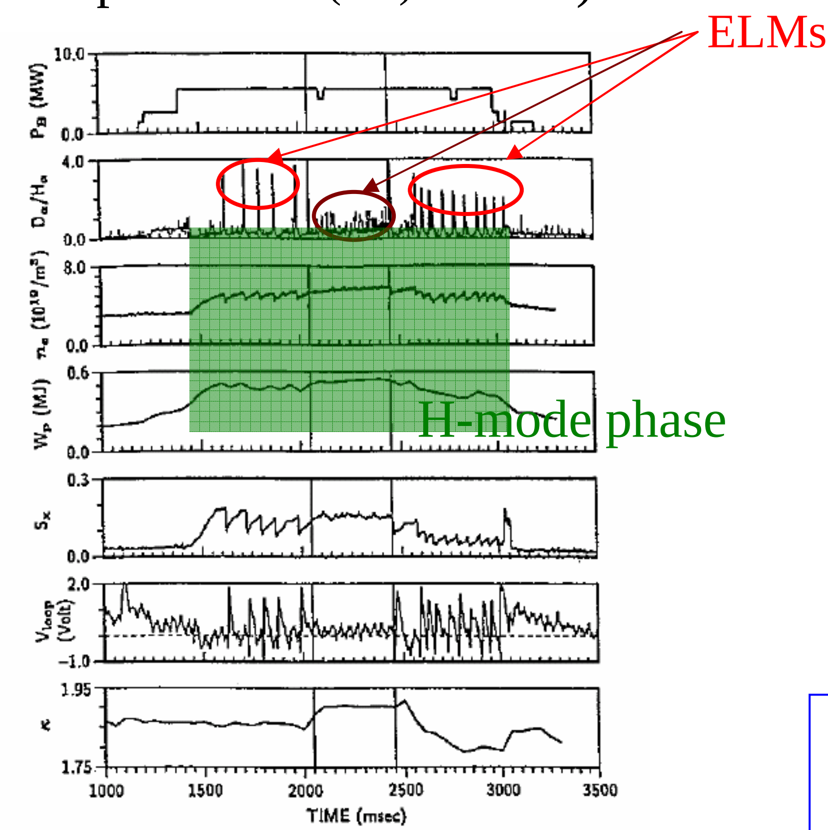

Fig. 1 Time traces of plasma parameters in a DIII-D discharge where type I ELMs are observed in t = 1,600 −2,000 ms and t = 2,600−3,000 ms, and type II ELMs in 2,050−2,450 ms at higher elongation and triangularity [5].

[5] T. Ozeki *et al.*, Nucl. Fusion 30, 1425 (1990).

When ELMs occur, the impurities like He are efficiently exhausted. In H-mode operation without ELM, it is not easy to remove the impurities. Though confinement improvement of H-mode with ELM is less that that without ELM, it is a favorable phenomenon for controlling the impurities and the understanding of the mechanism is important..

H-mode;
A kind of the improved confinement mode. the significant reduction of particle loss in the edge region is observed (Hα (Dα) signal is reduced). The steep gradients of the temperature and/or the density in the edge region appear.

ELM (Edge Localized Mode) II

Type I (giant) ELM Type II (grassy) ELM There are some types.

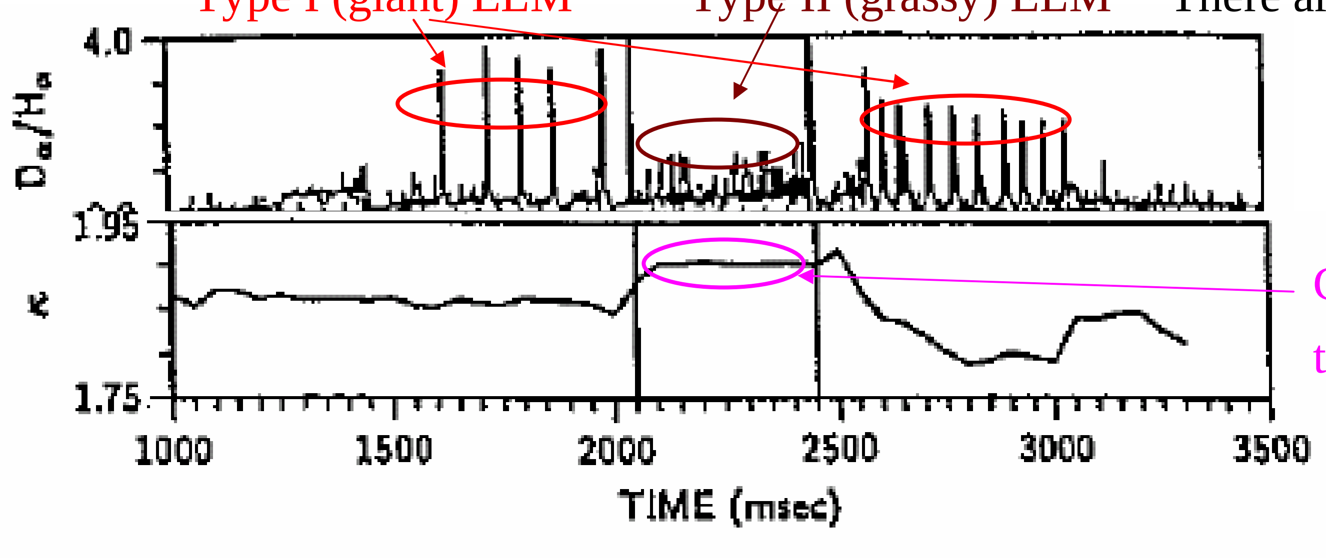

Config. changes

the shape is elongating

Frequency

Type I; 10~200Hz; proportional to the heating power across the separatrix.

Type II; higher than type I

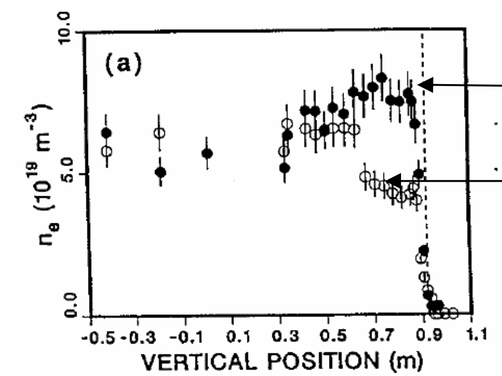

5ms before type I ELM.

11ms after type I ELM.

[6] P. Gohil *et al.*, Phys. Rev. Lett. **61**, 1603 (1988).

A probable candidate of driving mechanism of ELM

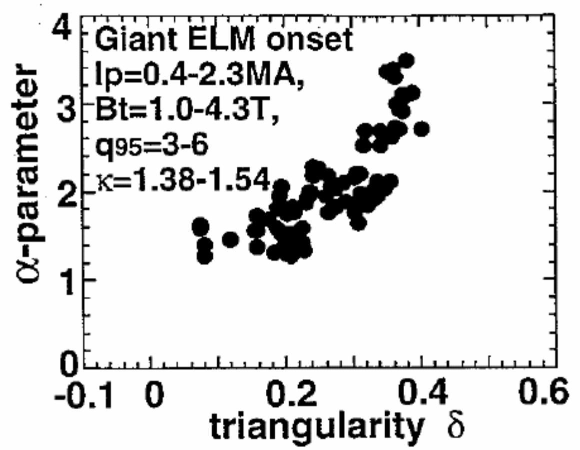

Fig. 5 The critical edge α parameter (the normalized edge pressure gradient) at onset of the first type I ELM after the ELM-free period increases with triangularity in JT-60U [15].

[15] Y. Kamada *et al., Proc. 16th IAEA Fusion Energy Conf.* Montreal, 1996 (1997) Vol.1, p.247.

Onset condition of type I ELM strongly depends on the triangularity.

The stability criterion also strongly depends on the triangularity.

=>
A probable candidate of the driving mechanism is ballooning mode.

A theoretical model of driving mechanism of ELM

ref. P.B. Snyder et al., Nucl. Fusion 44 (2004) 320.

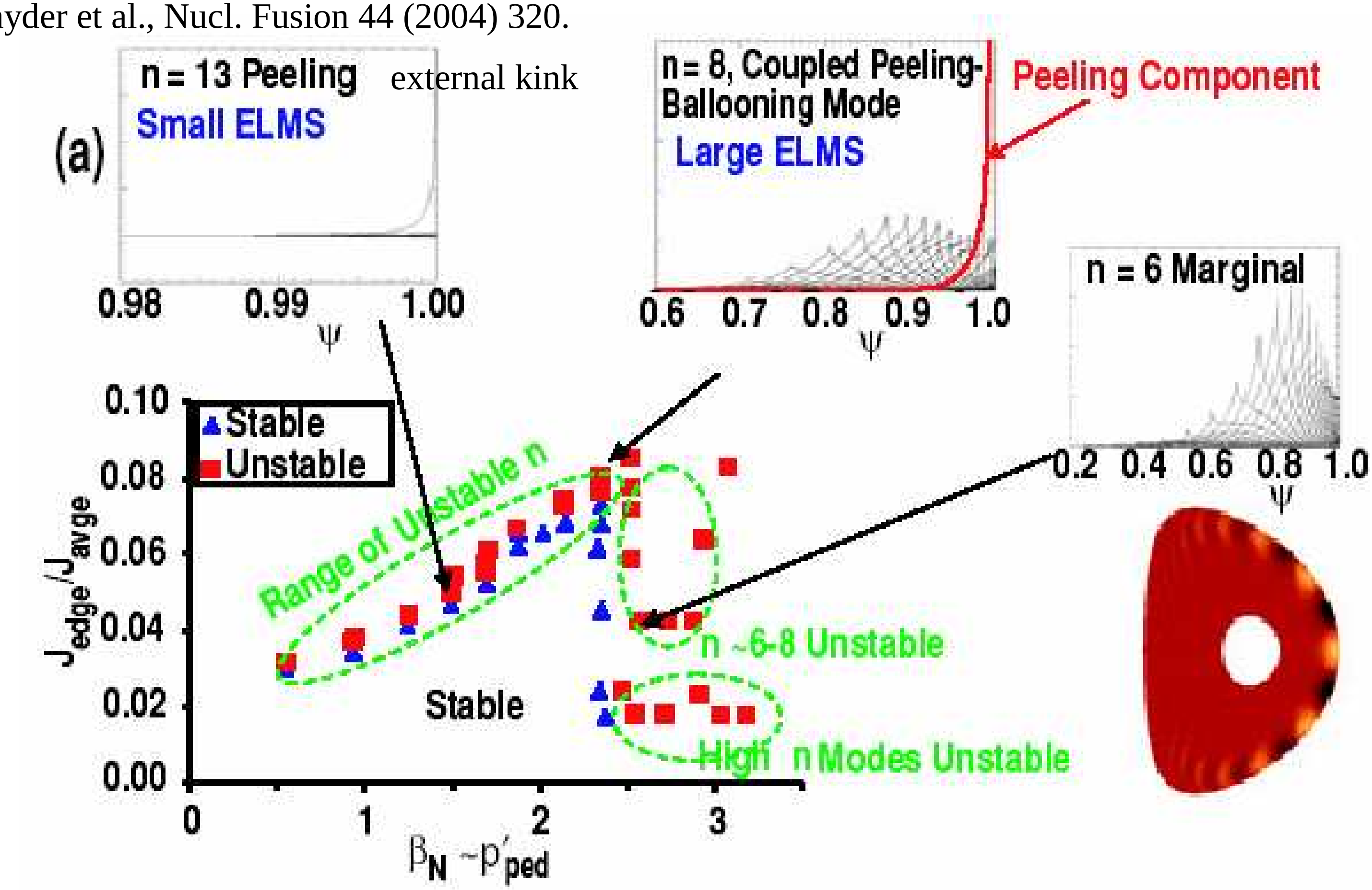

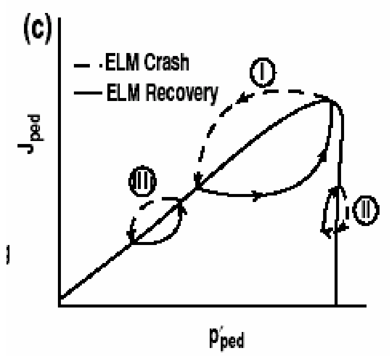

-ELM cycle

Cycle I ; Large ELMs (Type I ELM).

Cycle II; small ELMs (small Type I ELM or Type II.

Cycle III; low power, low density (Type III ELM).

Importance of the measurement of edge current profilefo ELM study

Observation of the current profile in the edge region is important to identify the driving mechanism of ELM

In DIII-D, Zeeman effect of the Li beam probe is used. Spatial resolution ΔR~5cm, 32 channel.

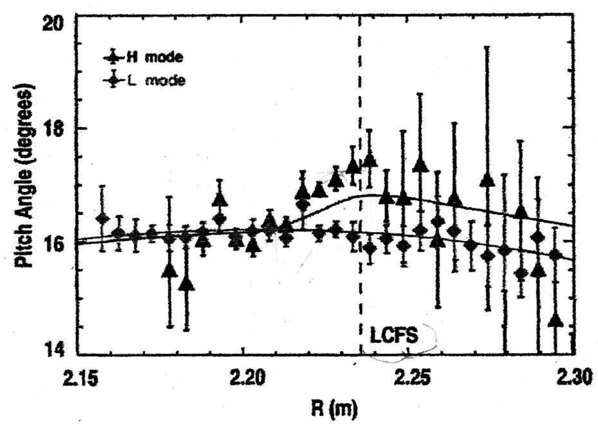

Application of the MSE measurement is not suitable fo edge current profile measurement because the NBI beam attenuation is very small in the edge region.

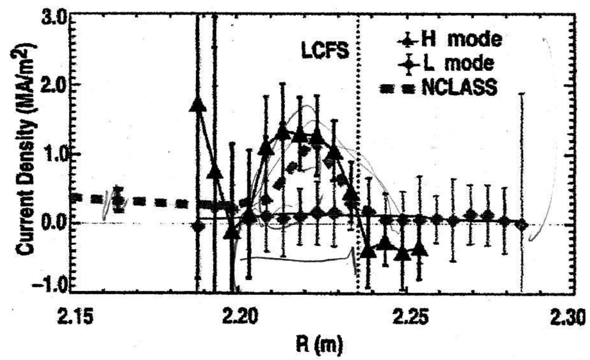

ref. D.M.Thomas et al., Phys. rev. Lett. 93, 065003-1 (2004).

Index of lecture

Physical picture of the current driven instabilities (kink modes)

m=0

B_θ; small

B_θ; large

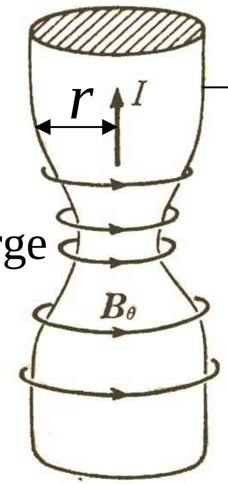

Mag. surfaces (press contour)

Situation
1. Mag. stress is balanced with press. gradient in equilibrium state.
2. Mag. field is produced by longitudinal current.

m=1

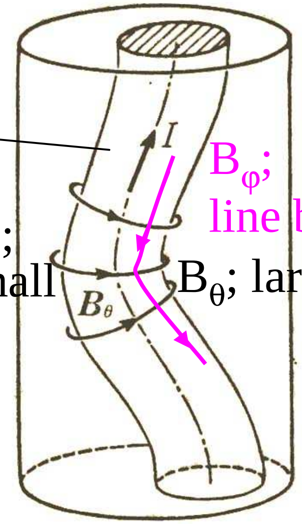

B_θ; small

B_φ; line bending

B_θ; large

Once cross-section of a mag. surf shrinks at a location, mag. field strength increases there, and mag. stress presses mag. surf. radially.
=> increases of mag. field strength.

Once column of mag. surface bends kink-like, mag. field strength increases in small curvature region and it decreases in large curv. region. Mag. stress in small curv. region is larger than that in large curv. region, and the column is pressed to bend more.
=> mag. field strength increases in small curvature region and it decreases in large curv. region.

$$B_\theta = I/2\pi r$$

$$p + \frac{B^2}{2\mu_0} = const.$$

Once plasma moves, it continues to move.
=> Unstable
Under presence of longitudinal field, additional force is affected as to suppress line bending. => Stabilizing effect

Linearized MHD Eq. I

$$\rho\left(\frac{\partial}{\partial t}+\mathbf{v}\cdot\nabla\right)\mathbf{v}=\mathbf{j}\times\mathbf{B}-\nabla p,$$

Starting from ideal MHD equations

$$\frac{\partial\rho}{\partial t}+\nabla\cdot(\rho\mathbf{v})=0,$$

$$\left(\frac{\partial}{\partial t}+\mathbf{v}\cdot\nabla\right)\left(\frac{p}{\rho^{\gamma}}\right)=0,$$

$$\mathbf{E}+\mathbf{v}\times\mathbf{B}=0 \quad (\eta\mathbf{j}),$$

$$\nabla\times\mathbf{B}=\mu_0\mathbf{j},\quad \nabla\times\mathbf{E}=-\frac{\partial\mathbf{B}}{\partial t},\quad \nabla\cdot\mathbf{B}=0.$$

Here some quantities are linearlized (separate the equilibrium part (suffix 0) and the perturbed part (suffix 1).).

$$\mathbf{v}(\mathbf{r},t)=\mathbf{v}_0(\mathbf{r})+\mathbf{v}_1(\mathbf{r},t),\ \mathbf{v}_0(\mathbf{r})=0,\qquad \mathbf{j}(\mathbf{r},t)=\mathbf{j}_0(\mathbf{r})+\mathbf{j}_1(\mathbf{r},t),\ |\mathbf{j}_1|<<|\mathbf{j}_0|,$$

$$\mathbf{B}(\mathbf{r},t)=\mathbf{B}_0(\mathbf{r})+\mathbf{B}_1(\mathbf{r},t),\ |\mathbf{B}_1|<<|\mathbf{B}_0|,\quad \mathbf{E}(\mathbf{r},t)=\mathbf{E}_0(\mathbf{r})+\mathbf{E}_1(\mathbf{r},t),\ \mathbf{E}_0(\mathbf{r})=0,$$

$$\rho(\mathbf{r},t)=\rho_0(\mathbf{r})+\rho_1(\mathbf{r},t),\ \rho_1<<\rho_0,\qquad p(\mathbf{r},t)=p_0(\mathbf{r})+p_1(\mathbf{r},t),\ p_1<<p_0.$$

The 1st order momentum equations are as follows:

$$\rho_0\frac{\partial\mathbf{v}_1}{\partial t}=-\nabla p_1+\mathbf{j}_1\times\mathbf{B}_0+\mathbf{j}_0\times\mathbf{B}_1,\ \frac{\partial\rho_1}{\partial t}+\nabla\cdot(\rho_0\mathbf{v}_1)=0,$$

$$\frac{\partial p_1}{\partial t}=-\mathbf{v}_1\cdot\nabla p_0-\gamma p_0\nabla\cdot\mathbf{v}_1,\ \mathbf{E}_1+\mathbf{v}_1\times\mathbf{B}_0=0,$$

$$\nabla\times\mathbf{B}_1=\mu_0\mathbf{j}_1,\quad \nabla\times\mathbf{E}_1=-\frac{\partial\mathbf{B}_1}{\partial t},\quad \nabla\cdot\mathbf{B}_1=0.$$

Linearized MHD Eq. II

Summarizing the above equations,

$$\rho_0 \frac{\partial^2 \mathbf{v}_1}{\partial t^2} = -\nabla\{\mathbf{v}_1 \cdot \nabla p_0 + \gamma p_0 \nabla \cdot \mathbf{v}_1\}_1 + \mathbf{j}_0 \times \{\nabla \times (\mathbf{v}_1 \times \mathbf{B}_0)\} + \frac{1}{\mu_0}[\nabla \times \{\nabla \times (\mathbf{v}_1 \times \mathbf{B}_0)\}] \times \mathbf{B}_0.$$

When $\mathbf{v}_1$ replaces a Lagrangian valiable, $\partial \xi / \partial t$,

$$\rho_0 \frac{\partial^2 \xi}{\partial t^2} = \mathbf{F}(\xi),$$

$$\mathbf{F}(\xi) \equiv -\nabla\{\xi \cdot \nabla p_0 + \gamma p_0 \nabla \cdot \xi\} + \frac{1}{\mu_0}(\nabla \times \mathbf{B}_0) \times \mathbf{Q} + \frac{1}{\mu_0}(\nabla \times \mathbf{Q}) \times \mathbf{B}_0.$$

where $\mathbf{Q} \equiv \nabla \times (\xi \times \mathbf{B}_0).$

In the linear stability analysis, the followin expression of the time evolution of the perturbation is useful,

$$\xi(\mathbf{r}, t) = \xi_\omega(\mathbf{r}) \exp(-\mathrm{i}\omega t).$$ If ω is imaginary, the mode grows (unstable).

Then

$$-\rho_0 \omega^2 \xi = \mathbf{F}(\xi).$$

Here it should be noticed that $\mathbf{F}$ is a self-adjoint operator, $\int dV \mathbf{x} \cdot \mathbf{F}(\mathbf{y}) = \int dV \mathbf{y} \cdot \mathbf{F}(\mathbf{x}).$

$$\frac{1}{2}\rho_0 \omega^2 \int \mathrm{d}V \xi^* \xi = -\frac{1}{2}\int \mathrm{d}V \xi^* \mathbf{F}(\xi), \; \frac{1}{2}\rho_0 \omega^{*2} \int \mathrm{d}V \xi \xi^* = -\frac{1}{2}\int \mathrm{d}V \xi \mathbf{F}(\xi^*).$$

$$\Rightarrow \frac{1}{2}\rho_0 \omega^2 \int \mathrm{d}V \xi^* \xi = \frac{1}{2}\rho_0 \omega^{*2} \int \mathrm{d}V \xi \xi^* \Rightarrow \omega^2 = \omega^{*2}.$$

=> ω^2 should be real.

Here * denotes a complex conjugate.

Linearized MHD Eq. III

$$\frac{1}{2}\rho_0\omega^2\int \mathrm{d}V\xi^*\xi = -\frac{1}{2}\int \mathrm{d}V\xi^*\mathbf{F}(\xi) \Rightarrow \mathrm{K} \equiv \frac{1}{2}\rho_0\int \mathrm{d}V\xi^*\xi,\ \delta\mathrm{W} \equiv -\frac{1}{2}\int \mathrm{d}V\xi^*\mathbf{F}(\xi).$$

$$\Rightarrow \omega^2\mathrm{K} = \delta\mathrm{W}.$$

$$\Rightarrow \omega^2 = \frac{\delta\mathrm{W}}{\mathrm{K}}.$$

Because K is positive, the sign of δW determines the stability of the system.
$\delta W>0$ => stable. $\delta W<0$ => unstable.
Here K and δW correspond to the kinetic energy and the potential energy.
After some calculations, δW is rewritten as

$$\delta W = \frac{1}{2}\int_{plasma}\mathrm{d}V\left[\gamma p_0(\nabla\cdot\xi)^2 + (\xi\cdot\nabla p_0)(\nabla\cdot\xi) + \frac{|\mathbf{Q}|^2}{\mu_0} + \mathbf{j}_0(\mathbf{Q}\times\xi)\right].$$

$$-\xi\cdot(\mathbf{j}_0\times\mathbf{B}_1)$$

Change of the internal energy of plasma without magnetic energy

Change of the magnetic energy

Work against the unbalanced magnetic force

Linearized MHD Eq. IV

$$\delta W = \frac{1}{2}\int_{plasma} \mathrm{d}V \left[\frac{|\mathbf{Q}_\perp|^2}{\mu_0} + \frac{B_0^{\ 2}}{\mu_0}\left|\nabla\cdot\xi_\perp + 2\xi_\perp\cdot\boldsymbol{\kappa}\right|^2 + \gamma p_0(\nabla\cdot\xi)^2 - 2(\xi_\perp\cdot\nabla p_0)(\xi_\perp\cdot\boldsymbol{\kappa}) - \mathbf{j}_{//}\cdot(\mathbf{Q}_\perp\times\xi_\perp) \right]$$

shear alfven wave
(line bending term)

$(k_\perp a)^2 (k_{//} a)^2$

sound wave of plasma

compressional alfven wave

stabilizing term

current driven
destabilizing term

$(k_\perp a)(k_{//} a)$

pressure driven
destabilizing term

$(k_\perp a)^2$

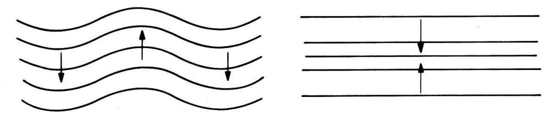

Bending of magnetic field lines

Compression of magnetic field

When the mode is localized $k_\perp a >> 1$,
pressure driven modeis dominant.

Current driven mode;
The global mode is more easily
unstable than the localized mode.
$k_\perp a \sim 1$

External kink I

$$\delta W=\frac{1}{2}\int_{plasma}\mathrm{d}V\left[\gamma p_0(\nabla\cdot\xi)^2+(\xi\cdot\nabla p_0)(\nabla\cdot\xi)+\frac{|\mathbf{Q}|^2}{\mu_0}-\mathbf{j}_0(\mathbf{Q}\times\xi)\right]+\int_{vacuum}\mathrm{d}V\left(\frac{B_V{}^2}{\mu_0}\right).$$

$$\beta\sim\varepsilon^2,\quad \frac{\partial}{\partial r}\sim\frac{1}{r}\frac{\partial}{\partial\theta}>>\frac{1}{R}\frac{\partial}{\partial\phi},\quad \nabla\cdot\xi=0 \text{ as the minimizing pertuurbation.}$$

$$\delta W=\pi R\int_0^a\left(\frac{|\mathbf{Q}|^2}{\mu_0}-j_{z0}(Q_r\xi_\theta-Q_\theta\xi_r)\right)\mathrm{d}\theta r\mathrm{d}r+\pi R\int_a^b\left(\frac{B_V{}^2}{\mu_0}\right)\mathrm{d}\theta r\mathrm{d}r.$$

where $|\mathbf{Q}|^2=Q_\rho{}^2+Q_\theta{}^2$, a is the plasma radius and b the radius of the perfect conducting wall. The perturbations are Fourier analyzed in the form $\exp[\mathrm{i}(m\theta-n\phi]$, and becomes

$$\xi_\theta=-\frac{\mathrm{i}}{m}\frac{\mathrm{d}}{\mathrm{d}r}(r\xi_r).$$

Here using $\mathbf{Q}=\nabla\mathrm{x}(\xi\mathrm{x}\mathbf{B}_0)$, then

$$Q_r=-\frac{\mathrm{i}mB_\varphi}{R}\left(\frac{n}{m}-\frac{1}{q}\right)\xi_r,\quad Q_\theta=\frac{B_\varphi}{R}\frac{\mathrm{d}}{\mathrm{d}r}\left[\left(\frac{n}{m}-\frac{1}{q}\right)r\xi_r\right].$$

where q ($=rB_\phi/RB_\theta$) is the safety factor. And $\mu_0 j_{z0}=\nabla\mathrm{x}\mathbf{B}_0$ ($=(1/r)[\mathrm{d}/\mathrm{d}r(rB_\theta)]$).

$$\delta W_p=\frac{\pi^2B_\varphi{}^2}{\mu_0 R}\int_0^a r\mathrm{d}r\{m^2\left(\frac{n}{m}-\frac{1}{q}\right)^2\xi_r{}^2+\left(\frac{\mathrm{d}}{\mathrm{d}r}\left[\left(\frac{n}{m}-\frac{1}{q}\right)r\xi_r\right]\right)^2$$

$$+\frac{1}{r}\frac{\mathrm{d}}{\mathrm{d}r}(rB_\theta)\left[\left(\frac{n}{m}-\frac{1}{q}\right)\xi_r\frac{\mathrm{d}}{\mathrm{d}r}(r\xi_r)+\frac{\mathrm{d}}{\mathrm{d}r}\left[\left(\frac{n}{m}-\frac{1}{q}\right)r\xi_r\right]\xi_r\right]\}$$

External kink II

After the integration by parts in the term involving $\xi_r d\xi_r/dr$,

$$\delta W_p = \frac{\pi^2 B_\varphi{}^2}{\mu_0 R}\int_0^a r\mathrm{d}r\left\{\left[\left(r\frac{\mathrm{d}\xi_r}{\mathrm{d}r}\right)^2 + (m^2-1)\xi_r{}^2\right]\left(\frac{n}{m}-\frac{1}{q}\right)^2\right\} + \left[\frac{2}{q_a}\left(\frac{n}{m}-\frac{1}{q_a}\right) + \left(\frac{n}{m}-\frac{1}{q_a}\right)^2\right]a^2\xi_{ra}{}^2.$$

where the subscript a denotes the value at $r=a$.

Next we consider the vacuum contribution to δW. In the vacuum, the perturbed magnetic field is expressed by a flux function Ψ as $B_{Vr1}=-(1/r)\,\partial\Psi/\partial\theta$ and $B_{V\theta 1}=\partial\Psi/\partial r$. Since

$$B_V{}^2 = B_{Vr12} + B_{V\theta 12} = \frac{\mathrm{m}^2}{r^2}\Psi + \left(\frac{\mathrm{d}\Psi}{\mathrm{d}r}\right)^2,$$ the δW_V is written as

$$\delta W_V = \frac{\pi^2 R}{\mu_0}\int_a^b r\mathrm{d}r B_V{}^2 = \frac{\pi^2 R}{\mu_0}\left\{\int_a^b r\mathrm{d}r\left[\frac{\mathrm{m}^2}{r^2}\Psi - \frac{\Psi}{r}\frac{\mathrm{d}}{\mathrm{d}r}\left(r\frac{\mathrm{d}\Psi}{\mathrm{d}r}\right)\right] + \left(r\Psi\frac{\mathrm{d}\Psi}{\mathrm{d}r}\right)\Bigg|_a^b\right\}.$$

Here it is noted that Ψ satisfies the following Laplace's equation, $\frac{1}{r}\frac{\mathrm{d}}{\mathrm{d}r}\left(r\frac{\mathrm{d}\Psi}{\mathrm{d}r}\right) - \frac{\mathrm{m}^2}{r^2}\Psi = 0.$

Then $$\delta W_V = \frac{\pi^2 R}{\mu_0}\left(r\Psi\frac{\mathrm{d}\Psi}{\mathrm{d}r}\right)\Bigg|_a^b.$$

Here we assume the solution of the Laplace's equation is written as $\Psi=\alpha r^{\mathrm{m}}-\beta r^{-\mathrm{m}}$.

For the conducting wall at $r=b$, $B_r(b)=0$ => $\Psi=0$ at $r=b$.

For the plasma surface $r=a$, $B_{Vr1}(a)=-\mathrm{i}m\Psi_a/a=Q_r(a)=-\mathrm{i}(mB_\varphi/R)(n/m-1/q_a)\xi_{ra}$ =>

$\Psi_a=B_{\theta a}(nq_a/m-1)\xi_{ra}$.

External kink III

The solution of the Ψ is given as $$\Psi = B_{\theta a}\left(\frac{nq_a}{m}-1\right)\frac{(r/b)^m-(b/r)^m}{(a/b)^m-(b/a)^m}\xi_{ra}.$$

Then the vacuum contribution δW_V is expressed as

$$\delta W_V = \frac{\pi^2 R}{\mu_0} m\lambda\left(\frac{n}{m}-\frac{1}{q_a}\right)a^2\xi_{ra}{}^2, \quad \text{where} \quad \lambda \equiv \frac{1+(a/b)^{2m}}{1-(a/b)^{2m}}.$$

When the conducting wall moves to infinity, (b=>inf.), λ=>1.

The above equation is added to the plasma contribution δW_p,

$$\delta W = \frac{\pi^2 B_\varphi{}^2}{\mu_0 R}\int_0^a r\mathrm{d}r\left\{\left[\left(r\frac{\mathrm{d}\xi_r}{\mathrm{d}r}\right)^2+(m^2-1)\xi_r{}^2\right]\left(\frac{n}{m}-\frac{1}{q}\right)^2\right\}+\left[\frac{2}{q_a}\left(\frac{n}{m}-\frac{1}{q_a}\right)+(1+m\lambda)\left(\frac{n}{m}-\frac{1}{q_a}\right)^2\right]a^2\xi_{ra}{}^2.$$

When $\xi_{ra}=0$, $\delta W\geq 0$. => stable *or* marginal stable.

The integral contribution (inside of the plasma) is always positive or zero. When we consider the case that the q_a>0, m>0, -inf<n<inf, the necessary condition for instability is

$$\left[\frac{2}{q_a}+(1+m\lambda)\left(\frac{n}{m}-\frac{1}{q_a}\right)\right]\left(\frac{n}{m}-\frac{1}{q_a}\right)<0 \quad => \quad \frac{m}{n}\frac{m\lambda-1}{m\lambda+1}<q_a<\frac{m}{n},$$

$$=> \quad \frac{m}{n}\frac{m-1}{m+1}<q_a<\frac{m}{n} \qquad (m=2, n=1 => 2/3<q_a<2, m=3, n=1 => 3/2<q_a<3) \ @ \ \lambda=1.$$

External kink IV

When m=1, $$\delta W = \frac{\pi^2 B_\varphi{}^2}{\mu_0 R}\int_0^a r\mathrm{d}r\left\{\left(r\frac{\mathrm{d}\xi_r}{\mathrm{d}r}\right)^2\left(n-\frac{1}{q}\right)^2\right\}+\left[\frac{2}{q_a}\left(n-\frac{1}{q_a}\right)+2\left(n-\frac{1}{q_a}\right)^2\right]a^2\xi_{ra}{}^2.$$

The minimizing eigenfunction in the plasma is given by $\xi_r(r)=\xi_{ra}$=constant. Then

$$\delta W = \left[2n\left(n-\frac{1}{q_a}\right)\right]a^2\xi_{ra}{}^2. \quad \Rightarrow \quad q_a > 1 \geq \frac{1}{n} \quad \text{(the condition of stabilization, Kruskal-Shafranov condition.)}$$

When m>=2, the trial function which minimizes the integral term (plasma term) should satisfy the following equation (Euler-Lagrange eq.)

$$\frac{\mathrm{d}_r}{\mathrm{d}r}\left[r^3\left(\frac{n}{m}-\frac{1}{q}\right)^2\frac{\mathrm{d}\xi_r}{\mathrm{d}r}\right]-r\left(m^2-1\right)\left(\frac{n}{m}-\frac{1}{q}\right)^2\xi_r = 0.$$

Assuming the above eq. can be solved for ξ_r, one can rewrite δW as follows:

$$\delta W = \left(\frac{n}{m}-\frac{1}{q_a}\right)\left[\left(m+\frac{a\xi_{ra}'}{\xi_{ra}}\right)\left(\frac{n}{m}-\frac{1}{q_a}\right)+\left(\frac{n}{m}+\frac{1}{q_a}\right)\right]a^2\xi_{ra}{}^2.$$

To evaluate δW the Euler-Lagrange eq. should be solved and $a\xi_r'/\xi_r$ be calculated. Assuming the mode structure is localized near the plasma boundary and after some calculation, we obtain the unstable criterion taking the current profile into account.

$$\frac{1}{n}\left(m-\frac{J_a}{\langle J\rangle}\right)<q_a<\frac{m}{n}, \quad \text{for} \quad J_a \neq 0, \quad \text{and} \quad \frac{1}{n}\left(m-\exp\left(\frac{2m\langle J\rangle}{aJ_a'}\right)\frac{J_a}{\langle J\rangle}\right)<q_a<\frac{m}{n}, \quad \text{for} \quad J_a = 0.$$

External kink V

How fast the current gradient must vanish is difficult estimate by the analytical methods.

The right figure is the numerical results of the unstable region for external kinks for a current profile $j(r)=j_0(1-\rho^2)^\nu$. $\rho=r/a$. $q=q_a\rho[1-(1-\rho)^{\nu+1}]^{-1}$.=> $q_a/q_0=\nu+1$.

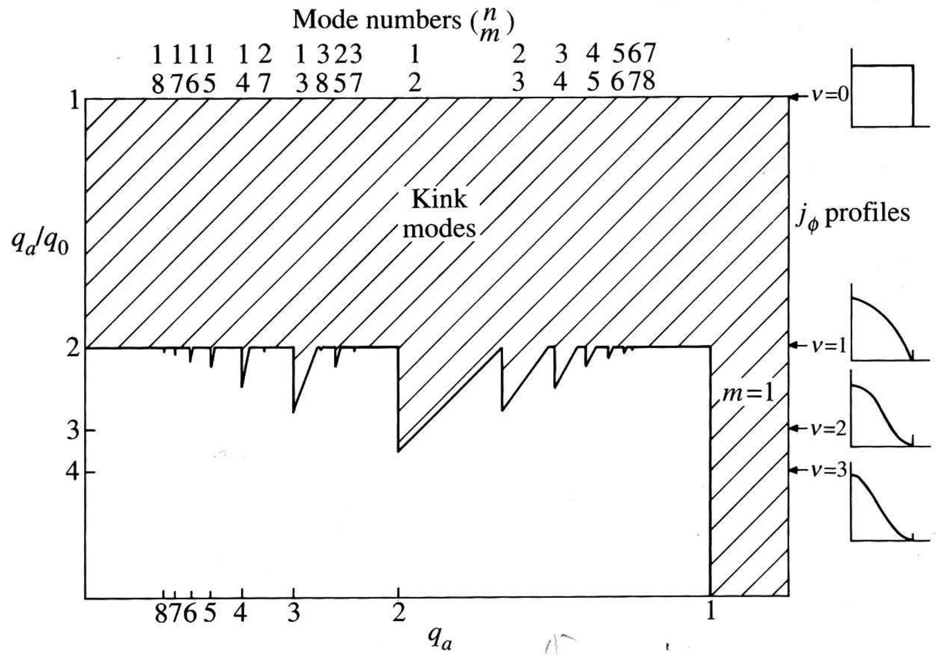

J.A.Wesson; Nucl. Fus. 18, 87 (1978).

When ν>2.5, all m>=2 modes are stable for any qa.
When 1<ν<2.5, the stability window of q_a exists.

External kink VI ---Observation of the mode structure of the external kink mode in TFTR---

$\beta = 0.5\%$, $\beta_N = 1.4$ and $\beta_p = 1.3$.

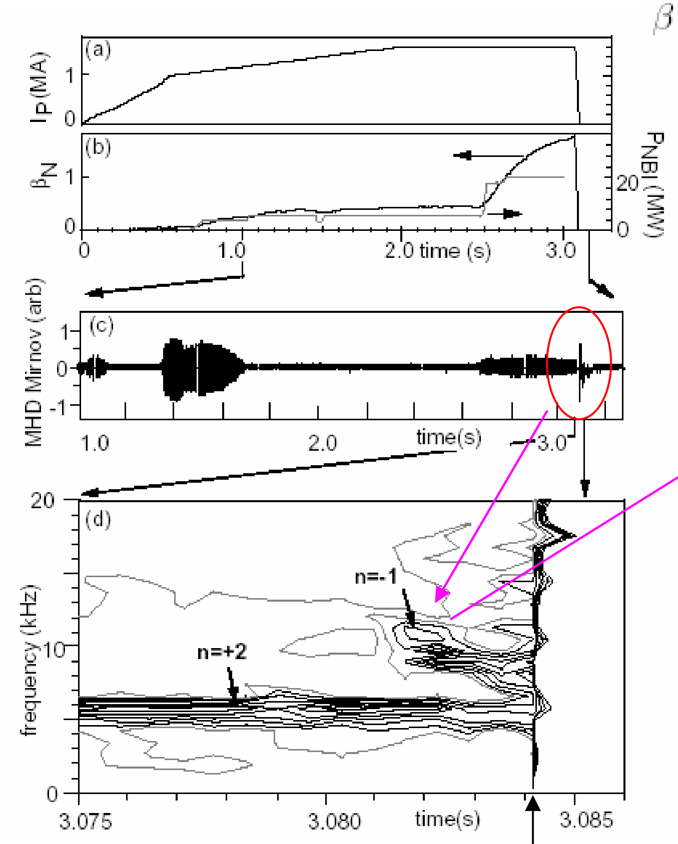

Disrupt

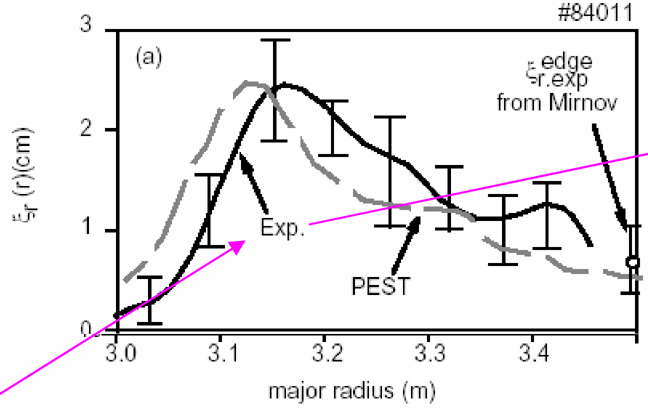

Profile of the radial displacement by ECE measurement and theoretical prediction

Mode structure is broad.

$$\xi_r = \tilde{T}_e / (-\nabla T_e)$$

	Small $r_{q_{min}}$
Shot	84011
Time (s)	3.08
τ_{growth} (μs)	$\simeq$150
$r_{q_{min}}/a$	0.53
$\xi^{max}_{r,exp}$ (mm)	25
$\xi^{edge}_{r,exp}$ (mm)	7
δB (G)	3
m/n	2/(−1)
$\omega_{obs}/2\pi$ (kHz	7

ω_A=1.7e4~5e4Hz

n_e=1e20~1e19m^{-3}, 5T

γ_{grow}/ω_A=0.5~0.2

$$\xi_\theta = -\frac{i}{m}\frac{d}{dr}(r\xi_r).$$

The prediction of the external kink mode is quite consistent with the observation on the mode structure.

M.Okabayashi et al; Nucl. Fus. 38, 1149 (1998).

Tearing mode --Physical picture--

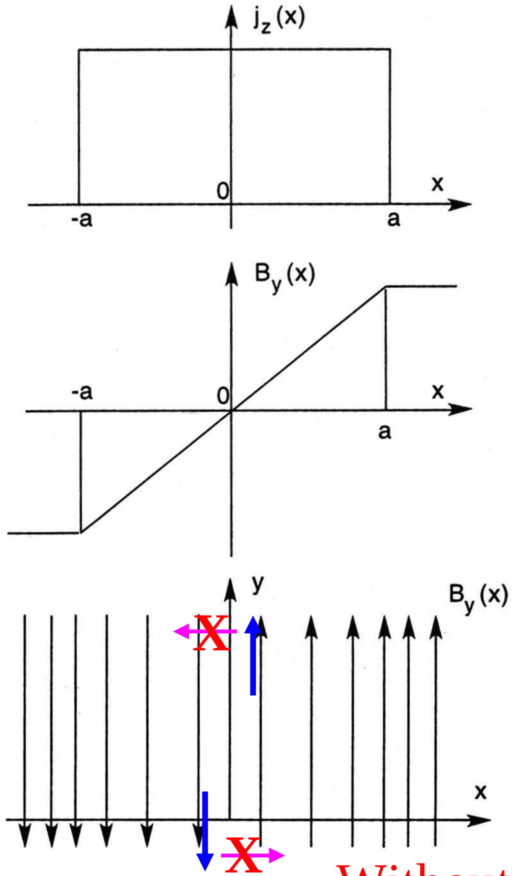

Without resistivity

$$j_z = \begin{cases} j_{z0} & -a < x < a \\ 0 & |x| > a \end{cases}$$

$$B_y(x) = \begin{cases} B'_{y0}x & -a < x < a \\ -B'_{y0}a & x < -a \\ B'_{y0}a & x > a \end{cases}$$

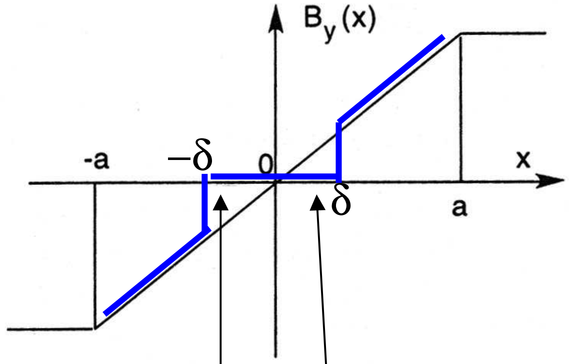

If $B_y = 0$ in $|x| < \delta$, $\int \left(B_y^{\,2}/2\right) dV$ is reduced.

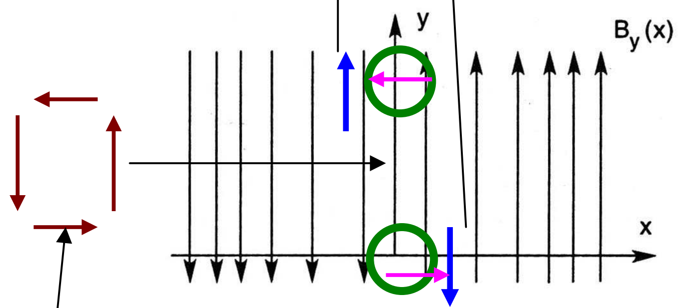

realize

With resistivity

from **div *B***=0

$$\frac{\partial \mathbf{B}}{\partial t} = -\nabla \times (\mathbf{v} \times \mathbf{B} - \eta \mathbf{j}) \Rightarrow \quad \mathrm{i}\omega B_x = -kB_{y0}u_{x1} - \eta \frac{\partial B_x^{\,2}}{\partial x^2}$$

If $\eta = 0$, $B_x = 0 @ x = 0$ because $B_{y0} = 0$. If $\eta \neq 0$, $B_x \neq 0 @ x = 0$

Goldston, Rutherford; Chap.20 in “Introduction to Plasma Physics”, IOP pub. Ltd. (1995).

Tearing mode I

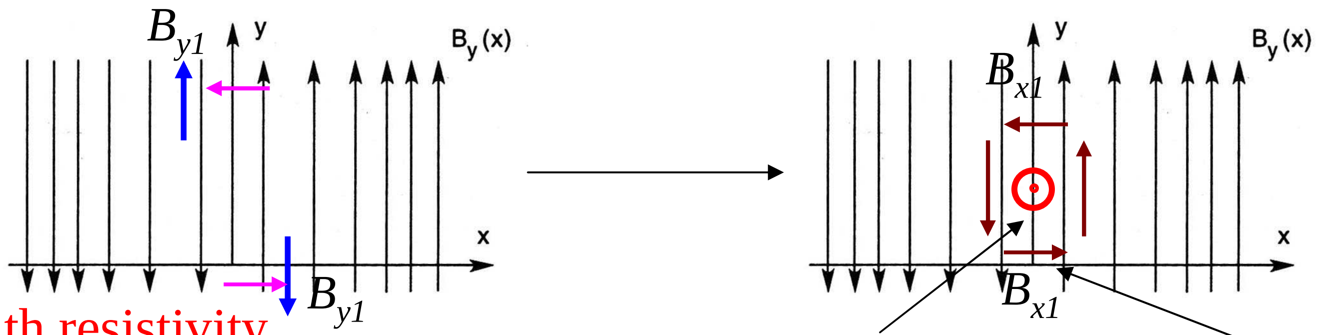

With resistivity
=> change of topology of magnetic field structure

=> current, j_{z1}, appears

from **div *B***=0

$$\boxed{\begin{array}{l}\dfrac{\partial \mathbf{B}}{\partial t} = -\nabla \times \left(\mathbf{v} \times \mathbf{B} - \eta \mathbf{j}\right) \Rightarrow \ \mathrm{i}\omega B_{x1} = -k_{y1} B_{y0} u_{x1} - \eta \dfrac{\partial B_{x1}{}^{2}}{\partial x^{2}} \\ \text{If } \eta = 0,\ B_{x1} = 0 @ x = 0 \text{ because } B_{y0} = 0.\ \text{If } \eta \neq 0,\ B_{x1} \neq 0 @ x = 0\end{array}}$$

$$\mu_0 j_{z1} = B_{y1}\Big|_{0+} - B_{y1}\Big|_{0-},\ \frac{\partial B_{x1}}{\partial x} + ikB_{y1} = 0,\ \Delta' B_{x1} \equiv \frac{\partial B_{x1}}{\partial x}\bigg|_{0+} - \frac{\partial B_{x1}}{\partial x}\bigg|_{0-}$$

$$\Rightarrow \mu_0 j_{z1} = -\mathrm{i}\Delta' B_{x1} / k_y$$

When j_{z1} exists, tearing mode is unstable.
Then ***Δ‘>0 => unstable***.

Tearing mode II

From linearized momentum eq.

$$\frac{\partial}{\partial x}\left[B_{y0}{}^{2} \frac{\partial}{\partial x}\left(\frac{B_{x1}}{B_{y0}} \right) \right] - k_y{}^{2} B_{y0} B_{x1} = 0, \qquad \text{for "outer-regions".}$$

$$-\omega\rho_0\mu_0 \frac{\partial^2 u_{x1}}{\partial x^2} = \frac{k_y B_{y0}}{i\eta}\left(\omega B_{x1} + k_y B_{y0} u_{x1} \right), \qquad \text{for "resistive layer } \left(|x| < \delta \equiv \frac{\eta}{k_y B_{y0}{}' u_{x1}} \frac{\partial^2 B_{x1}}{\partial x^2}, \right)\text{".}$$

Δ' is determined.

Relationship between Δ' and γ (-iω) is determined.

$$\gamma = \left(\frac{\tau_R}{\tau_A} \right)^{0.4} \frac{0.55\left(\Delta' a \right)^{4/5}}{\tau_R}.$$

Magnetic Reynolds number
~10^8 in JT-60.
=> very large

τ_R; magnetic diffusive time ~ min is very long,
but γ of tearing mode is farly large.
(τ_A~10^{-6}s)

Tearing mode III

When we solve the momentum eq. in the outer regions

$$\frac{\partial}{\partial x}\left[B_{y0}^{\ 2}\frac{\partial}{\partial x}\left(\frac{B_{x1}}{B_{y0}}\right)\right]-k_y^{\ 2}B_{y0}B_{x1}=0,$$

under the following configurations,

$$B_y(x)=\begin{cases} B'_{y0}x & -a<x<a \\ -B'_{y0}a & x<-a \\ B'_{y0}a & x>a \end{cases}$$

we obtain the solution,

$$\Delta' a=\frac{2k_y\left[\exp(-2k_ya)-2k_ya+1\right]}{\exp(-2k_ya)+2k_ya-1}.$$

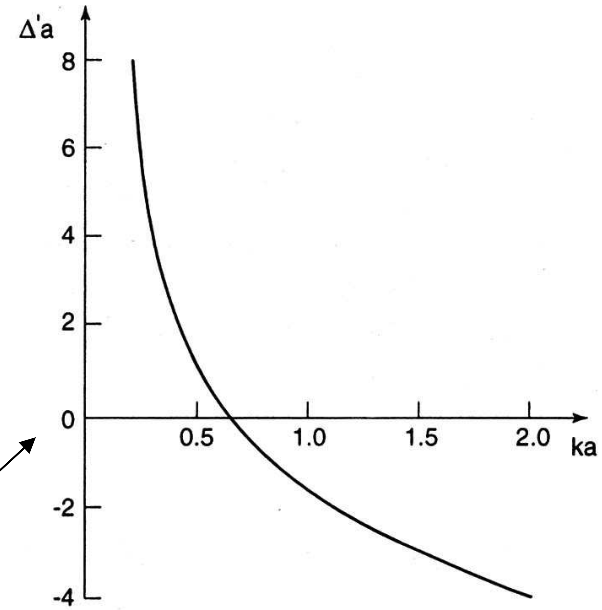

Generally speaking, when k_y is small, the tearing mode easily becomes unstable.
=> For the large k_y mode, the line-bending stabilization easily becomes large.

Neoclassical tearing mode --- Physical picture ---

The existence of bootstrap current is indispensability to obtaine the advanced tokamak plasmas because it helps to reduce the external current drive and to make the negative shear configuration.

However, when magnetic island exists, the bootstrap current affects the MHD stability through the neoclassical tearing mode.

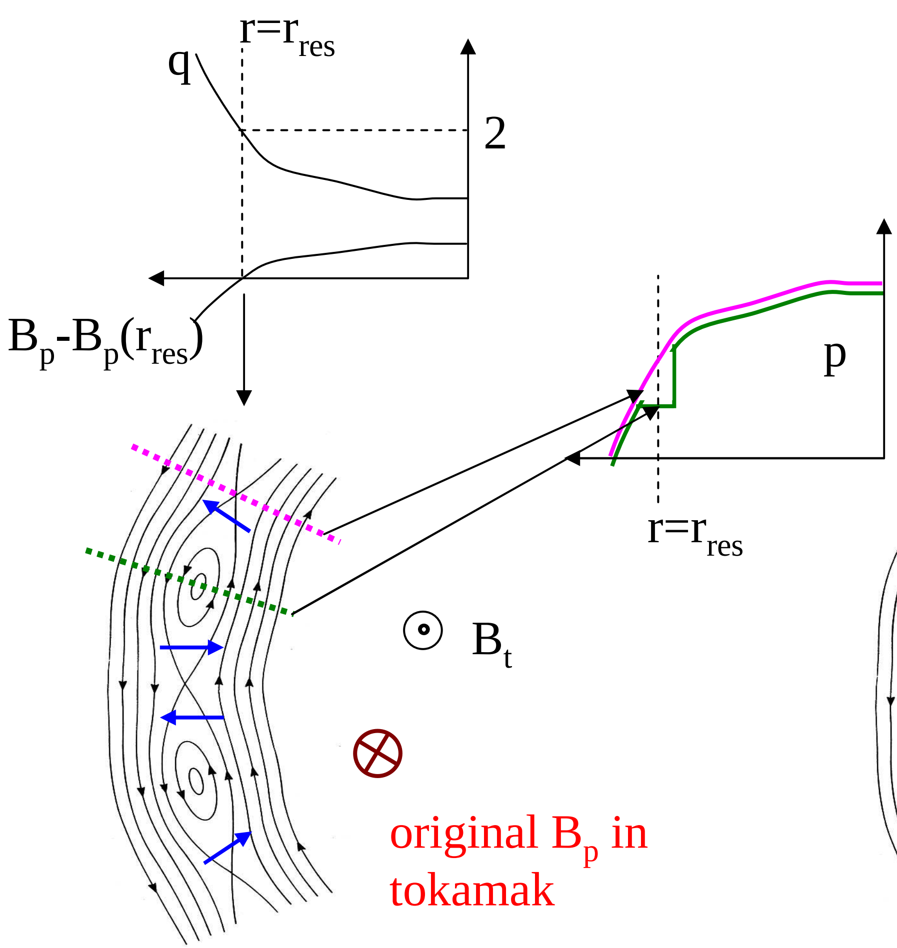

J$_{bs}$; proportional to dp/dr

⊗ J$_{bs}$; flows to enhance original B$_p$ in tokamak

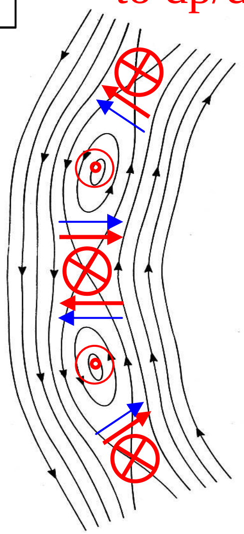

localized BS current in X-point enhances original mag. perturbation which produces mag.island.

=> Growth of Neoclassical Tearing mode

Neoclassical tearing mode

C.C. Hegna, Phys. Plasmas **4**, 2940 (1997).

The model eq. of the evolution of the island width (Modified Rutherford eq.)

$$\tau_R \frac{d}{dt}\left(\frac{w}{r_s}\right) = \Delta'(w)\, r_s - k_0 \varepsilon_s^2 \beta_{p_s} \frac{L_q^2}{L_p}(1 - q_s^{-2})\frac{1}{w} + k_1 r_s \sqrt{\varepsilon_s}\beta_{p_s}\frac{L_q}{L_p}\frac{w}{w^2 + w_d^2} - k_2 r_s \rho_p^2 \beta_{p_s}\left(\frac{L_q}{L_p}\right)^2 g(\nu_i, \varepsilon)\frac{1}{w^3} - k_3 \frac{16\mu_0 L_q I_{aux}}{\pi B_p}\frac{f_{aux}}{w^2}$$

the seed island due to tearing mode

destabilizing term due to BS current

stabilizing term due to external current

stabilizing term due to mag. well

stabilizing term due to polarization current

Example of observation of the neoclassical tearing mode

Neutron production rate due to DD reaction

in TFTR

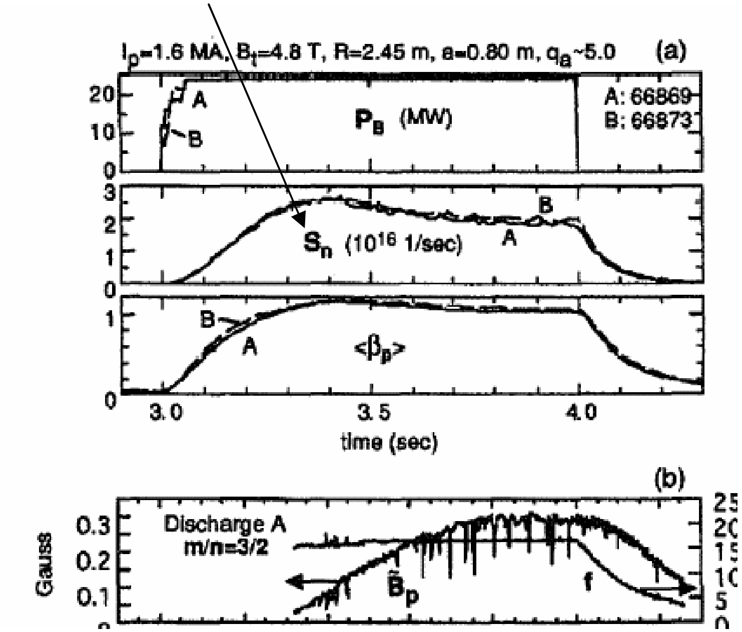

Z. Cheng et al., Phys. Rev. Lett. 74, 4663 (1995).

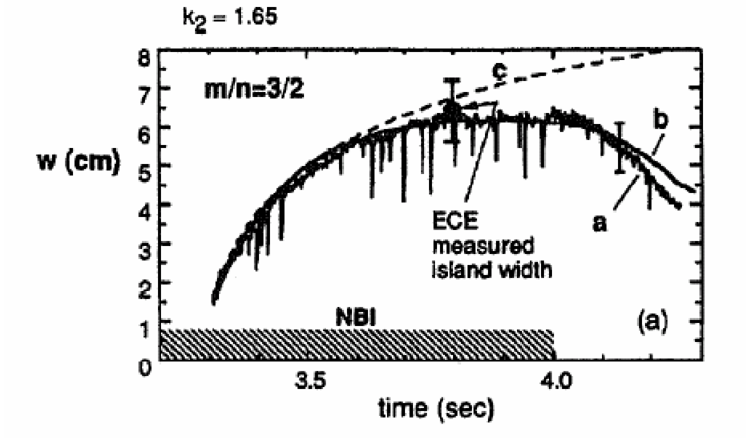

Comparison of the measured m/n = 3/2 island width (labeled 'a') with the neoclassical tearing mode theory (curve 'b' uses the time dependent parameters and 'c' uses fixed parameters)

Observation;

After b have exceeded 1.2%, it and S_n saturate, and just before the saturation, m/n=3/2 fluctuation starts increasing.

How is it identified?

Comparing measured m/n = 3/2 island width with the theory.

Mod. Rutherford model works well to explain the observation

Disruption I

A dramatic event in which the plasma confinement is suddenly destroyed.
In tokamak operations, it is often observed.
=> As a main cause, the instability related with the current driven mode and the subsequent destruction of the magnetic surfaces.

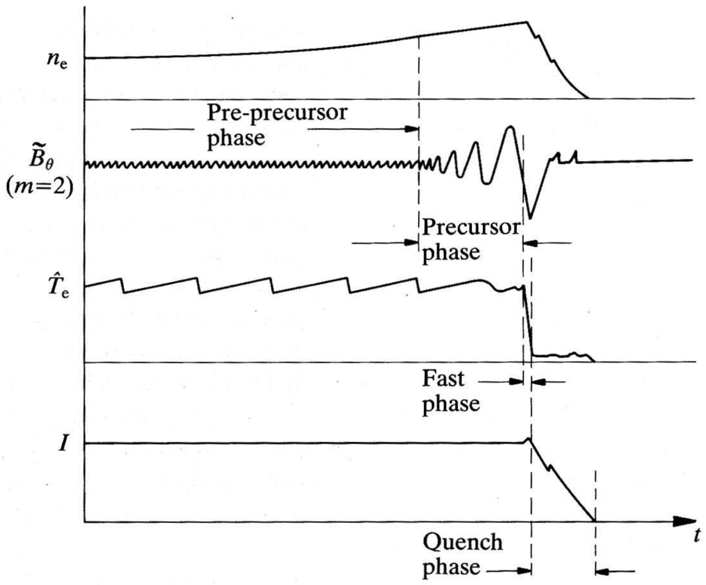

Typical sequence

1. Precursor in mag. probe signals are observed.
2. Temperature suddenly descreases.

2'. The equilibrium is destroyed less than once. And it is considered to be reconstructed.

3. Density and net toroidal current decrease slower than temperature does.

Decay time of density is mainly determined by particle confinement of the cold plasma, and that of net toroidal current is by L/R time.

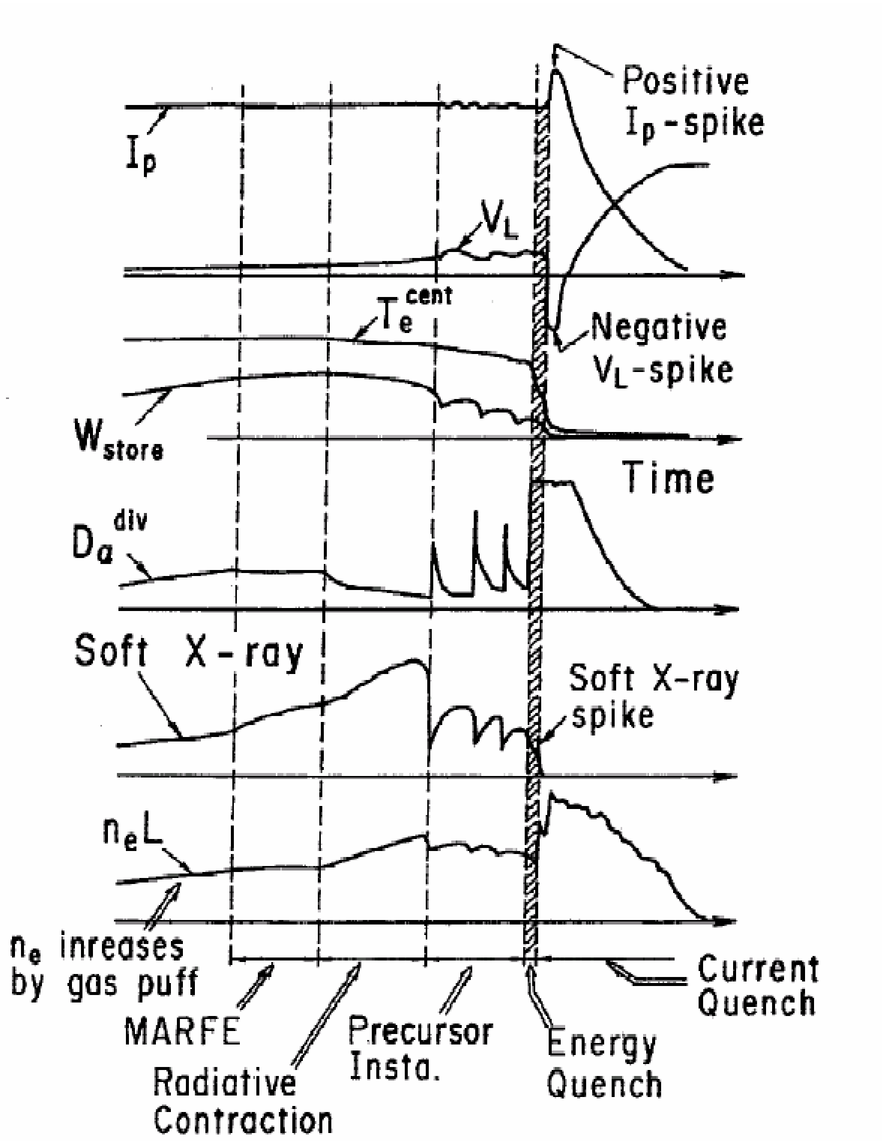
Positive
I_p-spike
I_p
V_L
T_e^{cent}
Negative
V_L-spike
W_{store}
Time
D_α^{div}
Soft X-ray
Soft X-ray
spike
n_eL
n_e inreases
by gas puff
MARFE
Radiative
Contraction
Precursor
Insta.
Energy
Quench
Current
Quench

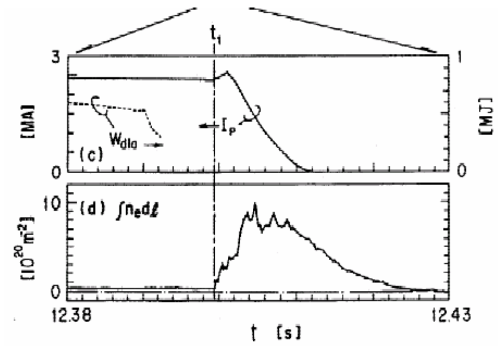
t_1
[MA]
[MJ]
(c)
W_{dia}
I_p
(d) $\int n_e d\ell$
$[10^{20} m^{-2}]$
12.38
12.43
t [s]

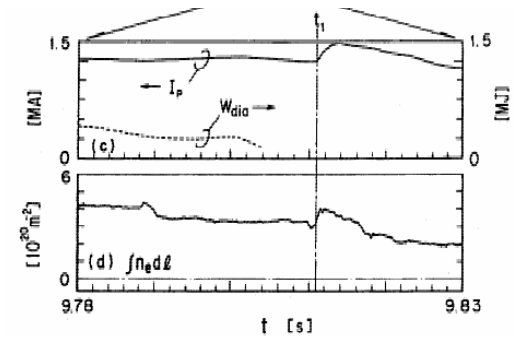
t_1
[MA]
[MJ]
I_p
W_{dia}
(c)
(d) $\int n_e d\ell$
$[10^{20} m^{-2}]$
9.78
9.83
t [s]

Disruption II

The radial over-rapping of tearing modes, a external kink and the positional instability are considered as main causes.

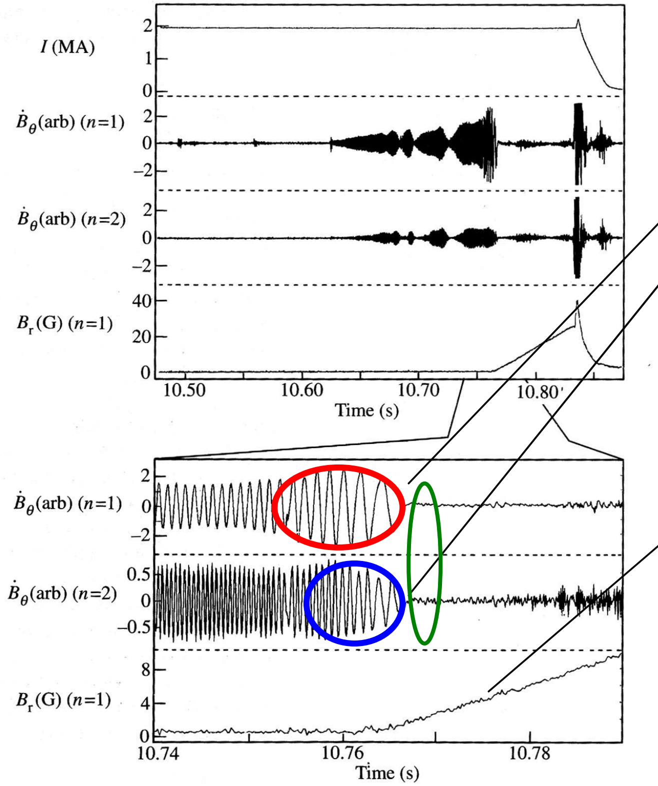

An example of the growth of MHD instabilities due to tearing modes in a disruption.

ref. J.A.Wesson et al., Nucl. Fusion 29, 641 (1989)

n=1/m=2?, n=2/m=3? tearing modes.
Oscillating periods become long.

Tearing modes are not annihilated.
Only oscillation have stopped (***mode locking***).

$$\left(-\dot{\mathbf{B}} = \nabla \times \mathbf{E}\right)$$

=>

B_r component monotonically increases.

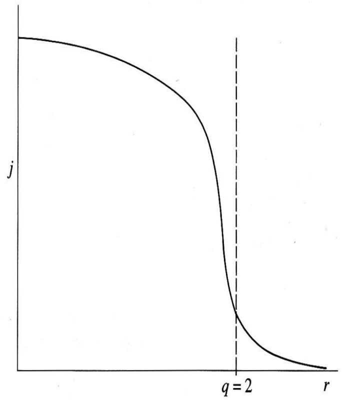

q_0 should be larger than 1. and the smaller toroidal current flows as the minor radius increases.
=> The central current profile is flattened. And the current gradient increases near q=2 surface.
=> The tearing mode becomes easily unstable.

Disruption III

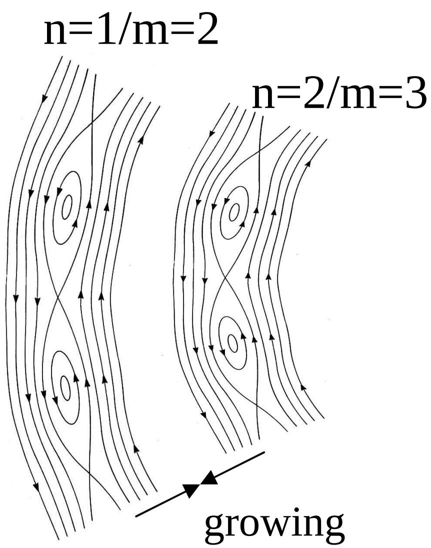

When over-rapping of the island due to tearing modes occur,
magnetic surfaces are destroyed, and the confinement will be lost.

When a external kink and the positional instability happen, the plasma losses rapidly due to a touch of the wall.
=> Rapid decay of temperature

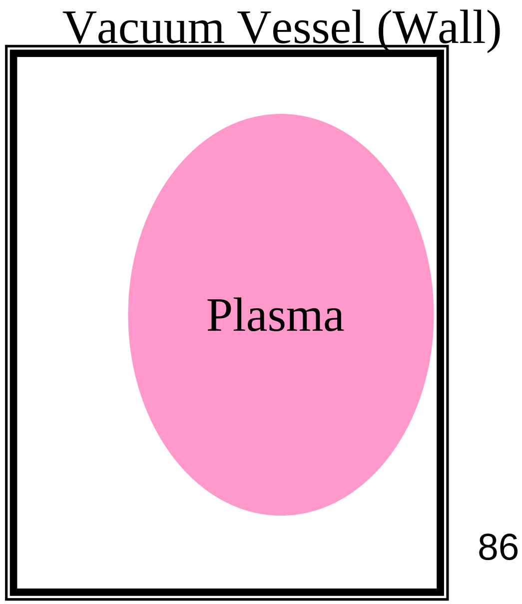

Sawtooth oscillation

Typical behavior

At first, the inner signal gradually increases and the outer one decreases. And at a time, the inner signal suddenly drops, and at the same time the outer signal increases. It is repeated.

=> The inner temperature (and/or density) suddenly drops, and the outer one increases.

The collapse is due to the instability with m/n=1/1 structure. It usually starts when a q=1 surface appear in plasma region.

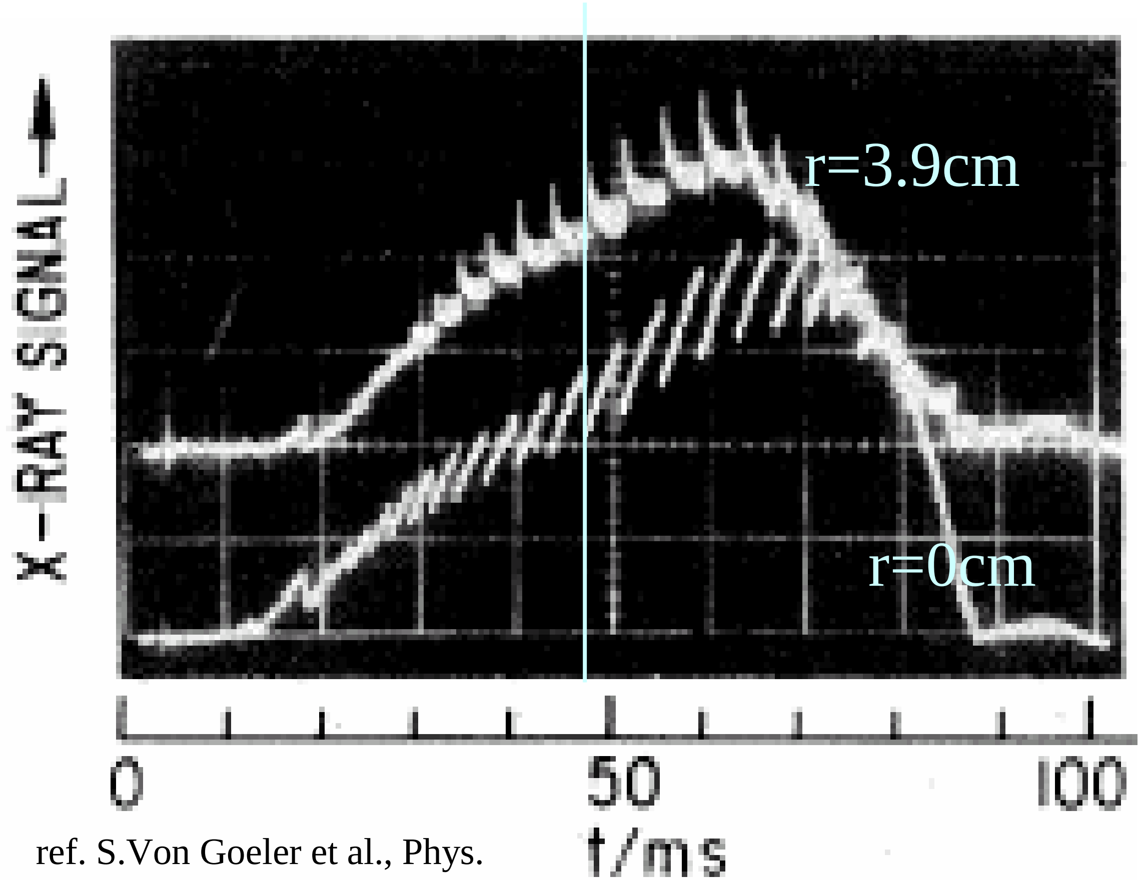

ref. S.Von Goeler et al., Phys. Rev. Lett. 33 1201 (1974).

ref. ASDEX team, Nucl. Fusion 29, 891 (1989).

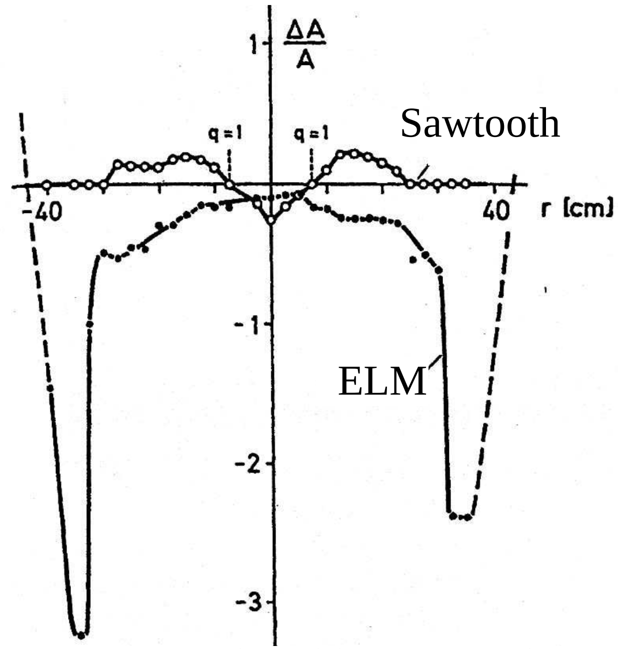

Radial profile of fluctuation of SX

A theoretical model for sawtooth oscillation

Kadomtsev's model

m/n=1/1 instability displaces the center region of plasma. The X point is created, the mag. field line breaks and reconnected where the magnetic flux is crowded.In intermediate state, a cooler core island is surrounding the displaced hot circular core.

time sequence

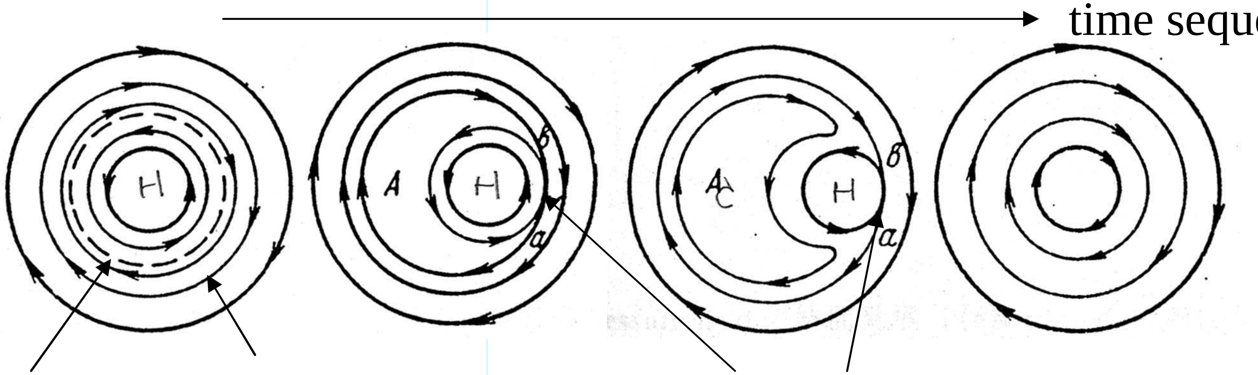

q=1 B_p-$B_p(r_1)$

reconnection of mag. filed line occurs due to resistivity

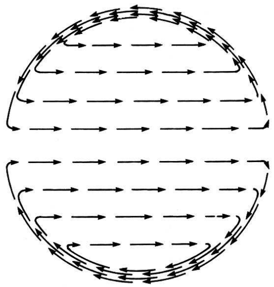

flow pattern of m/n=1/1
ideal kink mode (q_0=0.8)

According to Kadomtsev's model,
the collapse time is $\tau_R(\tau_A/\tau_R)^{0.5}$

ref J.Wesson; Chap.7.6 in "Tokamaks --2nd edit.--" Clarendon press (1997).

m=1 internal current driven modes

The leading order of δW respect with r/R is zero. When we consider higher order, the δW is expressed as the followings.

$$\delta W = \left(1 - \frac{1}{n^2}\right)\delta W_C + 2\pi^2 R \xi_0^{\ 2} \frac{B_\phi^{\ 2}}{\mu_0}\left(\frac{r_1}{R}\right)^4 \delta W_T \qquad \delta W_T = 3(1-q)\left(\frac{13}{144} - \beta_{p1}\right),\ \beta_{p1} = \frac{\int_0^{r_1}(p - p_1)2r\mathrm{d}r}{\mathrm{B}_{\theta 1}^{\ 2}/2\mu_0}.$$

Cylinder effect; in tokamaks, q>0.5. Then this term always positive.

Toroidal effect;
When β_{p1}>0.3, the ideal internal kink mode becomes unstable. However, the growth rate is small because δW is small. ***It should be noted that ideal internal kink mode is unstable just in finite pressure plasma.***

When we consider the resistiveity effect on the m/n=1/1 mode. That is unstable even without plasma pressure.

$$\gamma = \left(\frac{r}{R}\frac{aq'}{q}\right)^{2/3}\frac{1}{\tau_R}\left(\frac{\tau_R}{\tau_A}\right)^{2/3}.$$

$$\gamma = \left(\frac{\tau_R}{\tau_A}\right)^{0.4}\frac{0.55(\Delta' a)^{4/5}}{\tau_R}.$$

tearing mode

There are stronger effect of the resistiveity. When the resistivity becomes large, it more easily destabilized than m=2 tearing mode.

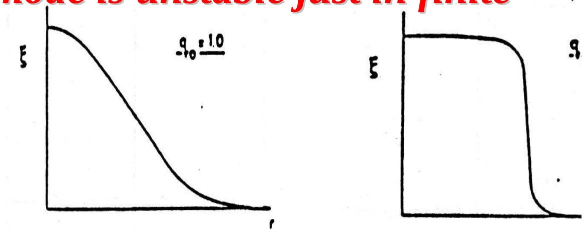

q_0=1 q_0=0.8

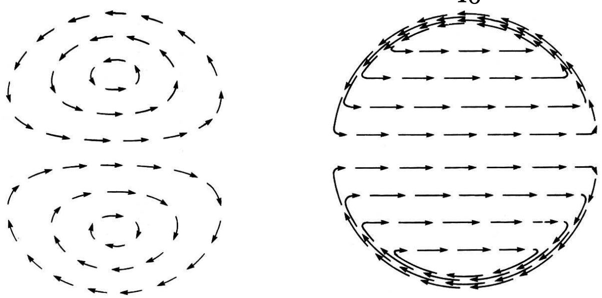

displacement and flow pattern of m/n=1/1 ideal kink mode

ref J.Wesson; Chap.6.10-11 in “Tokamaks --2nd edit.--” Clarendon press (1997).

Comparison between exp. observation and Kadomatsev’s mode

ref J.Wesson; Chap.7.6 in “Tokamaks --2nd edit.--” Clarendon press (1997).

Some discrepancies exist between observation and the model; ***still open question!***

(1) According to a observation of q_0, q_0 remains well below 1, which is conflict with the model which predicts full reconnection.
(2) According to the model, the collapse time is larger as the device becomes larger because of the increase of τ_A/τ_R, which is conflict with the experimental results that the collapse time hardly depends on the device size.
(3) According to a observation of fluc. contour, it looks that cold bubble invade the core, hot island is surrounding it, , which is conflict with the model which predicts a cooler core island is surrounding the displaced hot circular core.

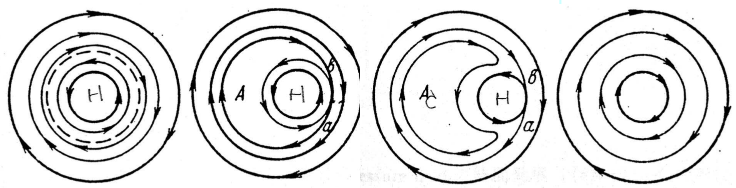

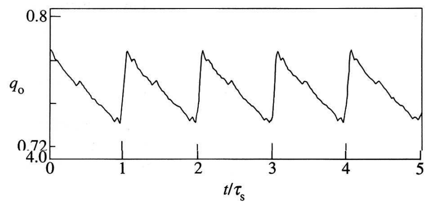

Time evolution of observed q_0
ref. H.Soltwisch et al, at 29th APS meeting, San Diego (1987)

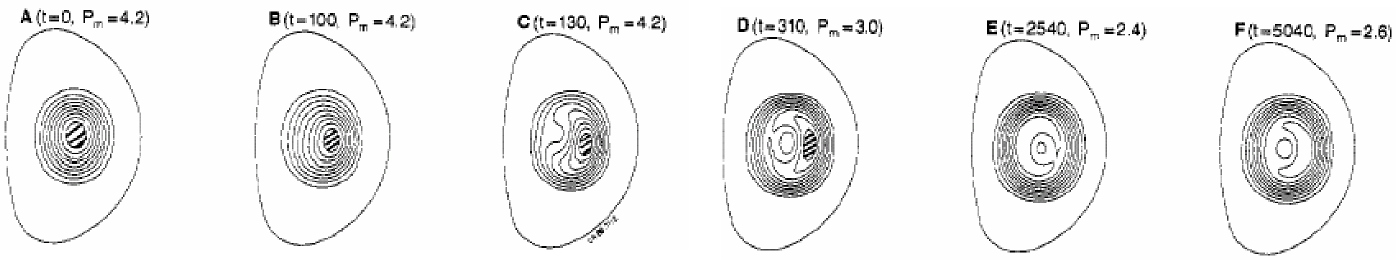

ECE tomography result in JET
ref. A.E.Costley et al, PPCF 30, 1455 (1988)

It looks that cold bubble invade the core, hot island is surrounding it.

Index of lecture

1. Introduction of MHD Jan. 5

2. MHD equilibrium Jan. 5

3. Pressure driven MHD instabilities
   Interchange mode Jan. 12
   Ballooning mode Jan. 19

4. Current driven MHD instabilities Jan. 19

5. Hot topics of MHD equilibrium and instability
   Jan. 27

On next phase of this class,

Start from Feb. 1 (Tue.) 13:30~
At meeting room on 7th floor.
Teacher; Prof. Miyazawa

Mode coupling

through configuration effects

through Non-linear process

Reduced MHD Equation

$$\rho\left(\frac{\partial}{\partial t}+\mathbf{v}\cdot\nabla\right)\mathbf{v}=\mathbf{j}\times\mathbf{B}-\nabla p,$$

Motion eq.

$$\frac{\partial\rho}{\partial t}+\nabla\cdot(\rho\mathbf{v})=0, \qquad \left(\frac{\partial}{\partial t}+\mathbf{v}\cdot\nabla\right)p=0,$$

Eq. of continuity and state for γ=0

$$\frac{\partial\mathbf{B}}{\partial t}=-\nabla\times\mathbf{E}, \quad \nabla\times\mathbf{B}=\mu_0\mathbf{j}, \quad \nabla\cdot\mathbf{B}=0, \quad \mathbf{E}+\mathbf{v}\times\mathbf{B}=0 \quad (\eta\mathbf{j}),$$

Ohm's low   Maxwell eq.

Here some quantities are linearized (separate the equilibrium part (suffix 0) and the perturbed part (suffix 1).).

$$\mathbf{v}(\mathbf{r},t)=0+\mathbf{v}_1(\mathbf{r},t), \qquad \mathbf{j}(\mathbf{r},t)=\mathbf{j}_0(\mathbf{r})+\mathbf{j}_1(\mathbf{r},t), \left|\mathbf{j}_1\right|<<\left|\mathbf{j}_0\right|,$$

$$\mathbf{B}(\mathbf{r},t)=\mathbf{B}_0(\mathbf{r})+\mathbf{B}_1(\mathbf{r},t), \left|\mathbf{B}_1\right|<<\left|\mathbf{B}_0\right|, \quad \mathbf{E}(\mathbf{r},t)=0+\mathbf{E}_1(\mathbf{r},t),$$

$$\rho(\mathbf{r},t)=\rho_0(\mathbf{r})+\rho_1(\mathbf{r},t), \rho_1<<\rho_0, \qquad p(\mathbf{r},t)=p_0(\mathbf{r})+p_1(\mathbf{r},t), p_1<<p_0.$$

The 1st order momentum equations are as follows:

$$\rho_0\frac{\partial\mathbf{v}_1}{\partial t}=-\nabla p_1+\mathbf{j}_1\times\mathbf{B}_0+\mathbf{j}_0\times\mathbf{B}_1,$$

$$\frac{\partial\rho_1}{\partial t}+\nabla\cdot(\rho_0\mathbf{v}_1)=0, \quad \frac{\partial p_1}{\partial t}=-\mathbf{v}_1\cdot\nabla p_0-\gamma p_0\nabla\cdot\mathbf{v}_1,$$

$$\mathbf{E}_1+\mathbf{v}_1\times\mathbf{B}_0=\mu\mathbf{j}_1,$$

$$\frac{\partial\mathbf{B}_1}{\partial t}=-\nabla\times\mathbf{E}_1, \quad \nabla\times\mathbf{B}_1=\mu_0\mathbf{j}_1, \quad \nabla\cdot\mathbf{B}_1=0.$$

$$\boxed{\begin{gathered}\rho_0\frac{\partial\mathbf{v}_1}{\partial t}=-\nabla p_1+\mathbf{j}_1\times\mathbf{B}_0+\mathbf{j}_0\times\mathbf{B}_1,\\ \frac{\partial\rho_1}{\partial t}+\nabla\cdot(\rho_0\mathbf{v}_1)=0, \quad \frac{\partial p_1}{\partial t}=-\mathbf{v}_1\cdot\nabla p_0,\\ \frac{\partial\mathbf{B}_1}{\partial t}=\nabla\times\left(\mathbf{v}_1\times\mathbf{B}_0-\eta\nabla\times\mathbf{B}_1\right), \quad \nabla\cdot\mathbf{B}_1=0.\end{gathered}}$$

Reduced MHD Equation II

The 1st order momentum equations are as follows:

$$\rho_0 \frac{\partial \mathbf{v}_1}{\partial t} = -\nabla p_1 + \mathbf{j}_1 \times \mathbf{B}_0 + \mathbf{j}_0 \times \mathbf{B}_1,$$
$$\frac{\partial \rho_1}{\partial t} + \nabla \cdot (\rho_0 \mathbf{v}_1) = 0, \quad \frac{\partial p_1}{\partial t} + \mathbf{v}_1 \cdot \nabla p_0 = 0,$$
$$\frac{\partial \mathbf{B}_1}{\partial t} = \nabla \times (\mathbf{v}_1 \times \mathbf{B}_0 - \eta \nabla \times \mathbf{B}_1), \quad \nabla \cdot \mathbf{B}_1 = 0.$$

Here $\nabla \cdot \mathbf{v}_1 = 0$ is assumed. $\frac{\partial \rho_1}{\partial t} + \mathbf{v}_1 \cdot \nabla \rho_0 = 0.$

incompressible approximation

Here $\nabla \cdot (\mathbf{B} \times)$ for 1st eq., and by using $\nabla \cdot \mathbf{v}_1 = 0$ and $\nabla \cdot \mathbf{B}_1 = 0$.

$$\mathbf{B} \cdot \frac{\rho_0}{B_0^2} \nabla \times \frac{\partial \mathbf{v}_1}{\partial t} = (\mathbf{B} \cdot \nabla) \frac{\mathbf{j}_1 \cdot \mathbf{B}_0}{B_0^2} + \mathbf{B} \cdot \frac{\nabla B_0^2 \times \nabla p_1}{B_0^4},$$
$$\frac{\partial p_1}{\partial t} + \mathbf{v}_1 \cdot \nabla p_0 = 0.$$
$$\frac{\partial \mathbf{B}_1}{\partial t} = (\mathbf{B}_0 \cdot \nabla) \mathbf{v}_1 - (\mathbf{v}_1 \cdot \nabla) \mathbf{B}_0 + \eta \nabla^2 \mathbf{B}_1.$$

vorticity eq. $\nabla \times \mathbf{v}_1$; vortecity

energy (density) conservation eq.

Faraday's law + Ampare, Ohms low

$\mathbf{v}_1 = \nabla U \times \vec{\varphi}$, and $\mathbf{B}_1 = \nabla \psi \times \vec{\varphi}$ are assumed. $\mathbf{B}_0 = B_0 \vec{\varphi} + \nabla \psi_{h0} \times \vec{\varphi}, \quad j_{\varphi 1} = -\nabla_\perp^2 \psi.$

$$\boxed{\rho_0 \frac{\partial}{\partial t} \nabla_\perp^2 U = -\mathbf{B}_0 \cdot \nabla \left(\nabla_\perp^2 \psi \right) - \hat{\varphi} \times \boldsymbol{\kappa}_r \cdot \nabla p_1, \quad \frac{\partial p_1}{\partial t} + \mathbf{v}_1 \cdot \nabla p_0 = 0, \quad \frac{\partial \psi}{\partial t} = \mathbf{B}_0 \cdot \nabla U + \eta \nabla_\perp^2 \psi.}$$

Mode coupling I

$$\rho_0 \frac{\partial}{\partial t}\nabla_\perp{}^2 U = -\mathbf{B}_0 \cdot \nabla\left(\nabla_\perp{}^2 \psi\right) - \hat{\varphi}\times\boldsymbol{\kappa}_r \cdot \nabla p_1,$$

$$\frac{\partial p_1}{\partial t} + \mathbf{v}_1 \cdot \nabla p_0 = 0,$$

$$\frac{\partial \psi}{\partial t} = \mathbf{B}_0 \cdot \nabla U + \eta \nabla_\perp{}^2 \psi.$$

$$\mathbf{v}_1 = \nabla U \times \vec{\varphi},$$

$$j_{\varphi 1} = -\nabla_\perp{}^2 \psi.$$

$$\rho_0 \frac{\partial^2}{\partial t^2}\nabla_\perp{}^2 U = -\mathbf{B}_0 \cdot \nabla\left(\nabla_\perp{}^2 \frac{\partial \psi}{\partial t}\right), \frac{\partial \psi}{\partial t} = \mathbf{B}_0 \cdot \nabla U$$

$$\boxed{\rho_0 \frac{\partial^2}{\partial t^2}\nabla_\perp{}^2 U \sim -\mathbf{B}_0{}^2 \cdot \nabla\nabla\left(\nabla_\perp{}^2 U\right)}$$

A kind of wave

Fourier-Laplace expansion; torus plasmas has 2 type of period.

$$\{U, p, A\} = \sum_{m,n}\{\hat{U}_{mn}, \hat{p}_{mn}, \hat{A}_{mn}\}\exp[\mathrm{i}(m\theta - n\varphi) - \mathrm{i}\omega t].$$

$\hat{U}_{mn}, \hat{p}_{mn}, \hat{A}_{mn}$ are function of ρ (radial variable; index of mag. surface)

Mode coupling II --through configuration effects--

$$\rho_0 \frac{\partial^2}{\partial t^2} \nabla_\perp{}^2 U \sim -\mathbf{B}_0{}^2 \cdot \nabla\nabla\left(\nabla_\perp{}^2 U\right)$$

$$\rho_0 \frac{\partial^2}{\partial t^2} \sum_{mn} X_{mn} \exp\left(i(m\theta - n\varphi) - i\omega t\right) \sim -\mathbf{B}_0{}^2 \cdot \nabla\nabla\left(\sum_{mn} X_{mn} \exp\left(i(m\theta - n\varphi) - i\omega t\right)\right)$$

When $\mathbf{B}_0$ (equilibrium field) is homogeneous case, there is no mode coupling.
=> $X_{mn}\exp(i(m\theta-n\phi)-i\omega t)$ is independent each other.

When $\mathbf{B}_0$ (equilibrium field) is inhomogeneous case like tokamaks [$\mathbf{B}_0 = B_0 * R_0/(R_0 + r*\cos\theta)$], mode coupling happens.=> mode coupling through equilibrium config.
=> When ω is fixed, Sum_$X_{mn}\exp(i(m\theta-n\phi)-i\omega t)$ is determined.

Notes!
There are some means in word "mode".
When ω is fixed, the space structure (combination set of m,n, $X_{mn}(\rho)$) is determined. The set including ω means a mode.
A component of Sum_$X_{mn}\exp(i(m\theta-n\phi)-i\omega t)$ is sometimes called "mode".

Example of mode coupling through equil. configuration

ref. P.B. Snyder et al., Nucl. Fusion 44 (2004) 320.

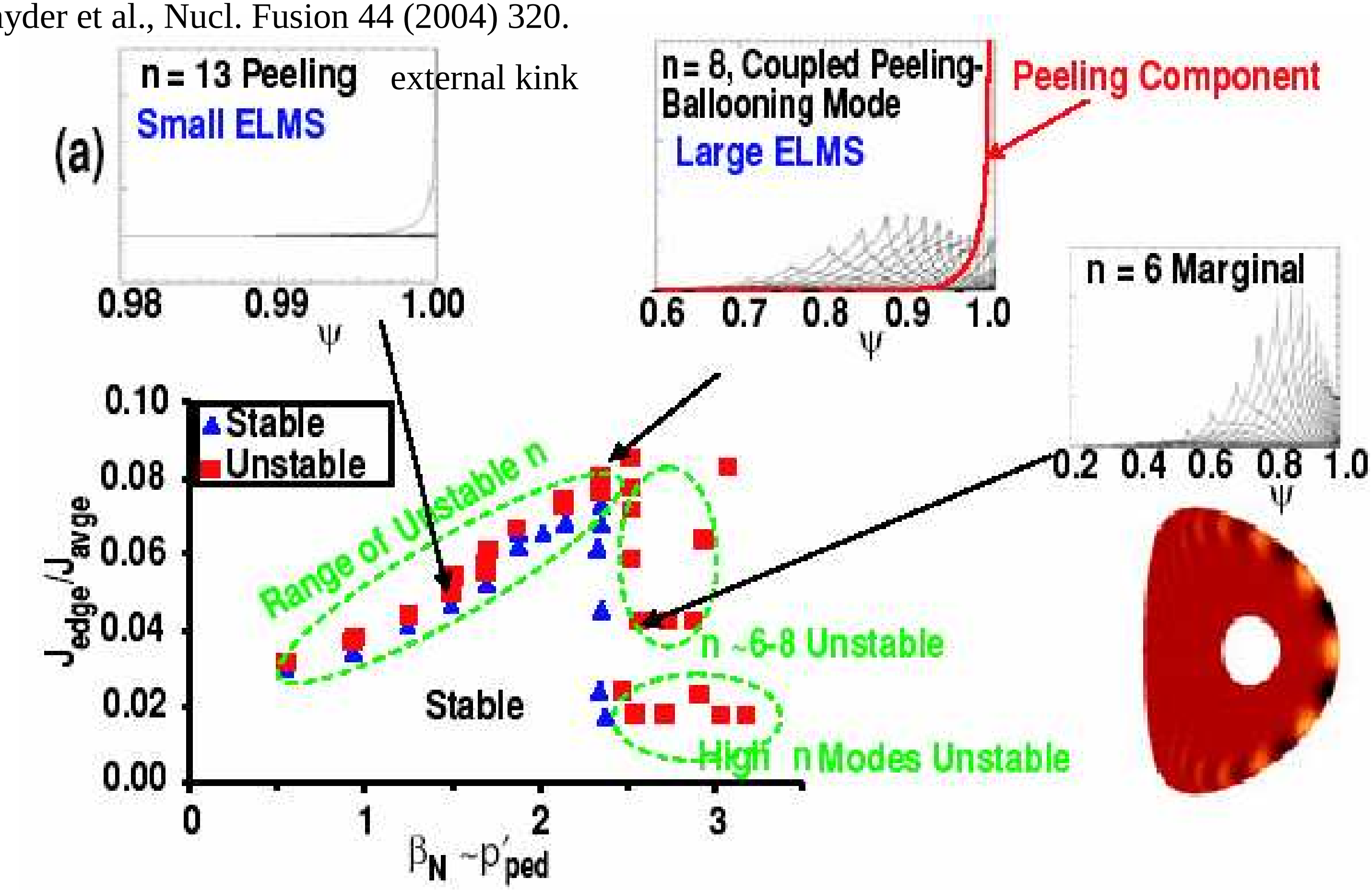

Tokamaks ballooning mode

Reduced MHD Equation II'

The 1st order momentum equations are as follows:

$$\boxed{\begin{aligned}&\rho_0 \frac{\partial \mathbf{v}_1}{\partial t} = -\nabla p_1 + \mathbf{j}_1 \times \mathbf{B}_0 + \mathbf{j}_0 \times \mathbf{B}_1 + \underline{\mathbf{j}_1 \times \mathbf{B}_1},\\ &\frac{\partial \rho_1}{\partial t} + \nabla \cdot \left(\rho_0 \mathbf{v}_1 + \underline{\rho_1 \mathbf{v}_1}\right) = 0, \quad \frac{\partial p_1}{\partial t} + \mathbf{v}_1 \cdot \nabla p_0 + \underline{\mathbf{v}_1 \cdot \nabla p_1} = 0,\\ &\frac{\partial \mathbf{B}_1}{\partial t} = \nabla \times \left(\mathbf{v}_1 \times \mathbf{B}_0 + \underline{\mathbf{v}_1 \times \mathbf{B}_1} - \eta \nabla \times \mathbf{B}_1\right), \quad \nabla \cdot \mathbf{B}_1 = 0.\end{aligned}}$$

$$\boxed{\begin{aligned}&\rho_0 \frac{\partial}{\partial t} \nabla_\perp{}^2 U = -\mathbf{B}_{0+1} \cdot \nabla\left(\nabla_\perp{}^2 \left(\psi_{h0} + \psi\right)\right) - \hat{\varphi} \times \boldsymbol{\kappa}_r \cdot \nabla p_1,\\ &\frac{\partial p_1}{\partial t} + \mathbf{v}_1 \cdot \nabla\left(p_0 + p_1\right) = 0,\\ &\frac{\partial \psi}{\partial t} = \mathbf{B}_{0+1} \cdot \nabla U + \eta \nabla_\perp{}^2 \psi.\end{aligned}}$$

$$\mathbf{B}_1 = \nabla \psi \times \vec{\varphi}.$$

$$\rho_0 \frac{\partial^2}{\partial t^2} \nabla_\perp{}^2 U = -\mathbf{B}_0 \cdot \nabla\left(\nabla_\perp{}^2 \frac{\partial \psi}{\partial t}\right) - \mathbf{B}_1 \cdot \nabla\left(\nabla_\perp{}^2 \frac{\partial \psi}{\partial t}\right), \frac{\partial \psi}{\partial t} = \mathbf{B}_0 \cdot \nabla U + \mathbf{B}_1 \cdot \nabla U$$

$$\boxed{\rho_0 \frac{\partial^2}{\partial t^2} \nabla_\perp{}^2 U \sim -\mathbf{B}_0{}^2 \cdot \nabla\nabla\left(\nabla_\perp{}^2 U\right) + \nabla_\perp{}^2 U \times \nabla\nabla\left(\nabla_\perp{}^2 U\right)}$$

Mode coupling III --through Non-linear process--

$$\rho_0 \frac{\partial^2}{\partial t^2}\nabla_\perp{}^2 U \sim -\mathbf{B}_0{}^2 \cdot \nabla\nabla\left(\nabla_\perp{}^2 U\right) + \nabla_\perp{}^2 U \times \nabla\nabla\left(\nabla_\perp{}^2 U\right)$$

$$\rho_0 \frac{\partial^2}{\partial t^2}\sum_{mn} X_{mn} \exp\left(i(m\theta - n\varphi) - i\omega t\right) \sim -\mathbf{B}_0{}^2 \cdot \nabla\nabla\left(\sum_{mn}\left(\sum_{m'n'} X_{m'n'} \exp\left(i(m'\theta - n'\varphi) - i\omega t\right)\right) X_{mn} \exp\left(i(m\theta - n\varphi) - i\omega t\right)\right)$$

Even if $\mathbf{B}_0$ (equilibrium field) is homogeneous case, mode coupling happens because perturbed terms are multiplied .
=> $X_{mn}\exp(i(m\theta\text{-}n\phi)\text{-}i\omega t)$ is not independent each other.

Method of mode structure analyzing I

The 1st order momentum equations are as follows:

$$\frac{\partial \rho_1}{\partial t} + \mathbf{v}_1 \cdot \nabla \rho_0 = 0,$$
$$\frac{\partial p_1}{\partial t} + \mathbf{v}_1 \cdot \nabla p_0 = 0$$

Here $\nabla \cdot \mathbf{v}_1$ is assumed.

$$\boldsymbol{\xi} \equiv \frac{\partial \mathbf{v}_1}{\partial t}$$

$$\longrightarrow$$

$$\rho_1 + \boldsymbol{\xi}_1 \cdot \nabla \rho_0 = 0,$$
$$p_1 + \boldsymbol{\xi}_1 \cdot \nabla p_0 = 0$$

$$\rho_1 = -\xi_{1r} \frac{d\rho_0}{dr},$$
$$p_1 = -\xi_{1r} \frac{dp_0}{dr}$$

$$\longrightarrow$$

$$\xi_{1r} = \rho_1 \Big/ \left(-\frac{d\rho_0}{dr} \right),$$
$$\xi_{1r} = p_1 \Big/ \left(-\frac{dp_0}{dr} \right)$$

Example of observation of mode structure

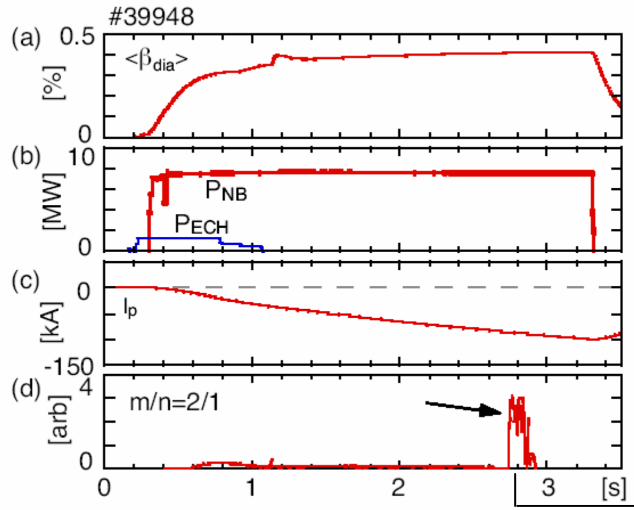

Poloidal and troidal mode structure m/n=2/1

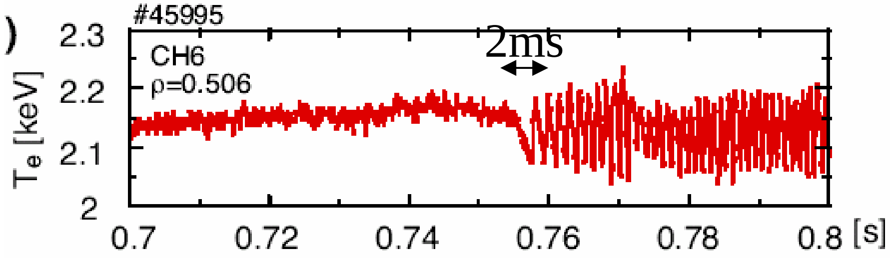

Evolution of the ECE perturbation

Toroidal Alfven freq. ~5.3×10^6Hz @2.75T, $n_e=10^{19}m^{-3}$, R_0=3,6m

According to theoretical prediction, the growth rate is around ~1.6×10^4Hz (63μs).

There is discrepancy between the prediction and observation in the growth rate.

Radial mode structure

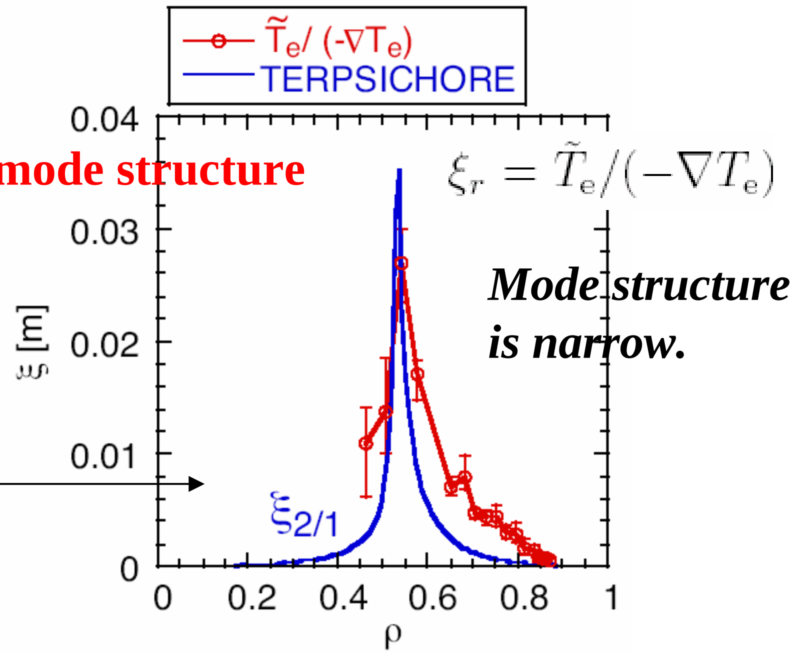

Mode structure is narrow.

Profile of the radial displacement by ECE measurement and theoretical prediction (Interchange mode)

The prediction of the ideal interchange mode is quite consistent with the observation on the mode structure.

A.Isayama et al; Plasma Phys. Contr. Fus. to be published (2005).

Method of mode structure analyzing II --tearing case--

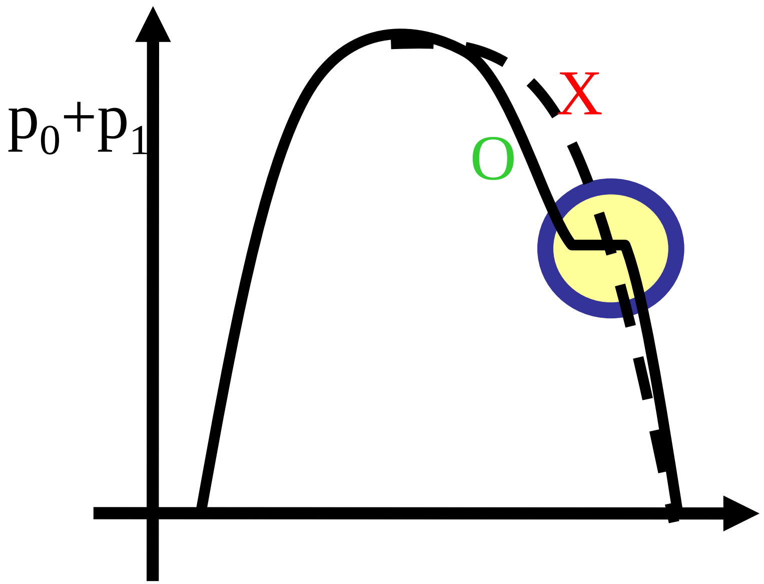

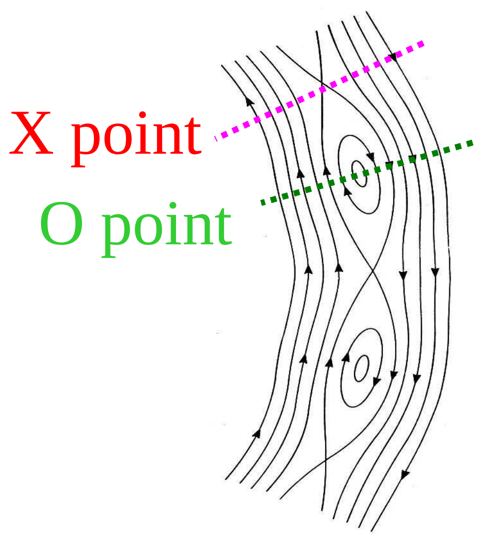

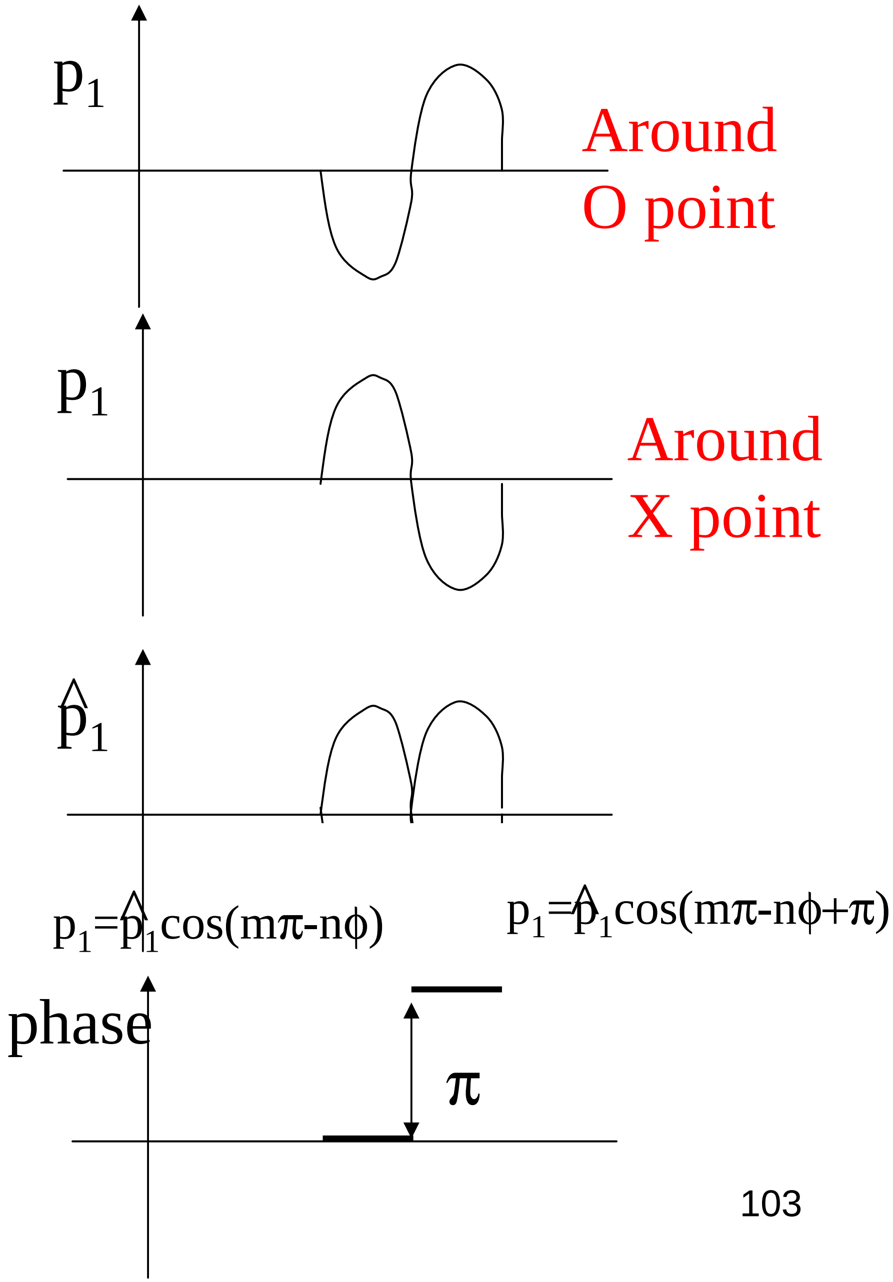

Characteristics MHD equil. related to stability in LHD

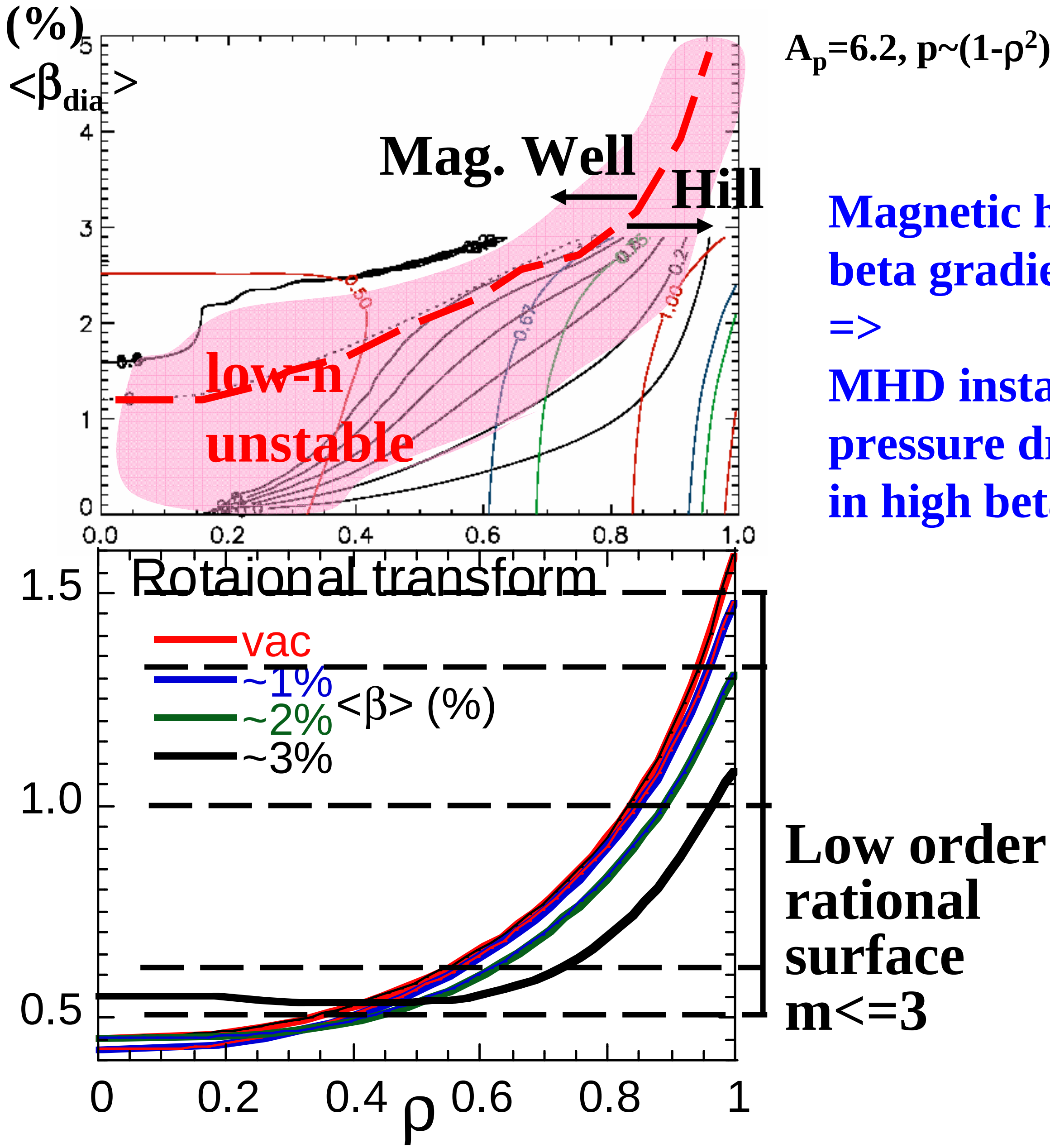

A_p=6.2, $p \sim (1-\rho^2)(1-\rho^8)$

Magnetic hill exists in the finite beta gradients region
=>
MHD instabilities (interchange/ pressure driven) would appear in high beta regime.

Characteristics MHD instability in LHD

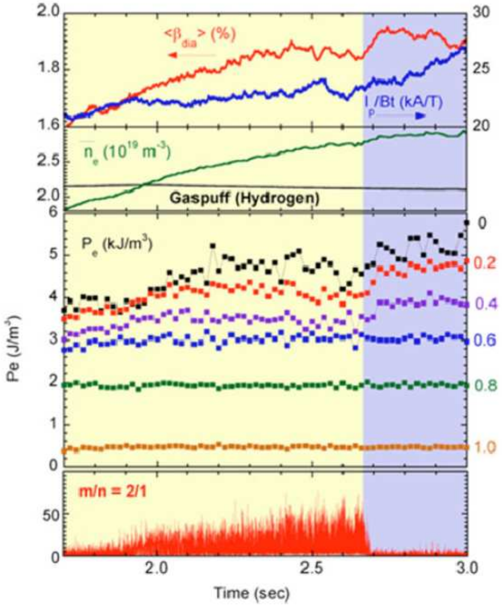

Fig. 1. Temporal changes of the averaged beta; plasma current normalized by toroidal field; electron density; electron pressure at ρ = 0.2, 0.4, 0.6, 0.8, and 1.0; and amplitude of m/n = 2/1 mode.

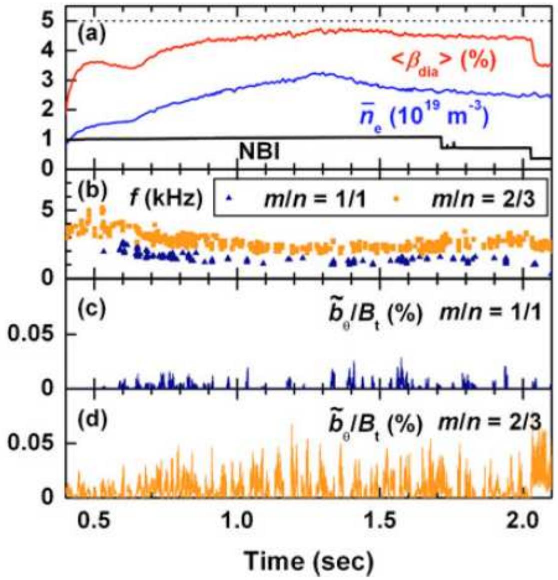

Fig. 4. Temporal changes of (a) $\langle \beta_{dia} \rangle$ and n_e, (b) frequencies of m/n = 1/1 and 2/3 modes, and amplitudes of (c) m/n = 1/1 and (d) m/n = 2/3 modes in typical high-β discharge.

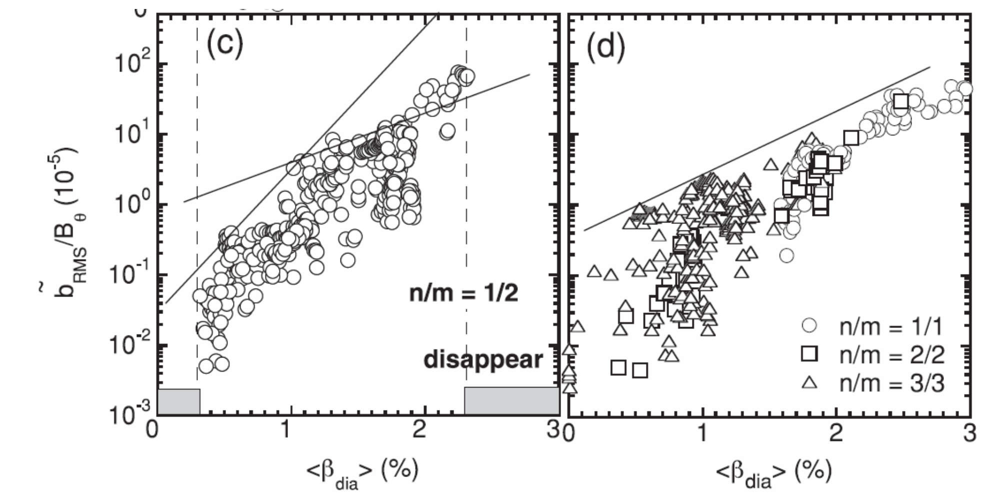

Quasi-steady high-β dischrage

<β>=4.8 %

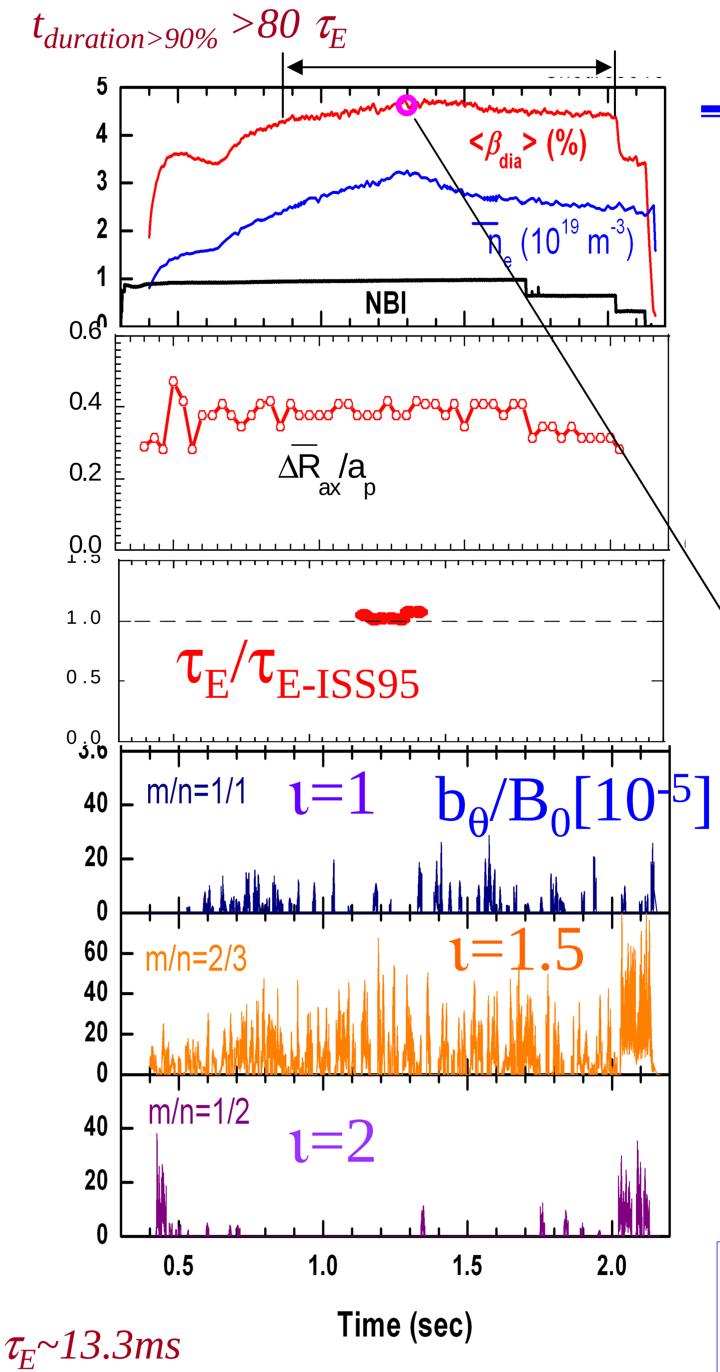

No disruptive high beta plasma is maintained during more than $80\tau_E$
Large shafranov shift Δ/a_p ~ 40%
Low-n,m MHD activities
- No observation of core resonant modes.
- Only resonating mode with peripheral surf. (m/n = 2/3 and 1/1) appear
Global confinement property is almost same with ISS95 scaling.

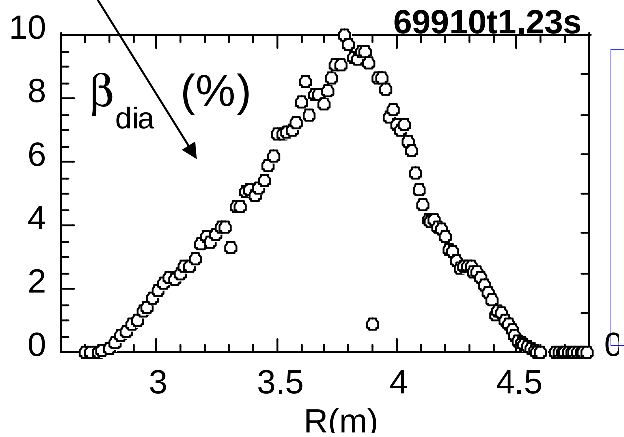

No large β flattening enough to affect a global confinement

Small flattening and asymmetric structures are observed

Comparison between peripheral pressure gradient and the prediction of linear MHD stability analysis

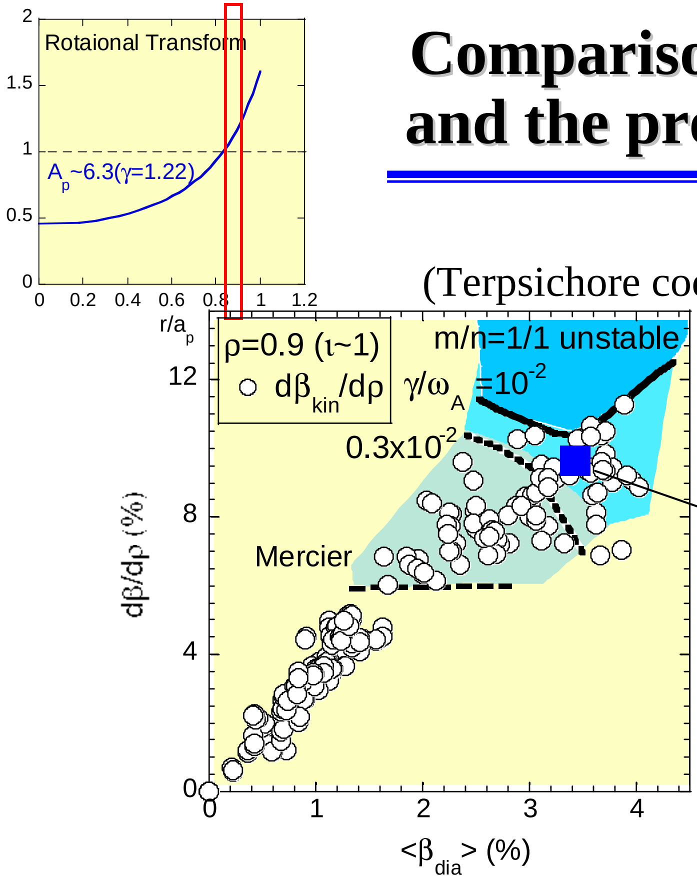

Observed kinetic beta gradients and a contour of growth rate of low-n ideal MHD mode

δ/a_p~3% (Ideal)

~5%(S=10^6) consistent with exp.

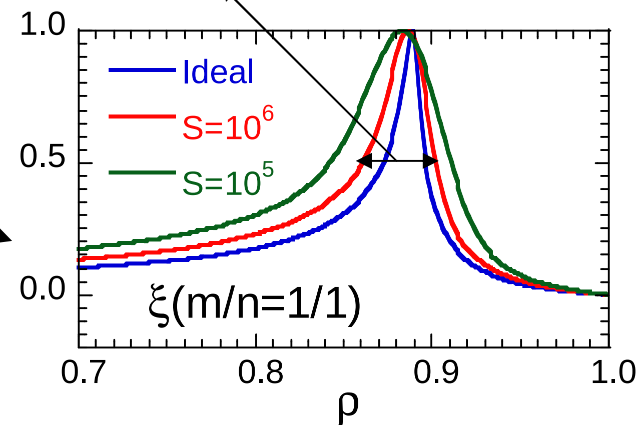

Calc. by FAR3D

Radial structure of low-n ideal and resitive MHD mode

In $<\beta_{dia}>$ ~4% plasmas, the global MHD mode is predicted unstable, but its radial mode width is narrow (~5% of a_p/ growth rate γ/ω_A~10^{-2})

No strong reduction of gradients

 # The gradients are averaged for Δρ=0.1.

even in the mode is expected linearly unstable, when the mode width is narrow, the effect on the confinement is quite small

Example of m/n=1/1 MHD instability in marginally stable discharge

Inducing impurity gas-puffing => S and grad p
changing magnetic config. => dι/dr and κ_n around the resonant surface
=>
Achievement of marginally unstable discharges with <β>~1% but similar $b^{\sim}$ level of <β>~5%

92000, R_{ax}^{V} 3.75m, 0.9T

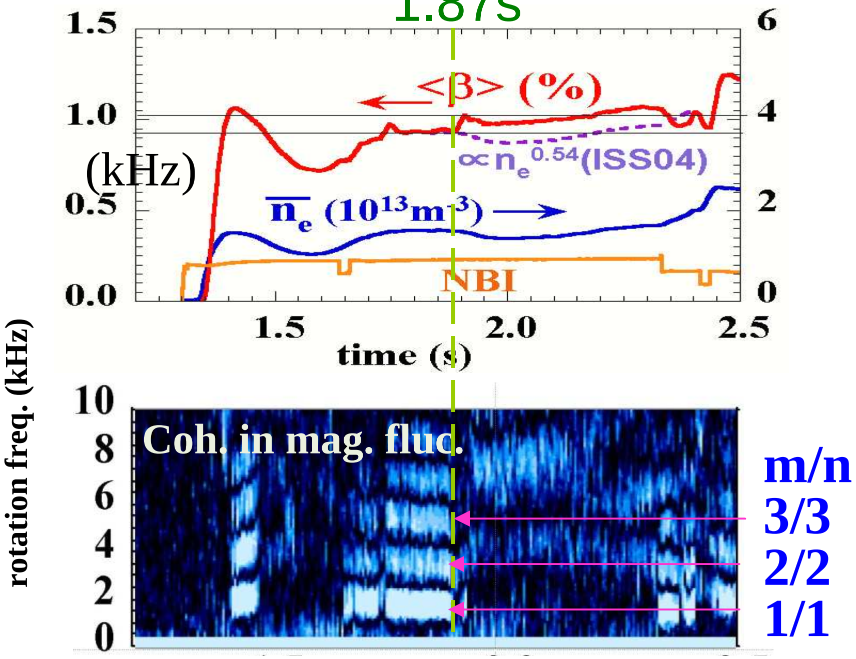

After disappearance of Mag. fluc., the beta increases

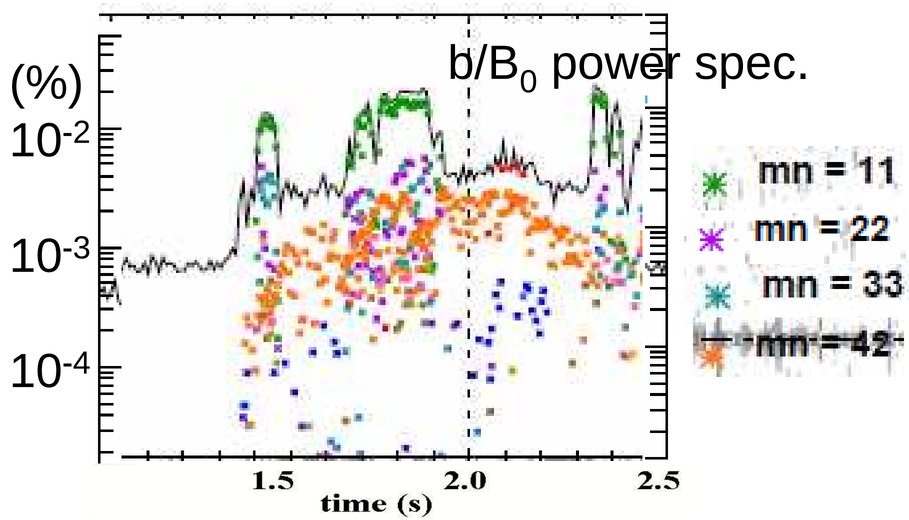

m/n=1/1 mag.fluc. is dominant in power spec..
Fluc. level ~0.03%
=> Same order with <β>~5% discharge

Characteristics of m/n=1/1 mode structure

92000, R_{ax}^{V} 3.75m, 0.9T

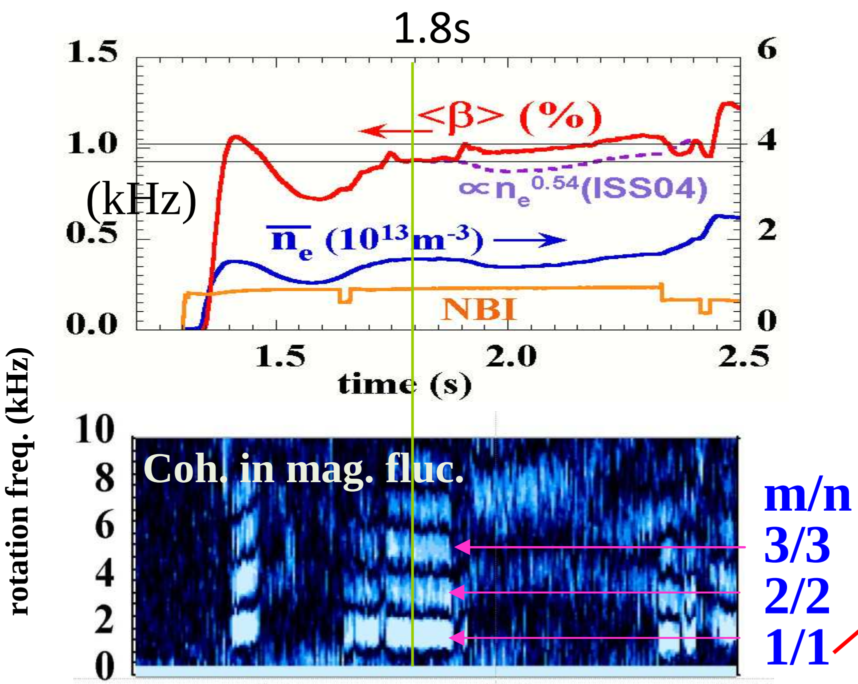

Radial profile of SXR fluctuation amplitude

t=1.8s

Line-integrated

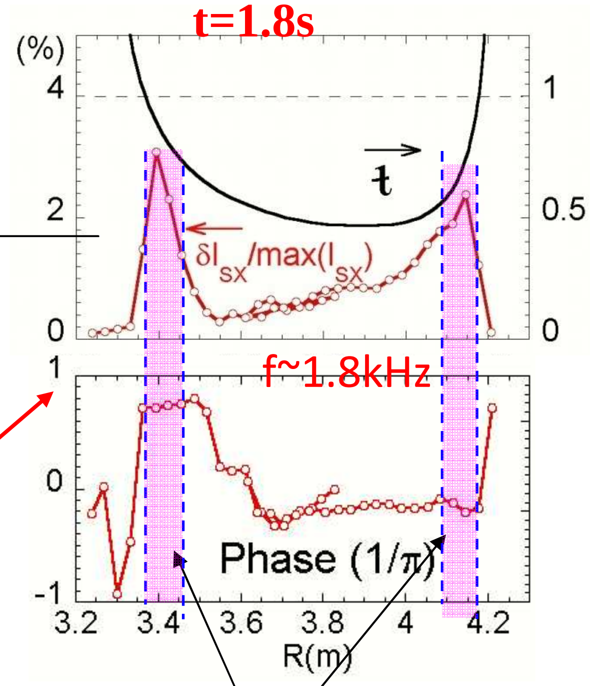

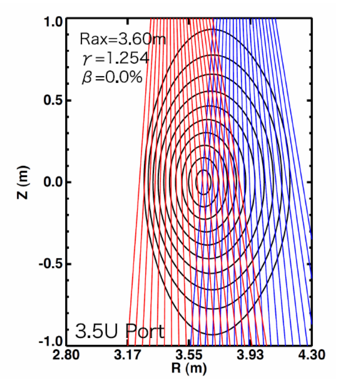

Sight lines of SX

No phase inversion
(No mag. island structure?)
=> Similar mode structure to linear theory prediction of res. interchange MHD insta.

Degradation Area due to the m/n=1/1 mode estimated from Te profile

B_0=0.9T, b/B_0~0.03%

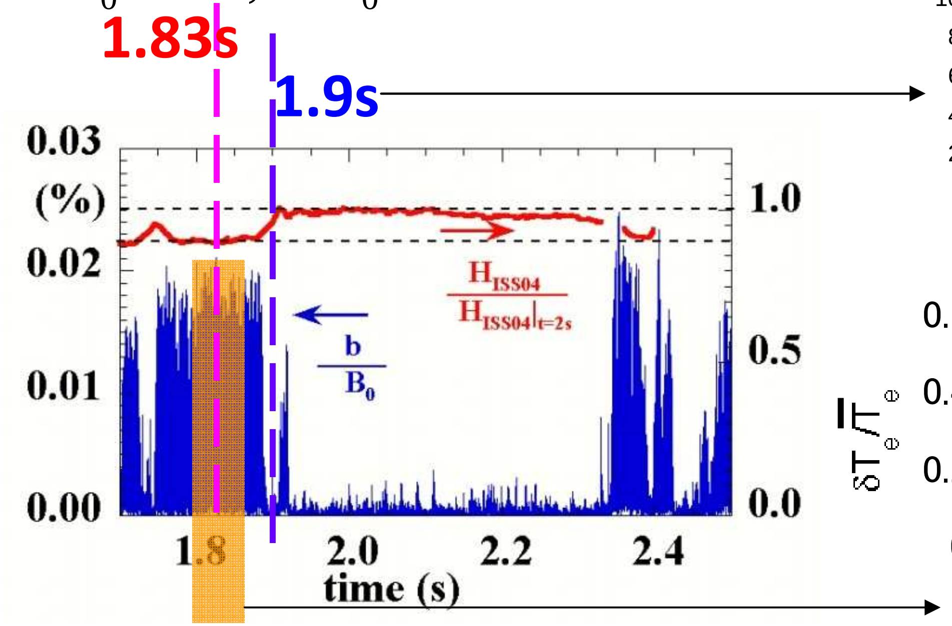

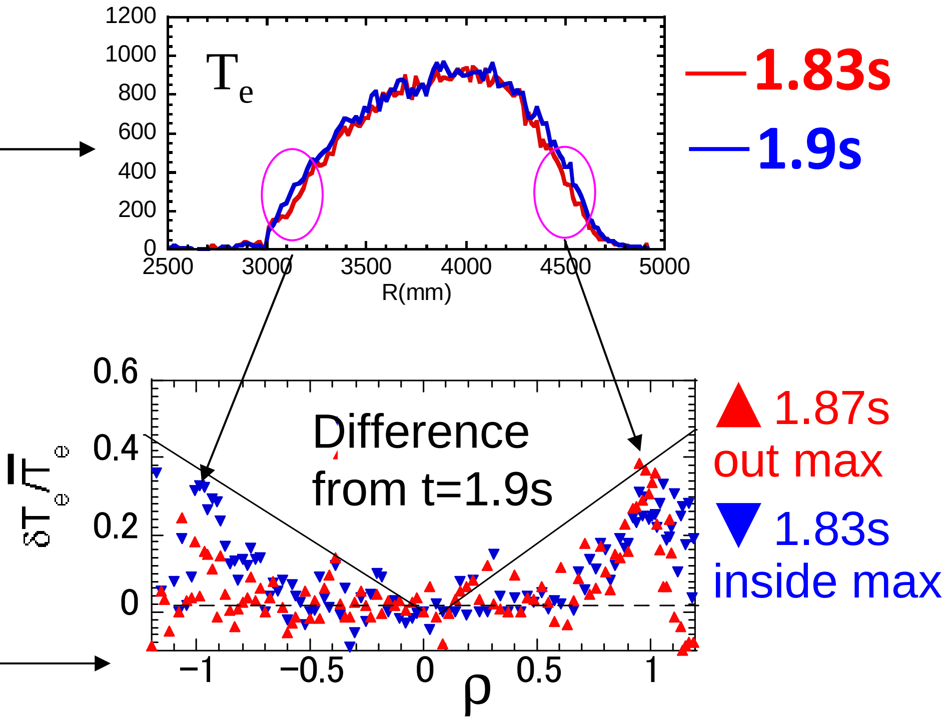

Decrease in Te is restricted to peripheral region around resonant rational surface by the m/n=1/1 mode =>
Impact on core region is quite small.

Estimation of m/n=1/1 mode internal structure based on Abel inv. and fitting method

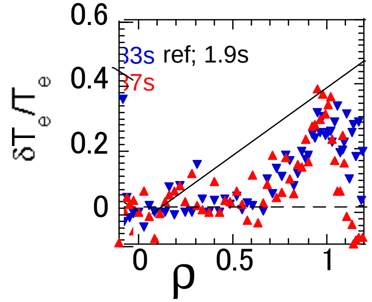

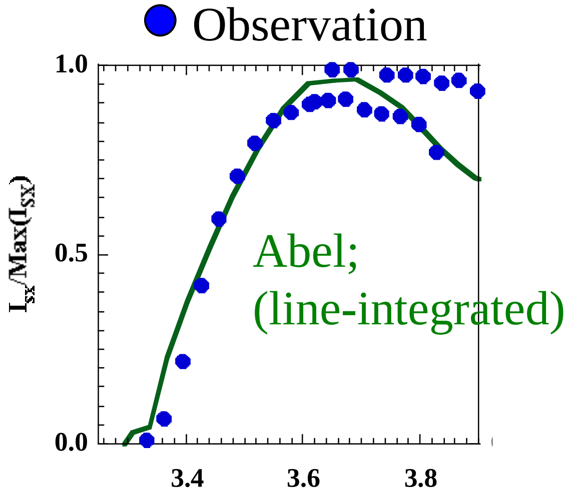

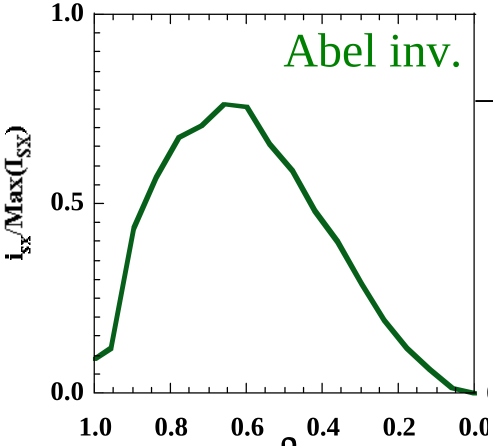

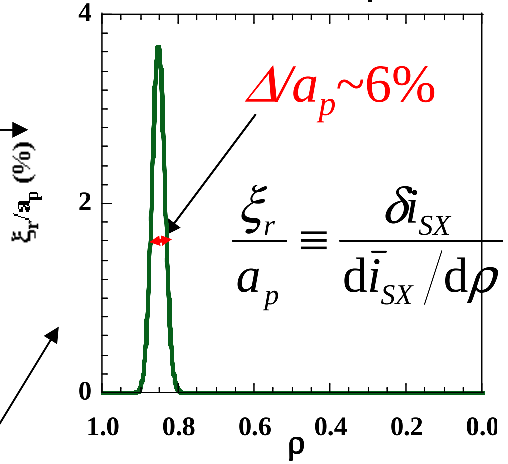

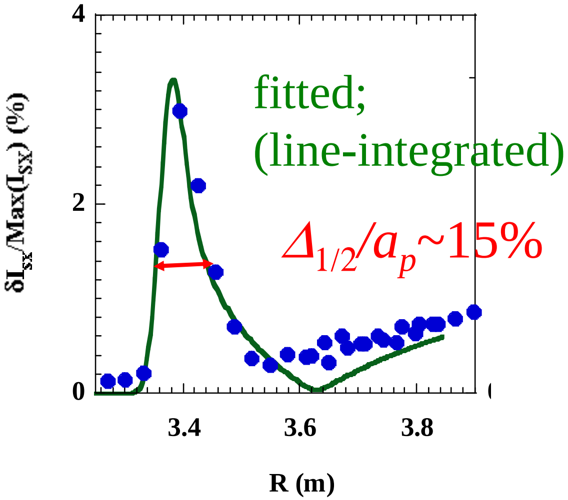

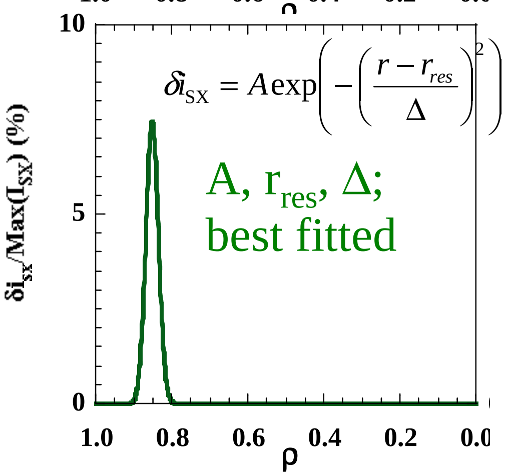

Δ/a_p~15%, $_{max}(\delta I/I_{SX\text{-}max})$~3%
in line-averaged fluc.
=>
Radial displacement
Δ/a_p~6%, ξ_r/a_p~4%

FWHM in local fluc. amplitude; less than half in line-averaged fluc. amp

Estimation of transport based on modeled perturb.

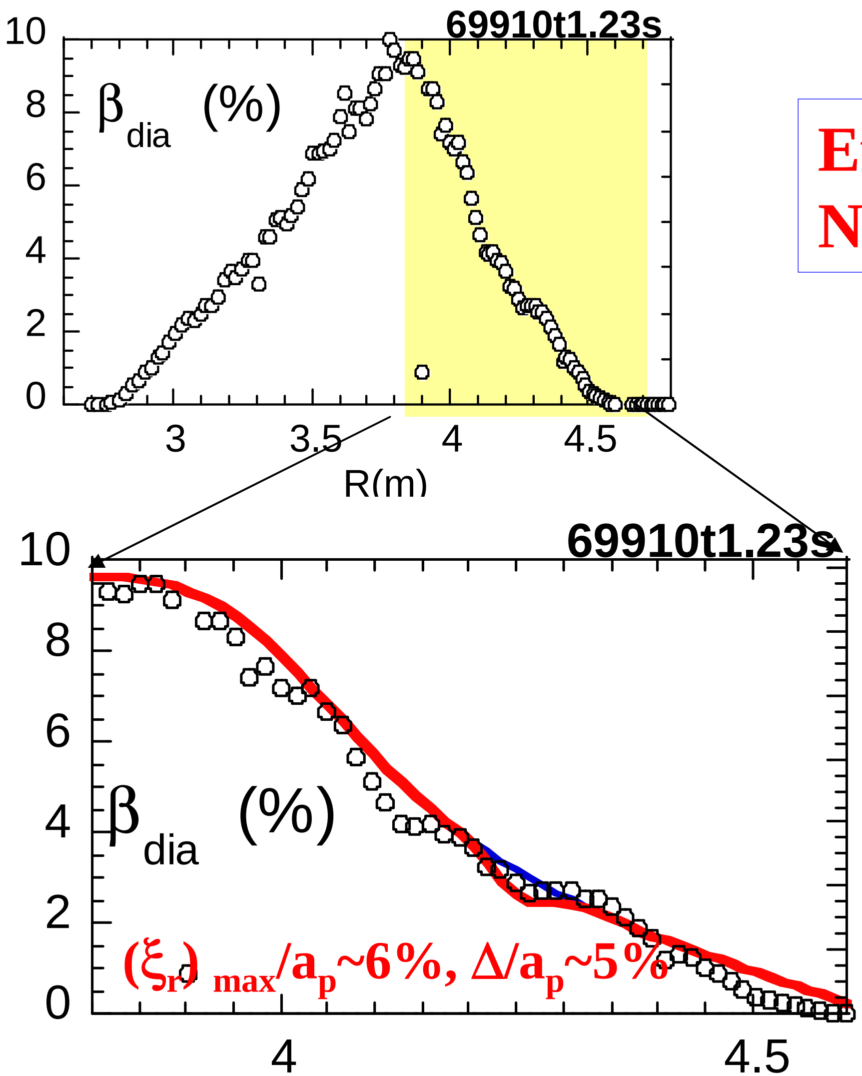

Effect on confinement? small??
Not clear yet!!

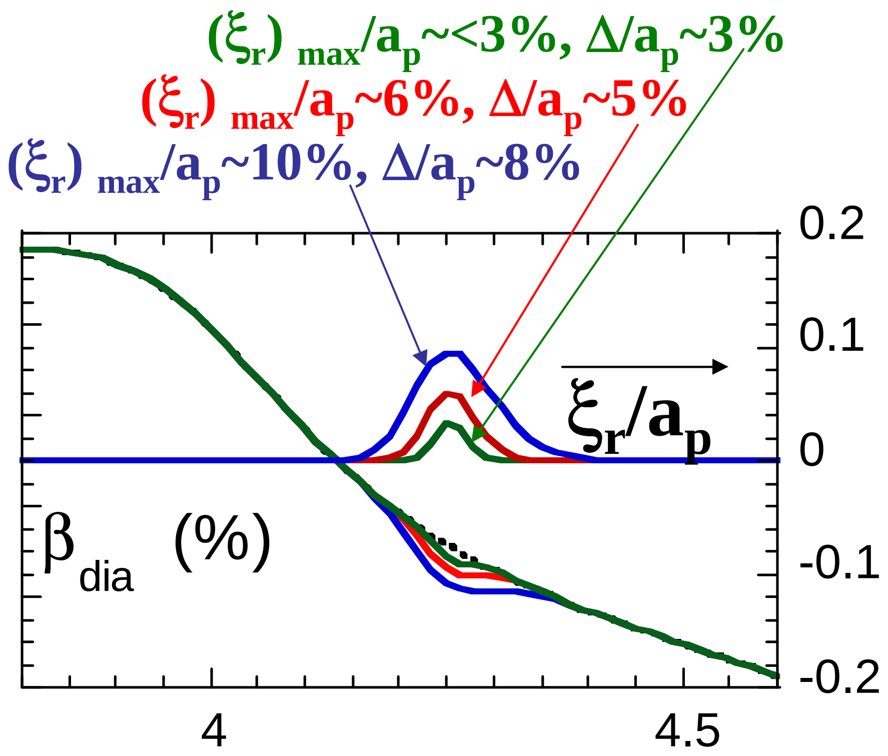

Effect of m/n=1/1 MHD mode on confinement

92000, R_{ax}^{V} 3.75m, 0.9T

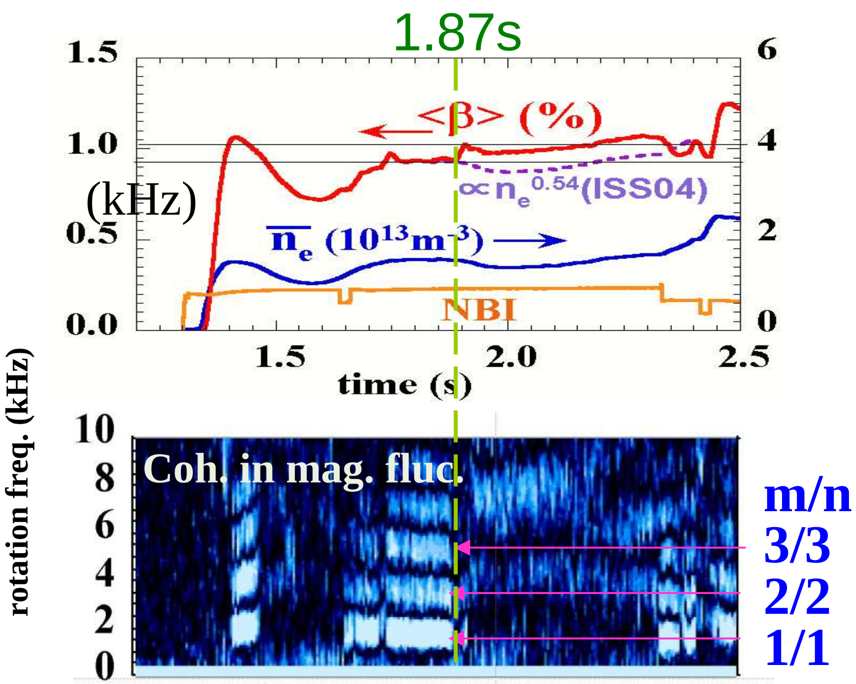

Confinement performance normalized by an empirical τ_E scaling (ISS04) in presence and disappearance

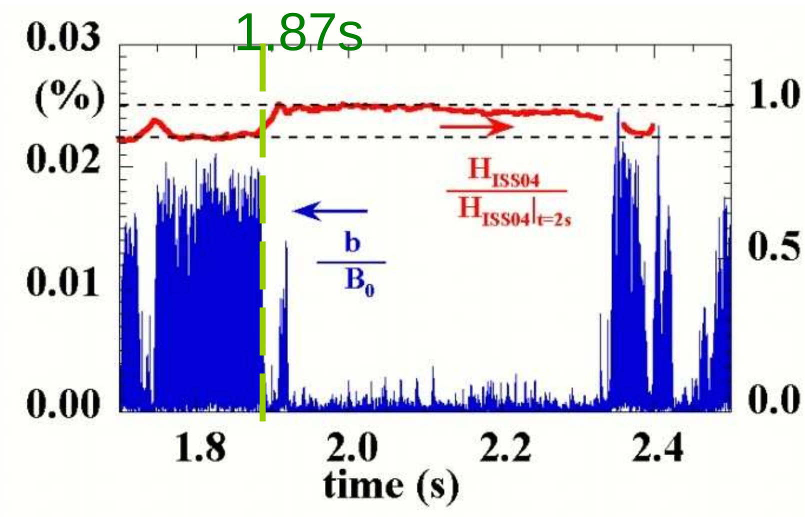

After disappearance of Mag. fluc., the beta increases

~10% degradation of the normalized global conf. time by a empirical scaling (ISS04) in the presence of the m/n=1/1 mode

No fatal effect of “global” mode on the helical plasma?

Helcal coil of LHD consists of 3 layers. By changing the current ratio in the 3 layers, plasma aspect ratio, mag.shear and mag. hill hight are controlled.

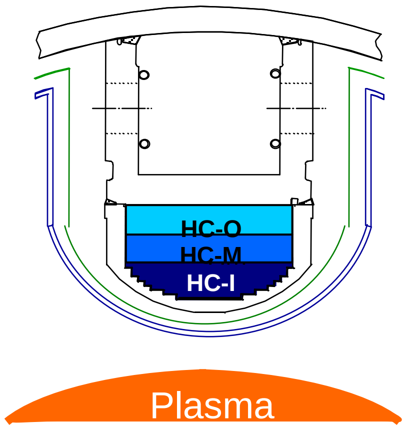

High aspect configuration (a special config.) has low magnetic shear and high magnetic hill in LHD

=> Interchange mode is more unstable

Magnetic curvature

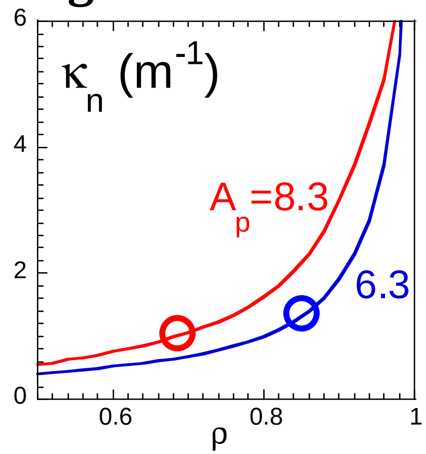

Rotaional transform

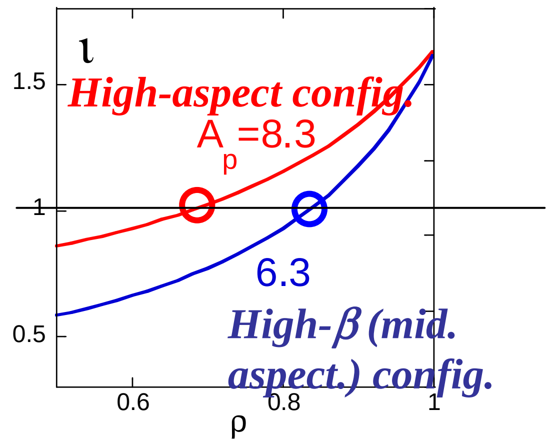

The magnetic shear of high aspect. conf. is much smaller than that of midium aspect. conf., and κ_n in both aspect ratio is almost same at the m/n=1/1 rational surface.

m/*n* = 1/1 mode in high aspect config. (low shear/high hill)

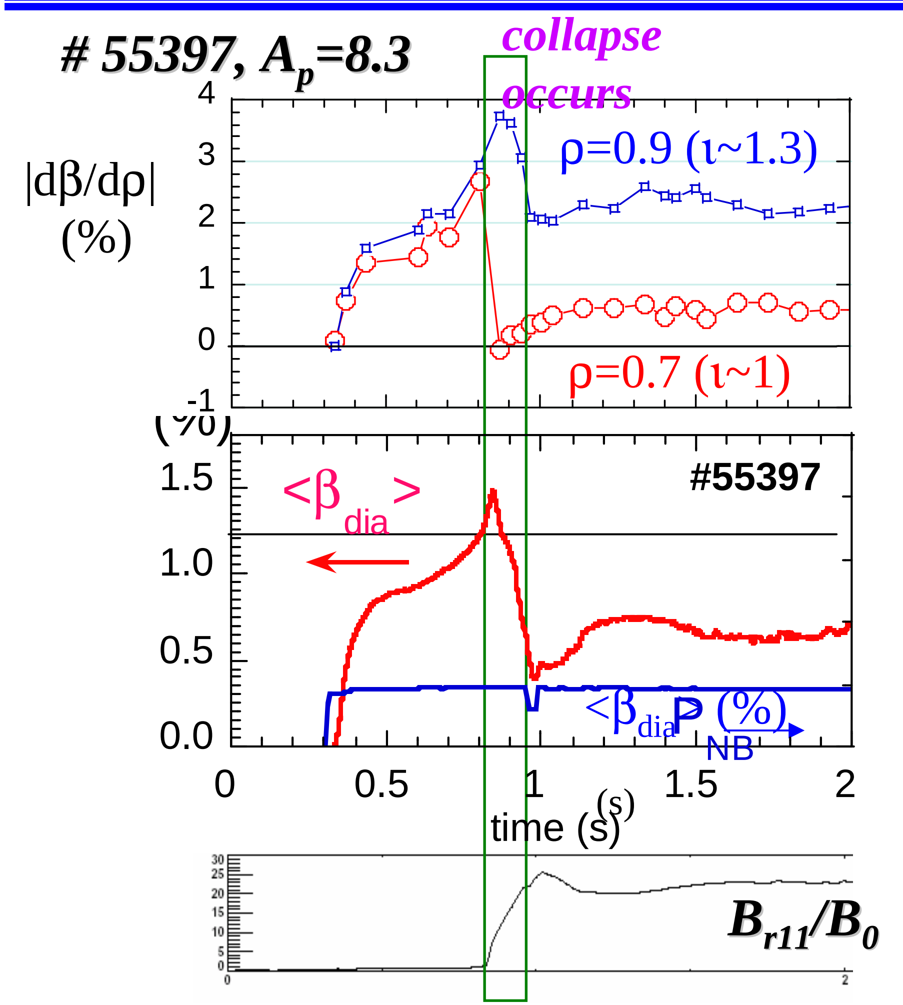

non-rotating

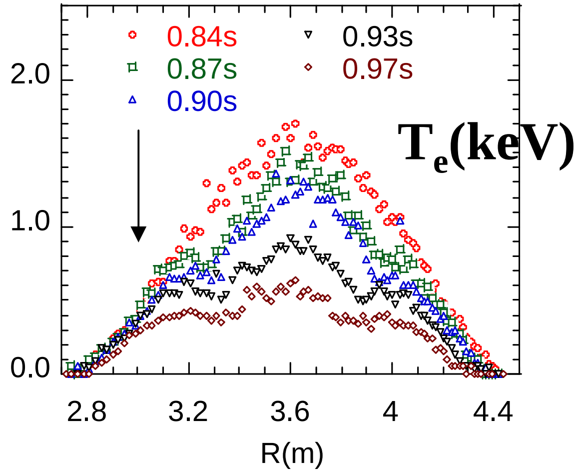

A collapse occurs in a high aspect plasma

Before the collapse occurs, stability condition of global MHD mode is strongly violated.

m/*n* = 1/1 mode in high aspect config. (low shear/high hill)

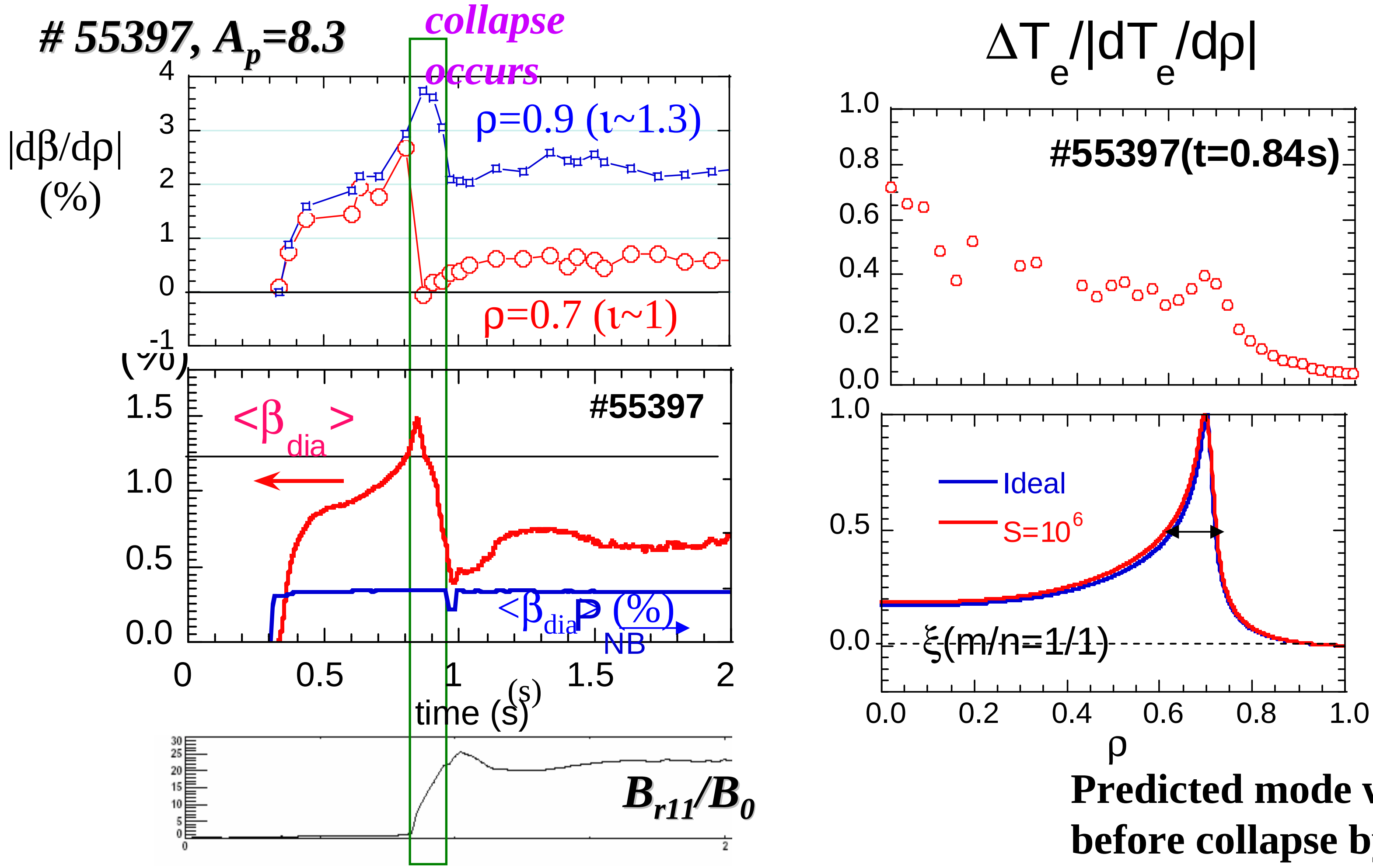

Predicted mode width before collapse by FAR3D

δ/a_p>10%
($\xi(0)$;finite)
$\gamma/\omega_A \sim 10^{-2}$

A collapse occurs in a high aspect plasma
Before the collapse occurs, stability condition of global MHD mode is strongly violated.

Mode width is much important for the effect on confinement!

Characteristics of m/n = 1/1 mode in LHD

Several differences of characteristics of the mode in different configurations.

Experiments	**“non-rotating” mode** *(High-A_p, and/or large I_p)*	**“rotating” mode** *(high-β)*
radial location	ρ ~ 0.7 (currentless)	ρ ~ 0.9
configuration	**weak shear**, magnetic hill (D_R>0)	magnetic hill (D_R>0)
Prediction	Ideal unstable **with large mode width**	Ideal stable, or unstable **with narrow mode width**
frequency	DC ~ several Hz	several kHz
spatial location	ϕ~ -120 deg (near natural error field)	rotating
S dependence	Low-S => not appears(?!)	**Low-S => large signal**
Interaction with static 1/1 island	**Suppression or growth**	Reduction of rotation, suppression
	“Ideal” mode	**“Resistive” mode**